Electronic Supplementary Material (ESI) for ChemComm.

Supporting Information for:

Complete reductive cleavage of CO facilitated by highly electrophilic borocations.

*Ewan R. Clark, Liam D. Curless, Alessandro Del Grosso, Jessica Cid and Michael J. Ingleson**

School of Chemistry, University of Manchester, Manchester, M13 9PL, U.K.

Table of Contents

1. General Comments

Unless otherwise stated, all manipulations were carried out using standard Schlenk techniques under argon, or in an MBraun UniLab glovebox, under an atmosphere of argon (< 0.1 ppm O_2/H_2O). Unless otherwise indicated, solvents were distilled from appropriate drying agents: *o*-Dichlorobenzene, *o*-$C_6H_4Cl_2$, (CaH_2) and *n*-hexane (NaK). *o*-$C_6H_4Cl_2$ was stored over activated 3Å molecular sieves while *n*-hexane was stored over a potassium mirror. All other compounds were purchased from commercial sources and used as received. Solvents for column chromatography were of technical grade and used without further purification. NMR spectra were recorded on Bruker AvanceIII-400 or Bruker Ascend-400 spectrometers. Chemical shifts are reported as dimensionless δ values and are frequency referenced relative to residual protio impurities in the NMR solvents for ^{1}H and ^{13}C $\{^{1}H\}$ respectively, while ^{11}B $\{^{1}H\}$, ^{19}F $\{^{1}H\}$ and ^{29}Si shifts are referenced relative to external BF_3-etherate, hexafluorobenzene and tetramethylsilane, respectively. Coupling constants *J* are given in Hertz (Hz) as positive values regardless of their real individual signs. The multiplicity of the signals are indicated as “s”, “d”, “t”, “q” “pent”, “sept” or “m” for singlet, doublet, triplet, quartet, pentet, septet or multiplet, respectively.

A number of NMR spectra are run in o-$C_6H_4Cl_2$. In these cases the ^{1}H NMR spectra are referenced to protio *o*-$C_6H_4Cl_2$, with the most up field peak at 7.154 ppm. A d_6-DMSO capillary is used to lock the signal. The ^{13}C NMR spectra are referenced to the d_6-DMSO peak at 39.51 ppm.

2. Amine Borane Activation with $Ph_3C^+[B(C_6F_5)_4]^-$

2.1 General Procedure 1

The reaction vessel was charged with a d_6-DMSO capillary and $Ph_3C^+[B(C_6F_5)_4]^-$ (46 mg, 0.05 mmol). This was dissolved in 0.6 ml of *o*-$C_6H_4Cl_2$ with subsequent addition of amine borane (1 equiv.). On addition of amine borane the tube was immediately sealed with the fitted Teflon valve and inverted for 10 min. The addition of amine borane leads to a colour change from a yellow to a colourless solution. NMR assay shortly following the observation of the colour change indicated formation of the H-bridged cation and Ph_3CH. The ^1H NMR spectrum is referenced to the protio o-$C_6H_4Cl_2$, with the most up field peak at 7.154 ppm. A d_6-DMSO capillary is used to lock the signal.

2.2 Et_3N-BH_3 activation with $Ph_3C^+[B(C_6F_5)_4]^-$

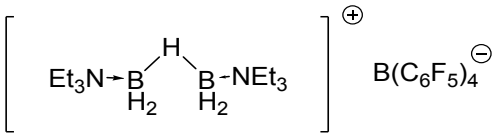

According to the general procedure 1, a J. Young's NMR tube was charged with $Ph_3C^+[B(C_6F_5)_4]^-$ (46 mg, 0.05 mmol) and dissolved in 0.6 ml *o*-$C_6H_4Cl_2$ before addition of Et_3N-BH_3 (15 µl, 0.1 mmol).

The signals corresponding to Ph_3CH are omitted and the resonances are comparable to that reported by Vedejs (which were recorded at -20°C in CD_2Cl_2).[1]

^1H NMR (*o*-$C_6H_4Cl_2$ 400 MHz) δ 2.75 (q, $^3J_{HH}$ 7.2 Hz, C*H*$_2$); 2.60 (br, B*H*$_2$); 1.13 (t, $^3J_{HH}$ 7.2 Hz, C*H*$_3$); -2.75 (br, B-*H*-B).

^{11}B NMR (*o*-$C_6H_4Cl_2$ 128 MHz) δ -3.9 (br, *B*H bridged species); -17.2 (s, *B*$(C_6F_5)_4$)

^{19}F NMR (*o*-$C_6H_4Cl_2$ 376 MHz) δ -132.7 (m, *o*-$(C_6F_5)_4$); -163.2 (t, $^3J_{FF}$ 20.8 Hz, *p*-$(C_6F_5)_4$); -167.1 (m, *m*-$(C_6F_5)_4$)

2.3 Et^iPr_2N-BH_3 activation with $Ph_3C^+[B(C_6F_5)_4]^-$

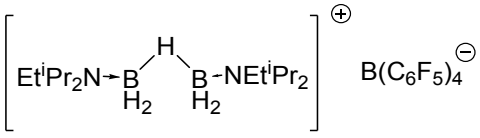

According to the general procedure 1, a J. Young's NMR tube was charged with $Ph_3C^+[B(C_6F_5)_4]^-$ (46 mg, 0.05 mmol) and dissolved in 0.6 ml *o*-$C_6H_4Cl_2$ before addition of Et^iPr_2N-BH_3 (17.5 µl, 0.1 mmol).

The signals corresponding to Ph_3CH are omitted.

^1H NMR (*o*-$C_6H_4Cl_2$ 400 MHz) δ 3.41 (sept, $^3J_{HH}$ 6.6 Hz, C*H*$(CH_3)_2$); 2.90 (q, $^3J_{HH}$ 7.2 Hz, C*H*$_2$); 2.72 (br, B*H*$_2$); 1.27 (d, $^3J_{HH}$ 6.6 Hz, CH(C*H*$_3$)$_2$); 1.23 (d, $^3J_{HH}$ 6.6 Hz, CH(C*H*$_3$)$_2$); 1.15 (t, $^3J_{HH}$ 7.2 Hz, C*H*$_3$); -2.53 (br, B-*H*-B).

^{11}B NMR (*o*-$C_6H_4Cl_2$ 128 MHz) δ -1.3 (br, *B*H bridged species); -17.2 (s, *B*$(C_6F_5)_4$)

^{19}F NMR (*o*-$C_6H_4Cl_2$ 376 MHz) δ -132.7 (m, *o*-$(C_6F_5)_4$); -163.2 (t, $^3J_{FF}$ 20.4 Hz, *p*-$(C_6F_5)_4$); -167.1 (m, *m*-$(C_6F_5)_4$)

3. Synthesis of O-Bridged borocation 3

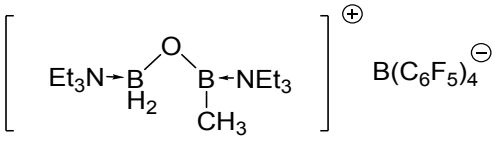

A J. Young's tube charged with the mixture of H-bridged cation **1** (0.1 mmol) and Ph_3CH in *o*-$C_6H_4Cl_2$ was subjected to three freeze pump thaw cycles before being back filled with CO at -78 °C. The J. Youngs NMR tube was placed in a 60 °C oil bath and periodically removed to be inverted to facilitate mixing. After 18 h NMR spectroscopy showed the predominant formation of a single new compound. The solution was layered with hexane to give crystalline needles.

^{1}H NMR (*o*-$C_6H_4Cl_2$ 400 MHz) δ 2.99 (q, $^3J_{HH}$ 7.3 Hz, C*H*$_2$); 2.72 (q, $^3J_{HH}$ 7.3 Hz, C*H*$_2$); 2.50 (br, B*H*$_2$); 1.10 (two overlapping triplets, CH_2CH_3); 0.66 (s, BC*H*$_3$).

^{11}B NMR (*o*-$C_6H_4Cl_2$ 128 MHz) δ 37.6 (br, O*B*CH_3); -2.3 (br, O*B*$H_2(NEt_3)$) -17.2 (s, *B*$(C_6F_5)_4$)

^{19}F NMR (*o*-$C_6H_4Cl_2$ 376 MHz) δ -132.7 (m, *o*-$(C_6F_5)_4$); -163.2 (t, $^3J_{FF}$ 20.8 Hz, *p*-$(C_6F_5)_4$); -167.1 (m, *m*-$(C_6F_5)_4$)

Accurate elemental analysis could not be obtained for this compound as solid sample were always contaminated with variable amounts of ammonium salts due to the sensitivity of this weakly stabilised borocation to trace protic impurities.

4. Boronium salt and Boroxine Formation

4.1 From Triethylamine borane H-bridged dimer

A J. Young's tube containing the H-bridged cation **1** (0.1 mmol) and Ph_3CH in *o*-$C_6H_4Cl_2$ was subjected to three freeze pump thawed cycles before being back filled with CO at -78 °C. The J. Youngs NMR tube was placed in a 100 °C oil bath and periodically removed to be inverted to facilitate mixing. The solution was layered with hexane to give crystalline needles.

Boronium 5

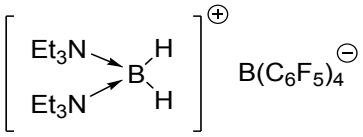

The ^{13}C NMR spectrum is referenced to the d_6-DMSO peak at 39.51 ppm. The signals corresponding to Ph_3CH and the anion $B(C_6F_5)_4$ are omitted.

^{1}H NMR (*o*-$C_6H_4Cl_2$ 400 MHz) δ 2.86 (q, $^{3}J_{HH}$ 7.2 Hz, CH_2); 1.80 (br, BH_2); 1.14 (t, $^{3}J_{HH}$ 7.3 Hz, CH_3).

^{11}B NMR (*o*-$C_6H_4Cl_2$ 128 MHz) δ -6.7 (br, BH_2) -17.2 (s, $B(C_6F_5)_4$)

^{13}C {^{1}H} NMR (*o*-$C_6H_4Cl_2$ 101 MHz) δ 49.4 (s, NCH_2); 6.2 (s, NCH_2CH_3).

^{19}F NMR (*o*-$C_6H_4Cl_2$ 376 MHz) δ -132.8 (m, *o*-$(C_6F_5)_4$); -163.0 (t, $^{3}J_{FF}$ 20.4 Hz, *p*-$(C_6F_5)_4$); -166. (m, *m*-$(C_6F_5)_4$)

Mass Spec (ESI+) Expected for **5**$^{+}$: 215.2659. Found 215.2667 m/z

Accurate elemental analysis could not be obtained for this compound as in our hands solid sample were always contaminated with between 5-10 % of the ammonium salt.

Boroxine 6

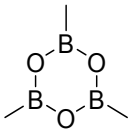

The ^{1}H NMR spectrum is referenced to the protio *o*-$C_6H_4Cl_2$, with the most up field peak at 7.154 ppm. A d_6-DMSO capillary is used to lock the signal. The ^{13}C NMR spectrum is referenced to the d_6-DMSO peak at 39.51 ppm. The signals corresponding to Ph_3CH and the anion $B(C_6F_5)_4$ are omitted.

^{1}H NMR (*o*-$C_6H_4Cl_2$ 400 MHz) δ 0.58 (BCH_3).

^{11}B NMR (*o*-$C_6H_4Cl_2$ 128 MHz) δ 32.0 (br, BCH_3)

^{13}C {^{1}H} NMR (*o*-$C_6H_4Cl_2$ 101 MHz) δ -2.0 (br, BCH_3)

4.2 Hunig's base borane H-bridged dimer

A J. Young's tube charged with the mixture containing H-bridged cation **8** (0.1mmol) and Ph_3CH in *o*-$C_6H_4Cl_2$ was subjected to three freeze pump thawed cycles before being back filled with CO at -78 °C. The J. Youngs NMR tube was continually inverted at 20 °C with NMR spectroscopy being recorded at regular intervals. After 24 h NMR spectroscopy indicated the formation of boroxine and the Hunig's base boronium salt 7.

Boronium Salt 7

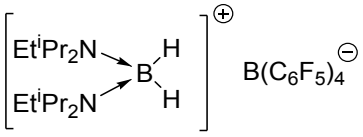

The signals corresponding to the anion $B(C_6F_5)_4$ are omitted.

^{1}H NMR (*o*-$C_6H_4Cl_2$ 400 MHz) δ 3.41 (sept, $^3J_{HH}$ 6.7 Hz, C*H*$(CH_3)_2$); 2.91 (q, $^3J_{HH}$ 7.2 Hz, CH_2); 1.56 (v. br, BH_2); 1.33 (d, $^3J_{HH}$ 6.6 Hz, CH(CH_3)$_2$, overlapping with broad feature); 1.25 (d, $^3J_{HH}$ 6.6 Hz, CH(CH_3)$_2$ overlapping with broad feature); 1.16 (t, $^3J_{HH}$ 7.2 Hz, CH_3).

^{11}B NMR (*o*-$C_6H_4Cl_2$ 128 MHz) δ -14.9 (br, *B*H_2) -17.2 (s, *B*$(C_6F_5)_4$)

^{13}C {^{1}H} NMR (*o*-$C_6H_4Cl_2$ 101 MHz) δ 55.7(*C*H$(CH_3)_2$); 46.4(CH_2); 16.9(CH(*C*H$_3$)$_2$); 16.5(CH(*C*H$_3$)$_2$); 8.3(*C*H$_3$).

^{19}F NMR (*o*-$C_6H_4Cl_2$ 376 MHz) δ -132.8 (m, *o*-$(C_6F_5)_4$); -163.2 (t, $^3J_{FF}$ 20.8 Hz, *p*-$(C_6F_5)_4$); -167.1 (m, *m*-$(C_6F_5)_4$)

Accurate elemental analysis could not be obtained for this compound as in our hands solid sample were always contaminated with between 5-10 % of the ammonium salt. Attempts to obtain mass spec were frustrated by decomposition of this compound.

Boroxine 6

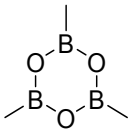

^{1}H NMR (*o*-$C_6H_4Cl_2$ 400 MHz) δ 0.59 (BC*H*$_3$).

^{11}B NMR (*o*-$C_6H_4Cl_2$ 128 MHz) δ 31.9 (br, *B*CH_3)

^{13}C {^{1}H} NMR (*o*-$C_6H_4Cl_2$ 101 MHz) δ -2.1 (br, B*C*H$_3$)

5. ^{13}CO Reactions

To facilitate reaction monitoring by ^{13}C NMR spectroscopy and obtain ^{13}C NMR spectra for the intermediate and final compounds the reactions were repeated under an atmosphere of ^{13}CO.

5.1 Synthesis of 3 under atmosphere of ^{13}CO

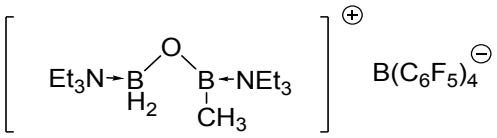

A J. Young's tube charged with the mixture containing the H-bridged cation **1** (0.1 mmol) and Ph_3CH in *o*-$C_6H_4Cl_2$ was subjected to three freeze pump thawed cycles before being back filled with ^{13}CO at -78 ^{o}C. The J. Youngs NMR tube was placed in a 60 ^{o}C oil bath and periodically removed to be inverted to facilitate mixing. After 18 h NMR spectroscopy showed the formation of one major new compound.

The sample was run in protio *o*-$C_6H_4Cl_2$ with a d_6-DMSO capillary. The ^{13}C NMR spectrum is referenced to the d_6-DMSO peak at 39.51 ppm. The signals corresponding to Ph_3CH and the anion $B(C_6F_5)_4$ are omitted. The ^{1}H and ^{11}B NMR spectra are comparable to that reported earlier.

$^{13}C\{^{1}H\}$ NMR (*o*-$C_6H_4Cl_2$ 101 MHz) δ 47.3 (s, N*C*H_2); 46.2 (s, N*C*H_2); 6.3 (s, NCH_2*C*H_3); 6.1 (s, NCH_2*C*H_3); -2.5 (br, B*C*H_3).

5.2 Synthesis of boroxine under atmosphere of ^{13}CO

A J. Young's tube charged with the mixture containing the H-bridged cation **1** (0.1 mmol) and Ph_3CH in *o*-$C_6H_4Cl_2$ was subjected to three freeze pump thawed cycles before being back filled with ^{13}CO at -78 ^{o}C. The J. Youngs NMR tube was placed in a 100 ^{o}C oil bath and periodically removed to be inverted to facilitate mixing. After 18 h NMR spectroscopy showed the formation of a new compound.

The sample was run in protio *o*-$C_6H_4Cl_2$ with a d_6-DMSO capillary. The ^{13}C NMR spectrum is referenced to the d_6-DMSO peak at 39.51 ppm. The signals corresponding to Ph_3CH and the anion $B(C_6F_5)_4$ are omitted.

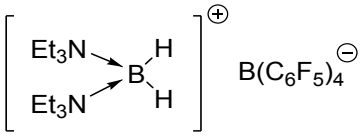

^{13}C {^{1}H} NMR (*o*-$C_6H_4Cl_2$ 101 MHz) δ 49.4 (s, N*C*H_2); 6.3 (s, NCH$_2$*C*H_3).

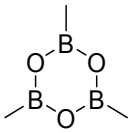

^{13}C {^{1}H} NMR (*o*-$C_6H_4Cl_2$ 101 MHz) δ -2.2 (br, B*C*H_3).

6. Independent formation of amine stabilised boronium salts

6.1 Triethylamine stabilised boronium

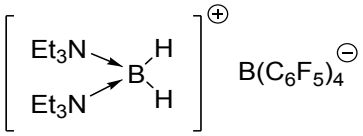

A J. Young's NMR tube was charged with a d_6-DMSO capillary and 0.6 ml of *o*-$C_6H_4Cl_2$. With subsequent addition of Et_3N (14 µl, 0.1 mmol) and Et_3N-BH_3 (15 µl, 0.1 mmol) and finally $Ph_3C^+[B(C_6F_5)_4]^-$ (92 mg, 0.1 mmol). On addition of $Ph_3C^+[B(C_6F_5)_4]^-$ the tube was immediately sealed with the fitted Teflon valve and inverted several times. A colour change of an initial yellow solution to purple on immediate addition of $Ph_3C^+[B(C_6F_5)_4]^-$ was shortly followed by formation of a pale yellow solution which was maintained. NMR spectroscopy showed the formation of Et_3N stabilised boronium with NMR spectra that closely matched that from reaction **4.1**.

^{1}H NMR (*o*-$C_6H_4Cl_2$ 400 MHz) δ 2.74 (q, $^3J_{HH}$ 7.1 Hz, C*H*$_2$); 1.80 (br, B*H*$_2$); 1.11 (t, $^3J_{HH}$ 7.2 Hz, C*H*$_3$).

^{11}B NMR (*o*-$C_6H_4Cl_2$ 128 MHz) δ -6.4 (br, *B*H$_2$) -17.2 (s, *B*$(C_6F_5)_4$)

^{13}C {^{1}H} NMR (*o*-$C_6H_4Cl_2$ 101 MHz) for the cation only: δ 49.4 (s, N*C*H$_2$); 6.2 (s, NCH$_2$*C*H$_3$).

^{19}F NMR (*o*-$C_6H_4Cl_2$ 376 MHz) δ -132.7 (m, *o*-$(C_6F_5)_4$); -163.2 (t, $^3J_{FF}$ 20.4 Hz, *p*-$(C_6F_5)_4$); -167.1 (m, *m*-$(C_6F_5)_4$)

Mass Spec (ESI+) Expected for **5**$^+$: 215.2659. Found 215.2667 m/z

6.2 Hunig's base stabilised boronium

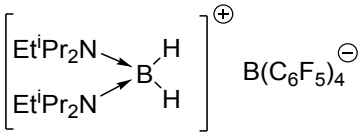

A J. Young's NMR tube was charged with a d_6-DMSO capillary and 0.6 ml of *o*-$C_6H_4Cl_2$. With subsequent addition of Hunig's base (17.5 µl, 0.1 mmol) and amine borane (17.5 µl, 0.1 mmol) and $Ph_3C^+[B(C_6F_5)_4]^-$ (92 mg, 0.1 mmol). On addition of $Ph_3C^+[B(C_6F_5)_4]^-$ the tube was immediately sealed with the fitted Teflon valve and inverted several times. A colour change of an initial yellow solution to purple on addition of $Ph_3C^+[B(C_6F_5)_4]^-$ was shortly followed to a pale yellow solution which was maintained. NMR spectrscopy showed the formation of Et(iPr)$_2$N stabilised boronium with NMR spectra that closely matched that from reaction **4.2**.

The ^{1}H NMR spectrum is referenced to the protio *o*-$C_6H_4Cl_2$, with the most up field peak at 7.154 ppm. A d_6-DMSO capillary is used to lock the signal. The signals corresponding to Ph_3CH are omitted.

^{1}H NMR (*o*-$C_6H_4Cl_2$ 400 MHz) δ 3.44 (sept, $^3J_{HH}$ 6.7 Hz, C*H*$(CH_3)_2$); 2.92 (q, $^3J_{HH}$ 7.2 Hz, C*H*$_2$); 1.67 (br, B*H*$_2$); 1.36 (d, $^3J_{HH}$ 6.6 Hz, CH(C*H*$_3$)$_2$, overlapping with broad feature); 1.28 (d, $^3J_{HH}$ 6.6 Hz, CH(C*H*$_3$)$_2$ overlapping with broad feature); 1.18 (t, $^3J_{HH}$ 7.2 Hz, C*H*$_3$ overlapping with broad feature).

^{11}B NMR (*o*-$C_6H_4Cl_2$ 128 MHz) δ -14.7 (br, *B*H_2); -17.2 (s, *B*$(C_6F_5)_4$).

^{13}C {^{1}H} NMR (*o*-$C_6H_4Cl_2$ 101 MHz) for the cation only: δ 55.5(*C*H$(CH_3)_2$); 46.3(CH_2); 16.9(CH(*C*$H_3)_2$); 16.5(CH(*C*$H_3)_2$); 8.3(*C*H_3).

^{19}F NMR (*o*-$C_6H_4Cl_2$ 376 MHz) δ -132.7 (m, *o*-$(C_6F_5)_4$); -163.2 (t, $^3J_{FF}$ 20.4 Hz, *p*-$(C_6F_5)_4$); -166.1 (m, *m*-$(C_6F_5)_4$)

(Et^{i}Pr$_2$N)BH$_3$

For comparison the data for the starting material (Et^{i}Pr$_2$N)BH_3 ran in identical solvent is provided below:

The ^{1}H NMR spectrum is referenced to the protio *o*-$C_6H_4Cl_2$, with the most up field peak at 7.154 ppm. A d_6-DMSO capillary is used to lock the signal.

^{1}H NMR (*o*-$C_6H_4Cl_2$ 400 MHz) δ 3.51 (2H sept, $^3J_{HH}$ 7.2 Hz, C*H*$(CH_3)_2$); 2.98 (2H quartet, $^3J_{HH}$ 7.2 Hz, C*H*$_2$); 2.06 (2H s, B*H*$_2$); 1.42 (6H d, $^3J_{HH}$ 6.6 Hz, CH(C*H*$_3)_2$); 1.31 (6H d, $^3J_{HH}$ 6.6 Hz, CH(C*H*$_3)_2$); 1.22 (3H t, $^3J_{HH}$ 6.6 Hz, C*H*$_3$ overlapping with broad feature).

^{11}B{^{1}H} NMR (*o*-$C_6H_4Cl_2$ 128 MHz) δ -13.4 (br, *B*H_3);

^{11}B NMR (*o*-$C_6H_4Cl_2$ 128 MHz) δ -13.4 (quartet, $^1J_{B\text{-}H}$ = 98 Hz, *B*H_3);

7. Independent Boroxine Reference

To confirm the presence of boroxine in the reaction, boroxine was dissolved and 0.6 ml of *o*-$C_6H_4Cl_2$ and charged with a d_6-DMSO capillary.

^{1}H NMR (*o*-$C_6H_4Cl_2$ 400 MHz) δ 0.58(BC*H*$_3$).

^{11}B NMR (*o*-$C_6H_4Cl_2$ 128 MHz) δ 32.4 (*B*CH_3).

^{13}C {^{1}H} NMR (*o*-$C_6H_4Cl_2$ 101 MHz) δ-1.7(B*C*H_3).

8. VT NMR Spectroscopy

A J. Young's tube was charged with $Ph_3C^+[B(C_6F_5)_4]^-$ (46 mg, 0.05 mmol) in 0.6 ml CD_2Cl_2. This was followed by the subsequent addition of triethylamine borane (15 µl, 0.1 mmol). On addition of amine borane the tube was immediately sealed with the fitted Teflon valve and inverted for 10 min. The addition of amine borane leads to a colour change from a yellow to a colourless solution. NMR assay shortly following the observation of the colour change indicated formation of the H-bridged cation **1** and Ph_3CH. The J. Young's tube was subjected to three freeze pump thaw cycles before being back filled with CO at -78 ^oC. After one hour ^1H, ^1H $\{^{11}B\}$, ^{11}B, ^{11}B $\{^1H\}$ NMR spectra were recorded at -78 ^oC. The reaction was warmed to 20 ^oC and monitored by NMR spectroscopy, which showed the formation of the O-bridged cation **3** (ca 25 %) after 24 hours at 20 ^oC, but no intermediates in the reduction process were observed.

9. Reactions with silanes

To a J. Young's tube charged with the H-bridged cation **1** (0.1 mmol) in *o*-$C_6H_4Cl_2$ was added Et_3SiH (48 µl, 0.3 mmol) before being subjected to three freeze pump thaw cycles before being back filled with ^{13}CO at -78 ^oC. The J. Youngs NMR tube was placed in a 60 ^oC oil bath and periodically removed to be inverted to facilitate mixing. After 18 h NMR spectroscopy showed the formation of **3** (o-bridged cation) and the presence of unreacted silane.

10. Reactions Catalytic in Trityl Salt- Addition of Excess Hunig's base borane

According to the general procedure 1, a J. Young's NMR tube was charged with $Ph_3C^+[B(C_6F_5)_4]^-$ (46 mg, 0.05 mmol) and dissolved in 0.6 ml *o*-$C_6H_4Cl_2$ before addition of Et^iPr_2N-BH_3 (17.5 µl, 0.1 mmol). This generated **8**, which was subjected to three freeze pump thaw cycles before being back filled with CO at -78 ^oC. The J. Young's NMR tube was left to invert at 20 ^oC with NMR spectroscopy being recorded at regular intervals. After 24 h NMR spectroscopy indicated the formation of boroxine and Hunig's base boronium. To this reaction mixture was added excess Hunig's base borane (51 µl, 0.3 mmol). The J. Young's NMR tube was placed in a 60 ^oC oil bath and inverted at regular intervals. There was no observed increase in the formation of boroxine via NMR spectroscopy. On heating 100 ^oC unidentified decomposition products were observed by ^{11}B NMR spectroscopy.

11. Reactions with $B(C_6F_5)_3$

11.1 Triethylamine Borane Activation with $B(C_6F_5)_3$

A J. Young's tube was charged with a d_6-DMSO capillary and $B(C_6F_5)_3$ (0.26 mg, 0.05 mmol). This was dissolved in 0.6 ml of *o*-$C_6H_4Cl_2$ with subsequent addition of triethylamine borane (15 µl, 0.1 mmol). On addition of amine borane the tube was immediately sealed with the fitted Teflon valve and inverted for 10 min. NMR analysis indicated formation of the H-bridged cation.

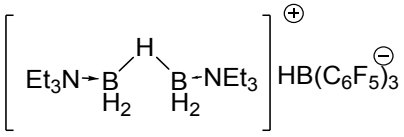

^{1}H NMR (*o*-$C_6H_4Cl_2$ 400 MHz) δ 4.47 (br, *H*B$(C_6F_5)_3$) 2.73 (q, $^3J_{HH}$ 7.2 Hz, C*H*$_2$); 2.56 (br, B*H*$_2$); 1.11 (t, $^3J_{HH}$ 7.2 Hz, C*H*$_3$); -2.79 (br, B-*H*-B).

^{11}B NMR (*o*-$C_6H_4Cl_2$ 128 MHz) δ -3.9 (br, *B*H$_2$) -25.5 (d, $^1J_{HB}$ 84.1 Hz, H*B*$(C_6F_5)_3$)

^{19}F NMR (*o*-$C_6H_4Cl_2$ 376 MHz) δ -133.3 (m, *o*-$(C_6F_5)_3$); -164.4 (t, $^3J_{FF}$ 20.4 Hz, *p*-$(C_6F_5)_3$); -167.3 (m, *m*-$(C_6F_5)_3$)

11.2 H-Bridged Dimer reactions with CO

To a J. Young's tube charged with the H-bridged cation (0.1 mmol) as the $[HB(C_6F_5)_3]$ salt in *o*-$C_6H_4Cl_2$ was subjected to three freeze pump thaw cycles before being back filled with CO at -78 °C. The J. Youngs NMR tube was placed in a 100 °C oil bath and inverted on regular intervals. NMR spectroscopy showed the formation of a new compound. The ^{11}B and ^{19}F spectra were not consistent with the retention of the anion $HB(C_6F_5)_3$ with signals present at 33.4 ppm and -15.0 ppm in the ^{11}B spectrum and -128.6, -158.9, -164.7 ppm in the ^{19}F spectrum. These signals were consistent with the previously reported ligand scrambling products $H_2B(C_6F_5)$ and $(Et_3N)BH_2(C_6F_5)$.[2] The reaction was repeated but in the absence of CO. After heating to 100 °C for 18 h there were signals present in the ^{11}B and ^{19}F spectra consistent with those previously seen at 34 and -15.0 ppm and -128, -158 and -164 ppm in the ^{11}B and ^{19}F spectra respectively, indicating there was no reactivity with CO.

12. NMR Spectra

12.1

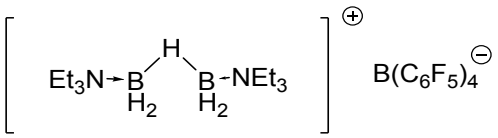

^{1}H NMR Spectrum: $Et_3N\text{-}BH_3$ activation with $Ph_3C^{+}[B(C_6F_5)_4]^{-}$

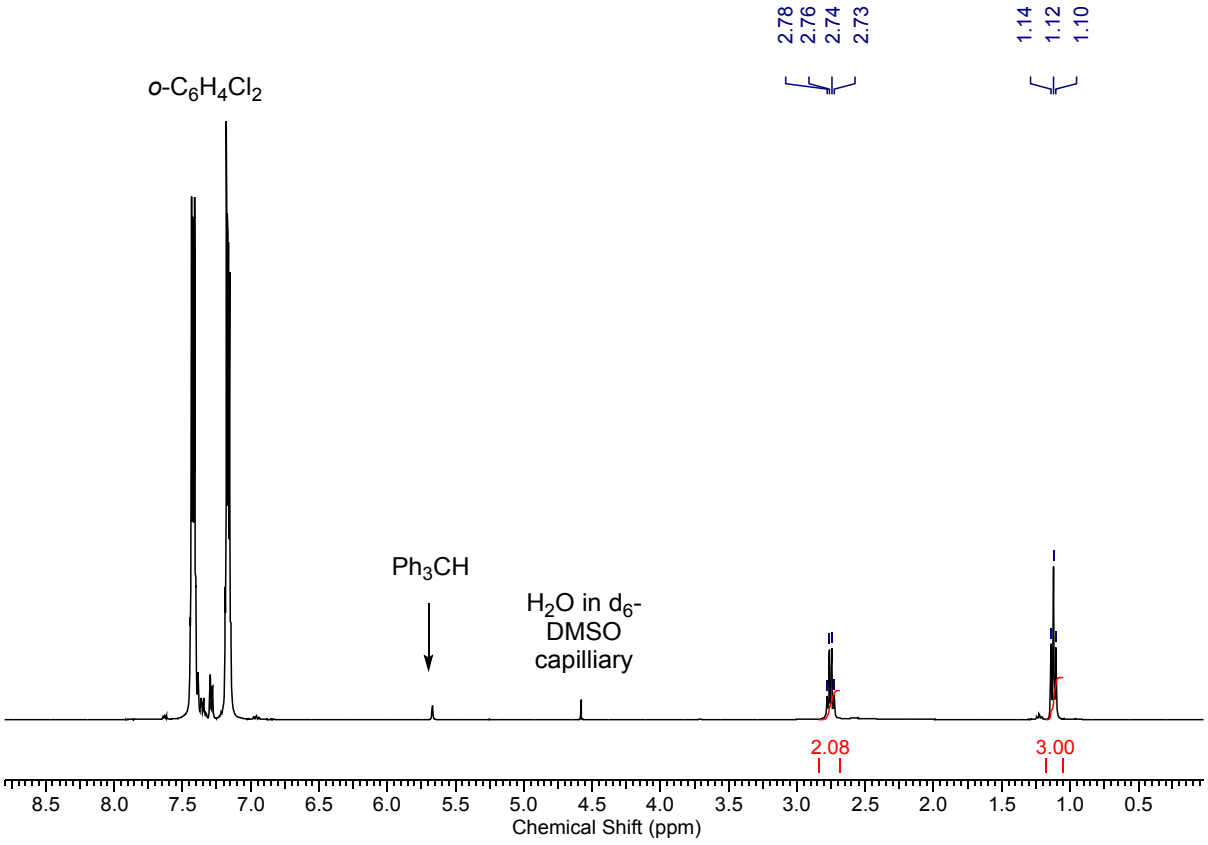

^{1}H {^{11}B} NMR Spectrum: Et_3N-BH_3 activation with $Ph_3C^+[B(C_6F_5)_4]^-$

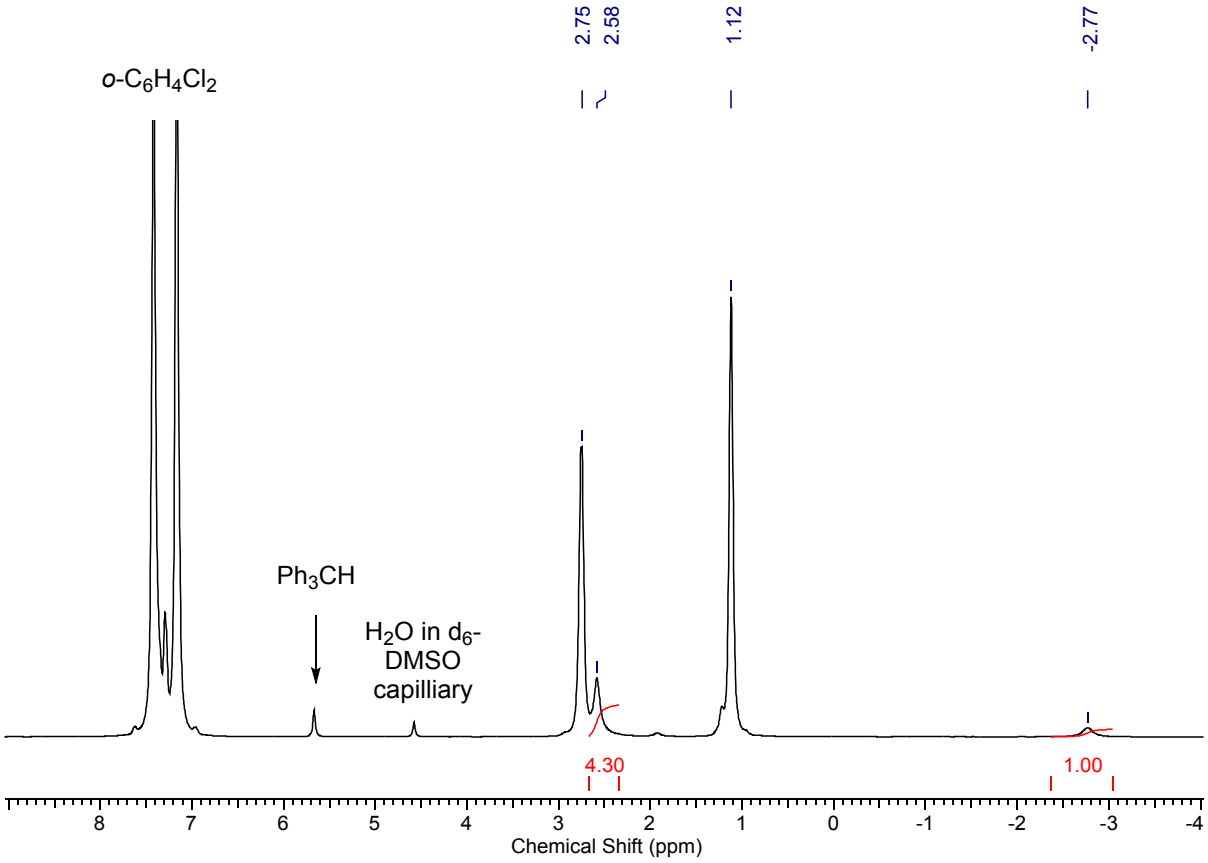

^{11}B NMR Spectrum: Et_3N-BH_3 activation with $Ph_3C^+[B(C_6F_5)_4]^-$

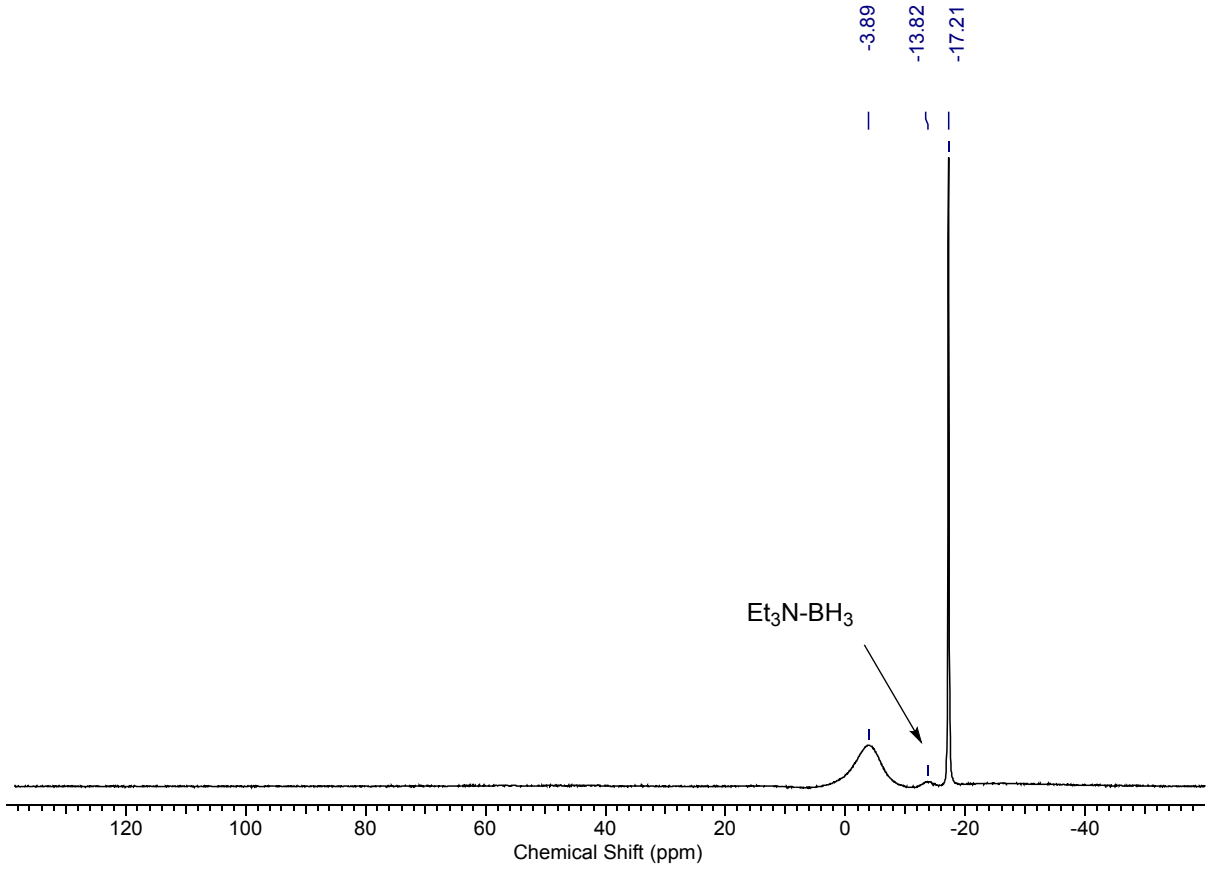

^{11}B {^{1}H} NMR Spectrum: Et_3N-BH_3 activation with $Ph_3C^+[B(C_6F_5)_4]^-$

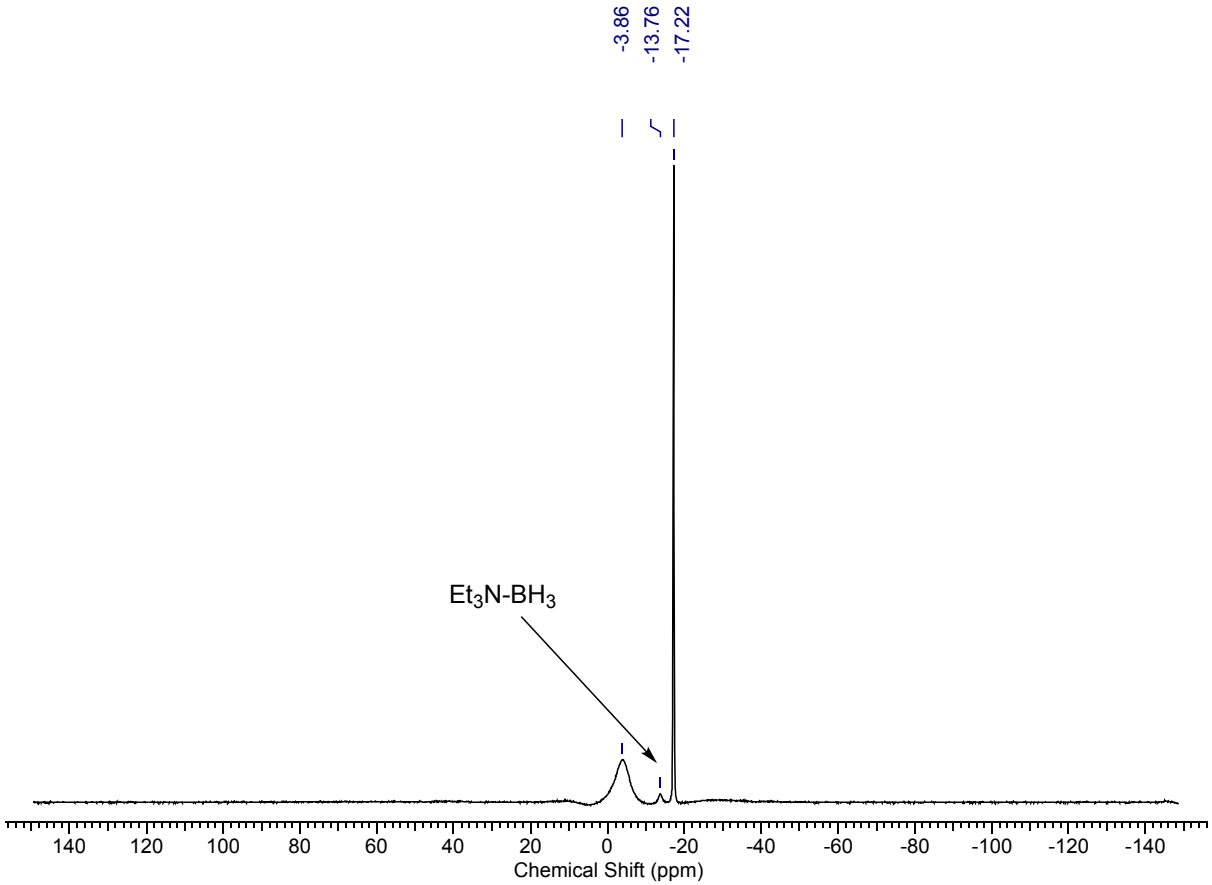

^{19}F {^{1}H} NMR Spectrum: Et_3N-BH_3 activation with $Ph_3C^+[B(C_6F_5)_4]^-$

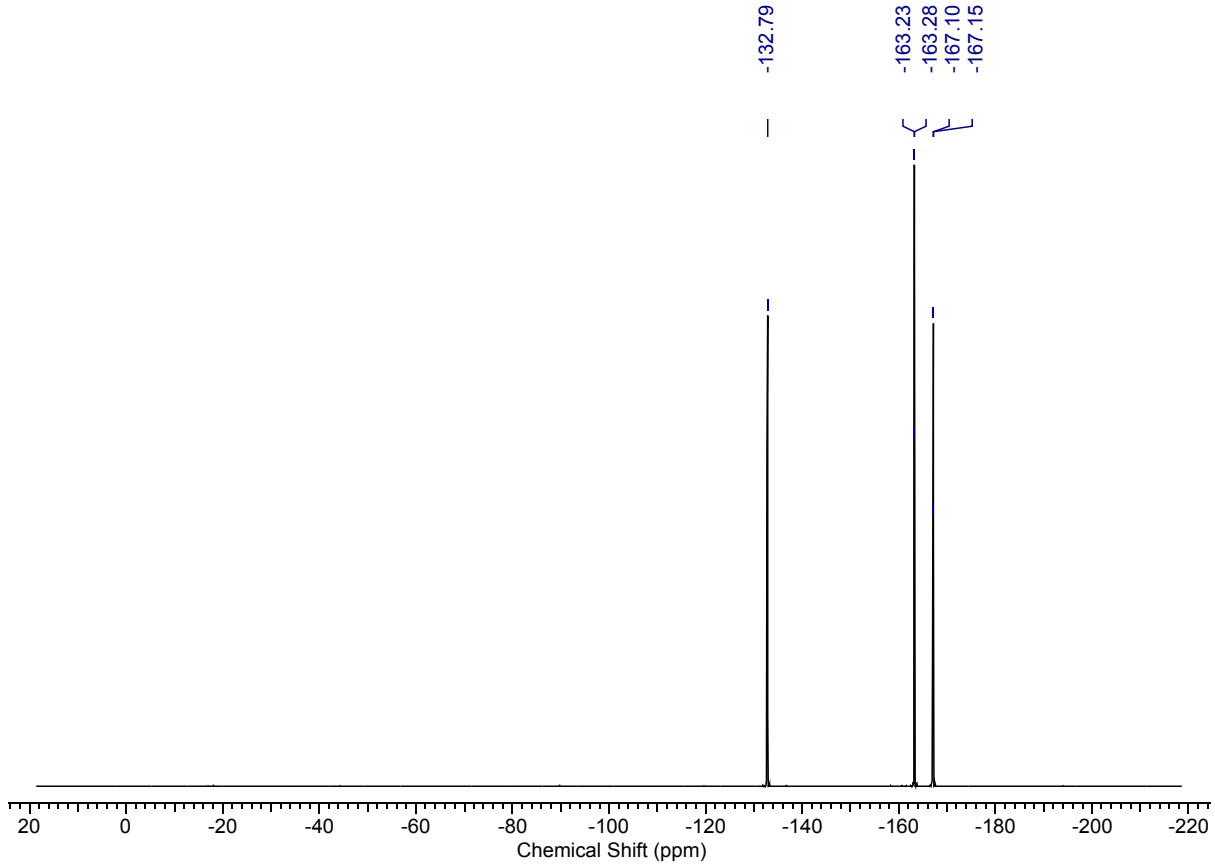

12.2

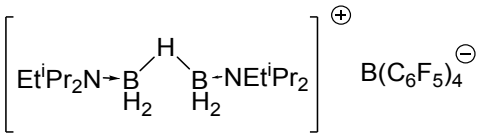

^{1}H NMR Spectrum: Et^{i}Pr$_2$N-BH$_3$ activation with Ph$_3$C$^+$[B(C$_6$F$_5$)$_4$]$^-$

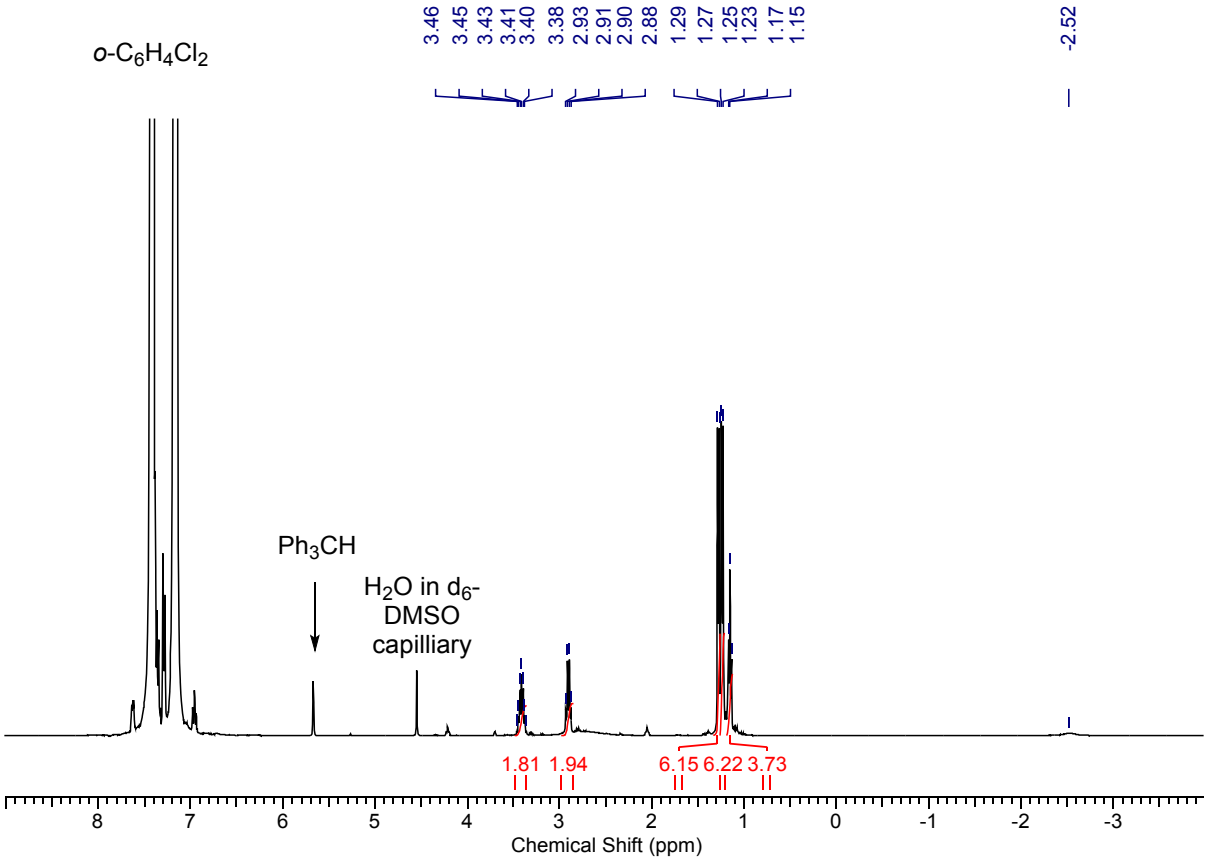

^{1}H {^{11}B} NMR Spectrum: $Et^{i}Pr_2N$-BH_3 activation with $Ph_3C^{+}[B(C_6F_5)_4]^{-}$

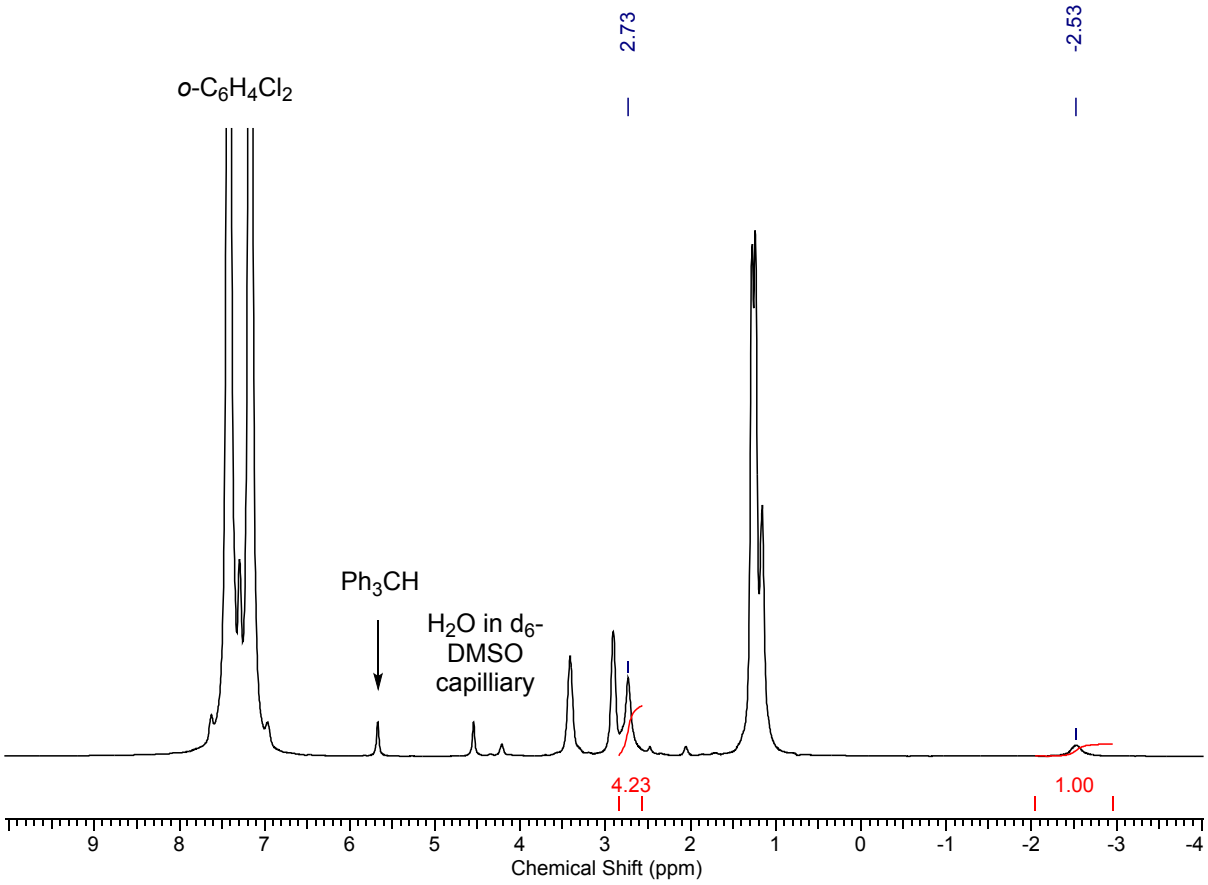

^{11}B NMR Spectrum: $Et^{i}Pr_2N\text{-}BH_3$ activation with $Ph_3C^{+}[B(C_6F_5)_4]^{-}$

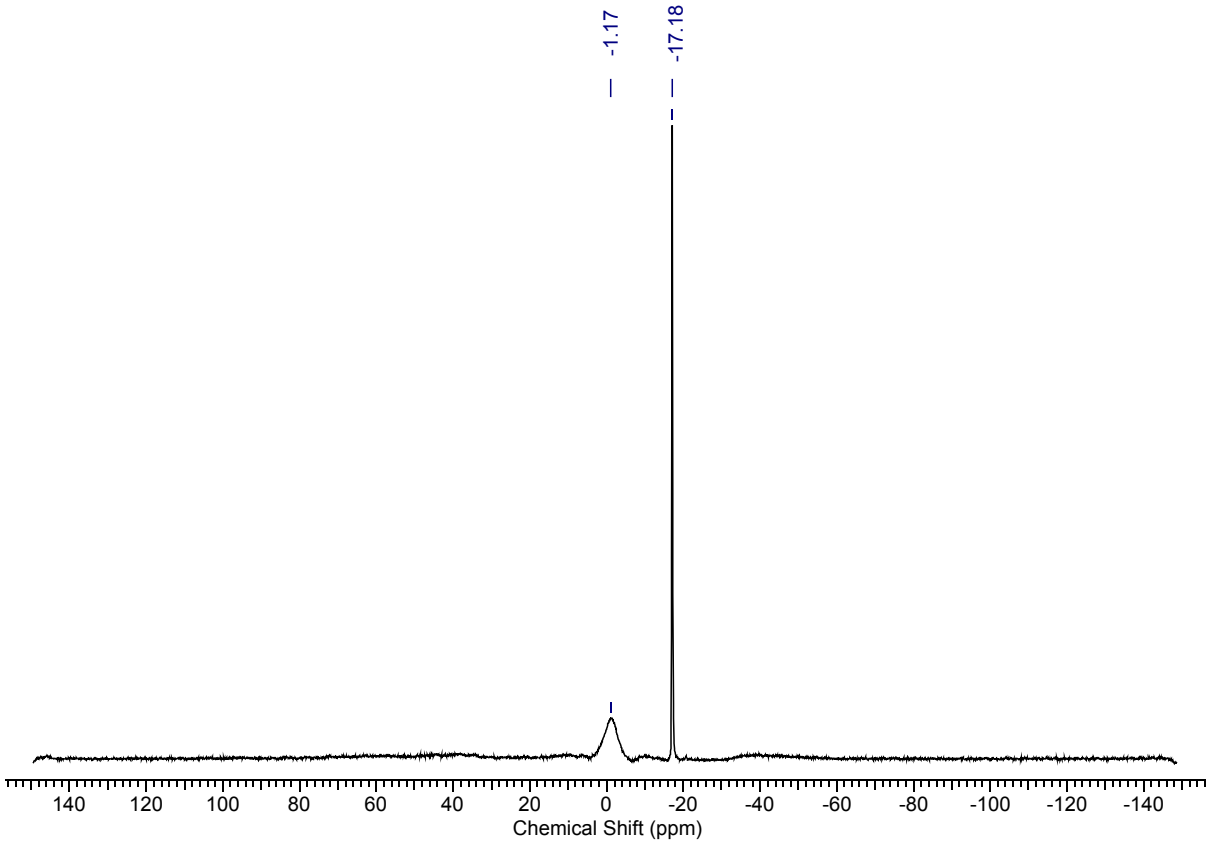

^{11}B {^{1}H} NMR Spectrum: $Et^{i}Pr_2N\text{-}BH_3$ activation with $Ph_3C^{+}[B(C_6F_5)_4]^{-}$

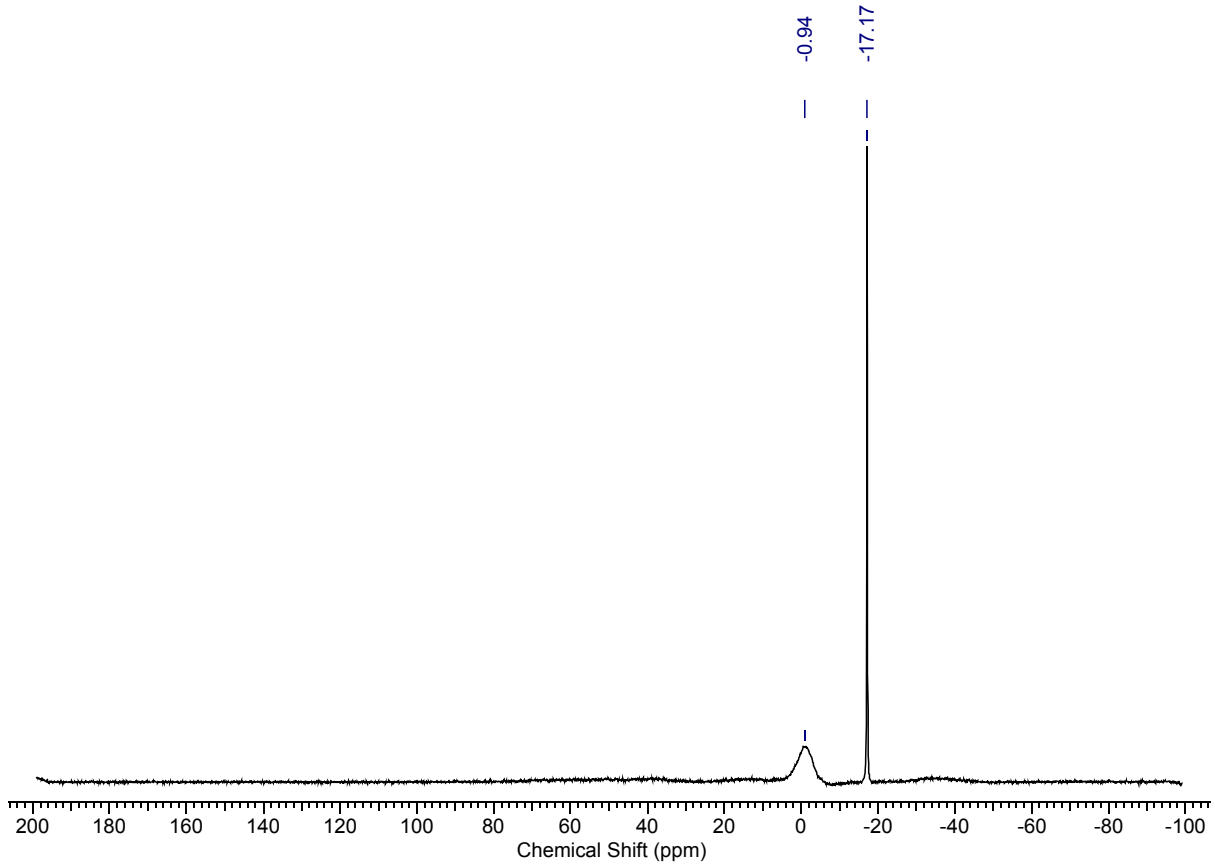

^{19}F {^{1}H} NMR Spectrum: $Et^{i}Pr_2N\text{-}BH_3$ activation with $Ph_3C^{+}[B(C_6F_5)_4]^{-}$

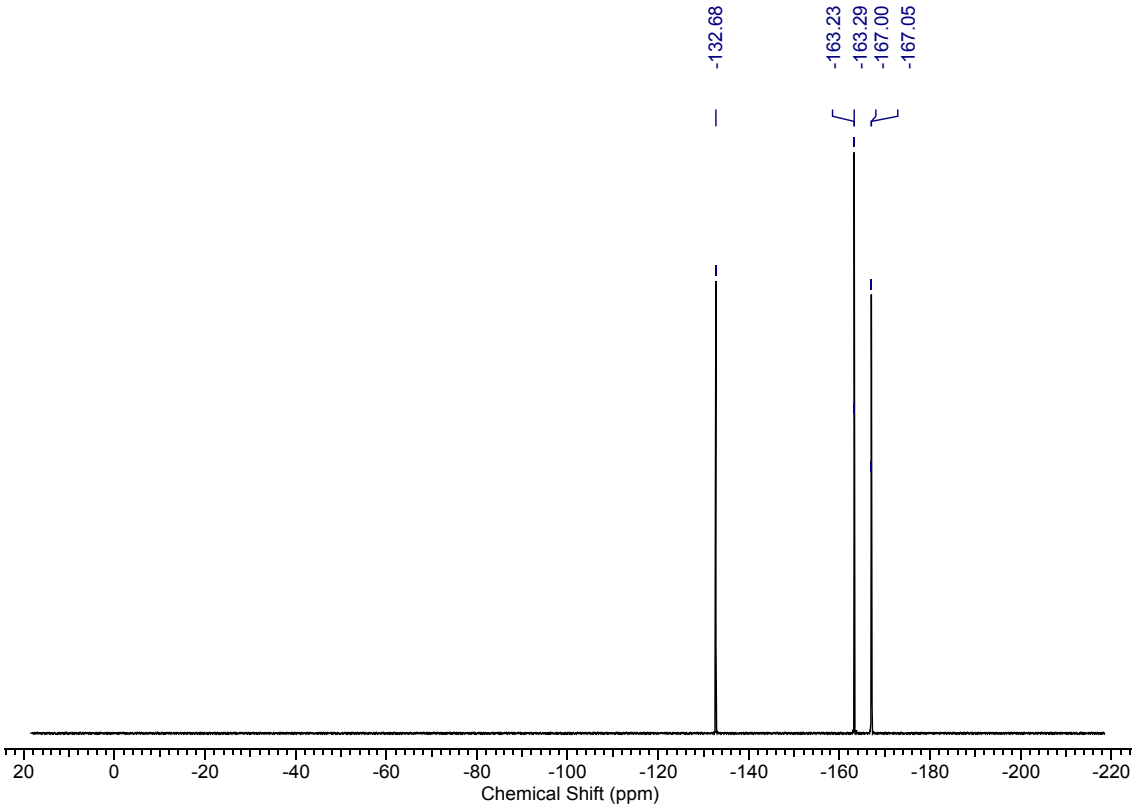

12.3

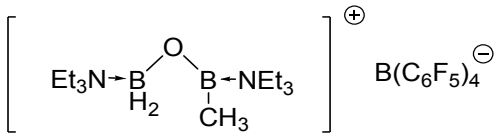

In-situ ^{1}H NMR Spectrum: O-Bridged borocation

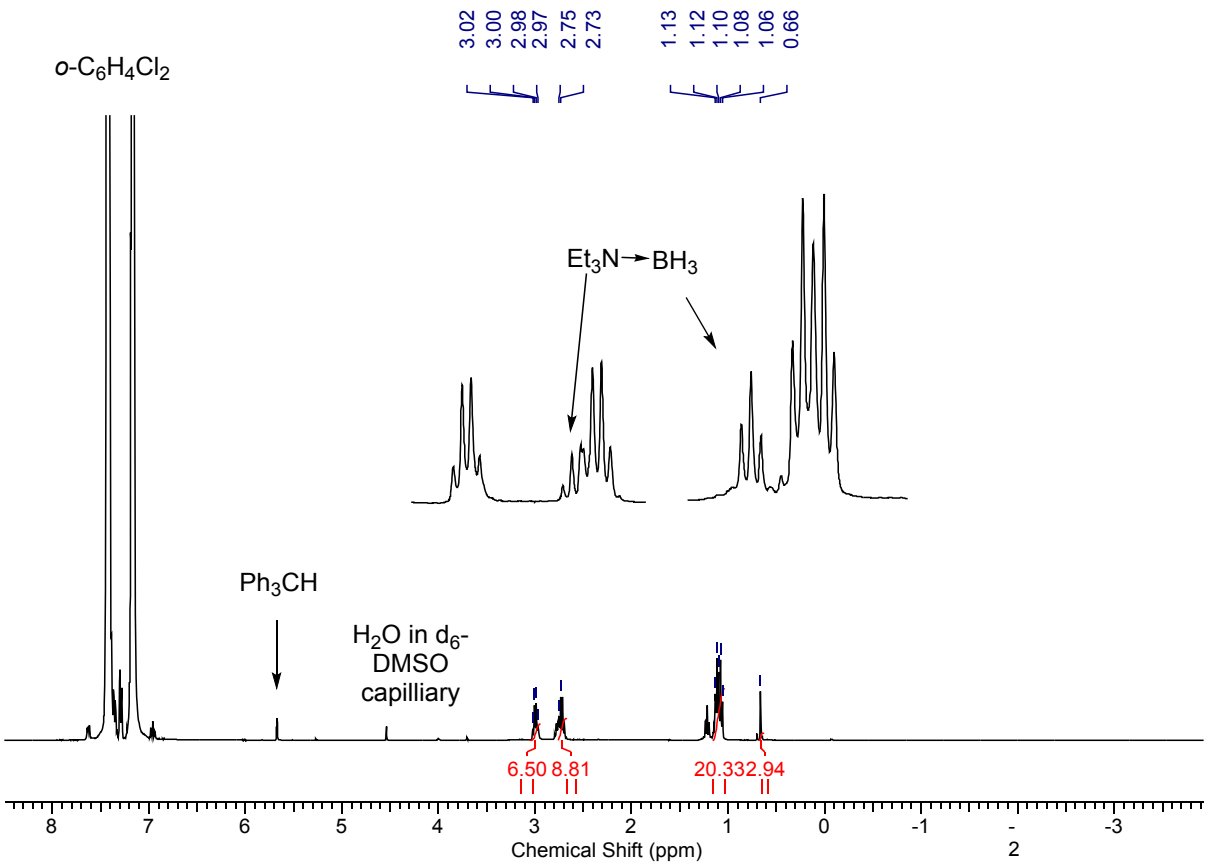

^{1}H {^{11}B} NMR Spectrum: O-Bridged borocation

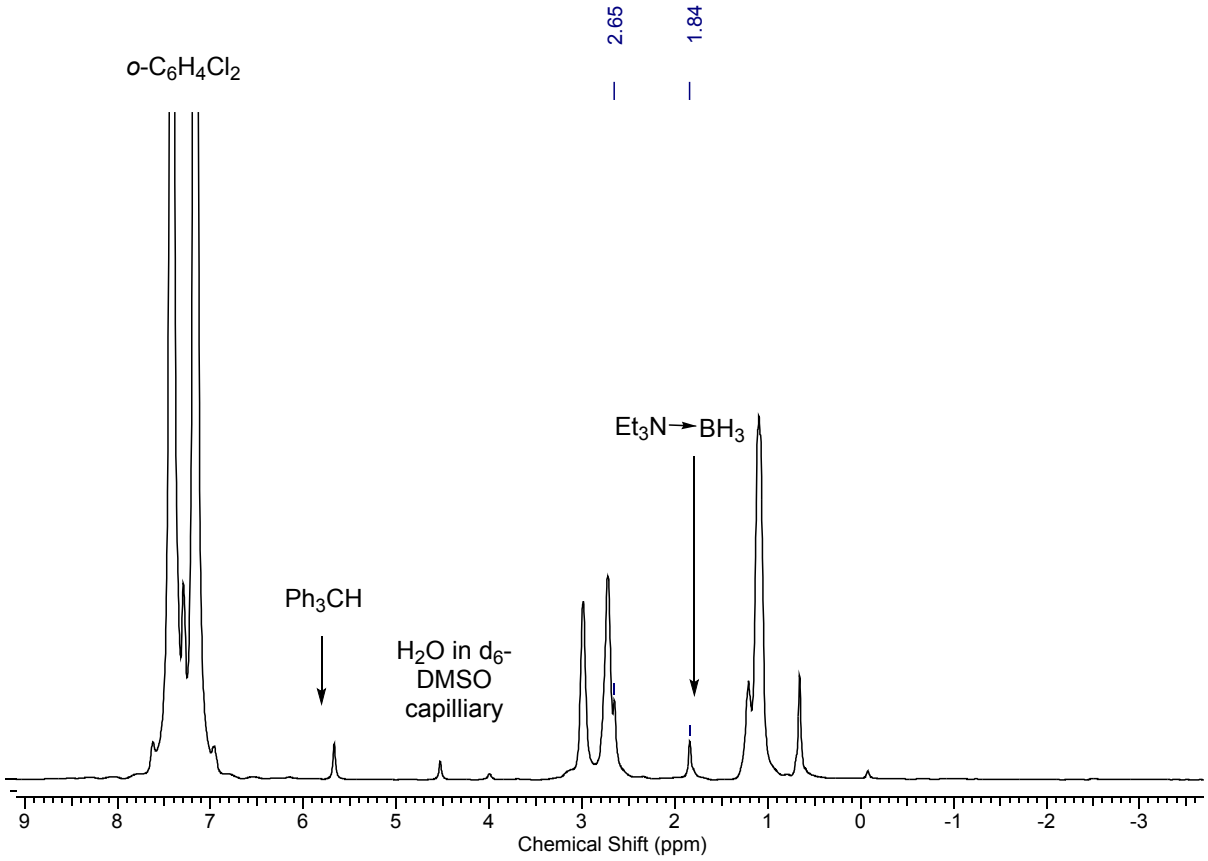

^{11}B NMR Spectrum: O-Bridged borocation

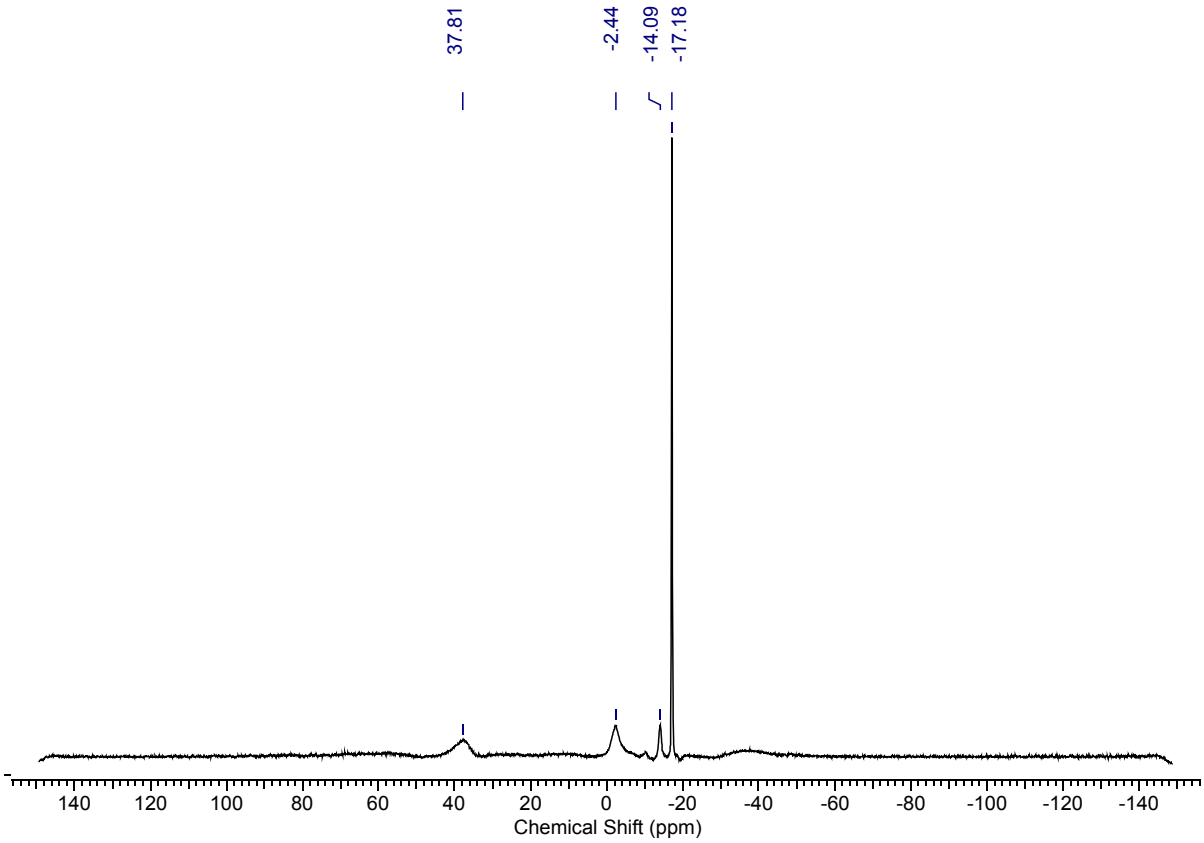

^{11}B {^{1}H} NMR Spectrum: O-Bridged borocation

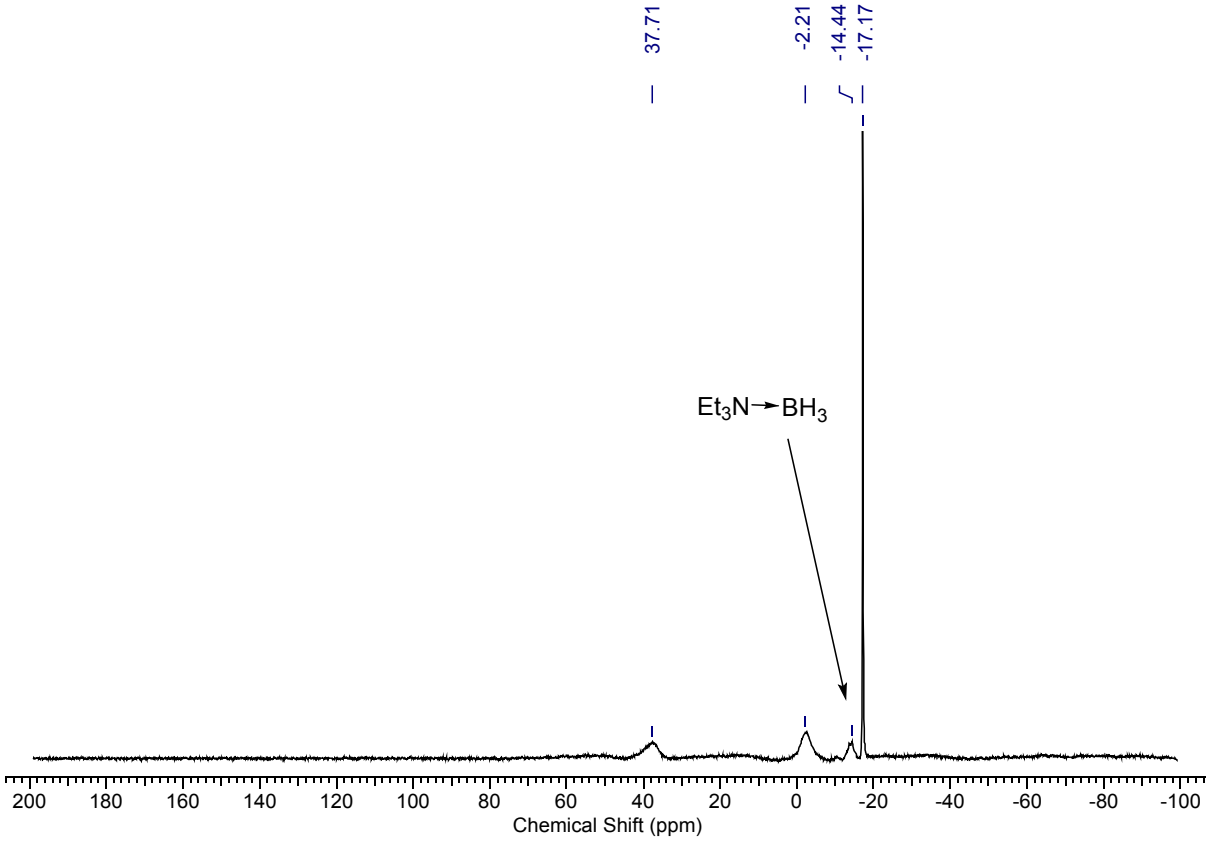

^{19}F {^{1}H} NMR Spectrum: O-Bridged borocation

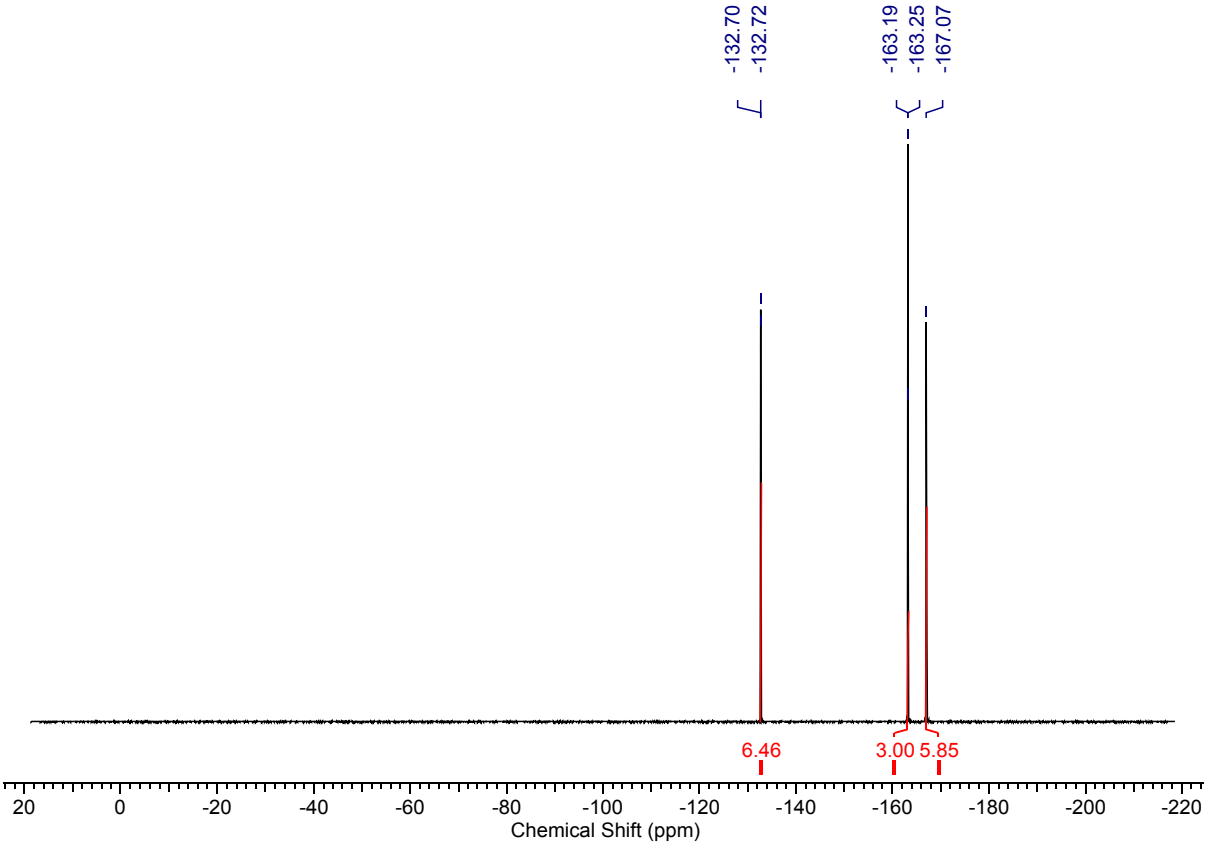

12.4

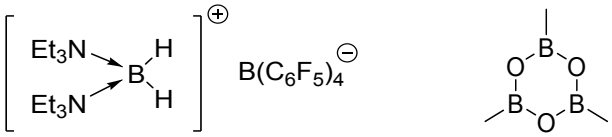

^{1}H NMR Spectrum: In situ NMR of boroxine formation and NEt_3 boronium

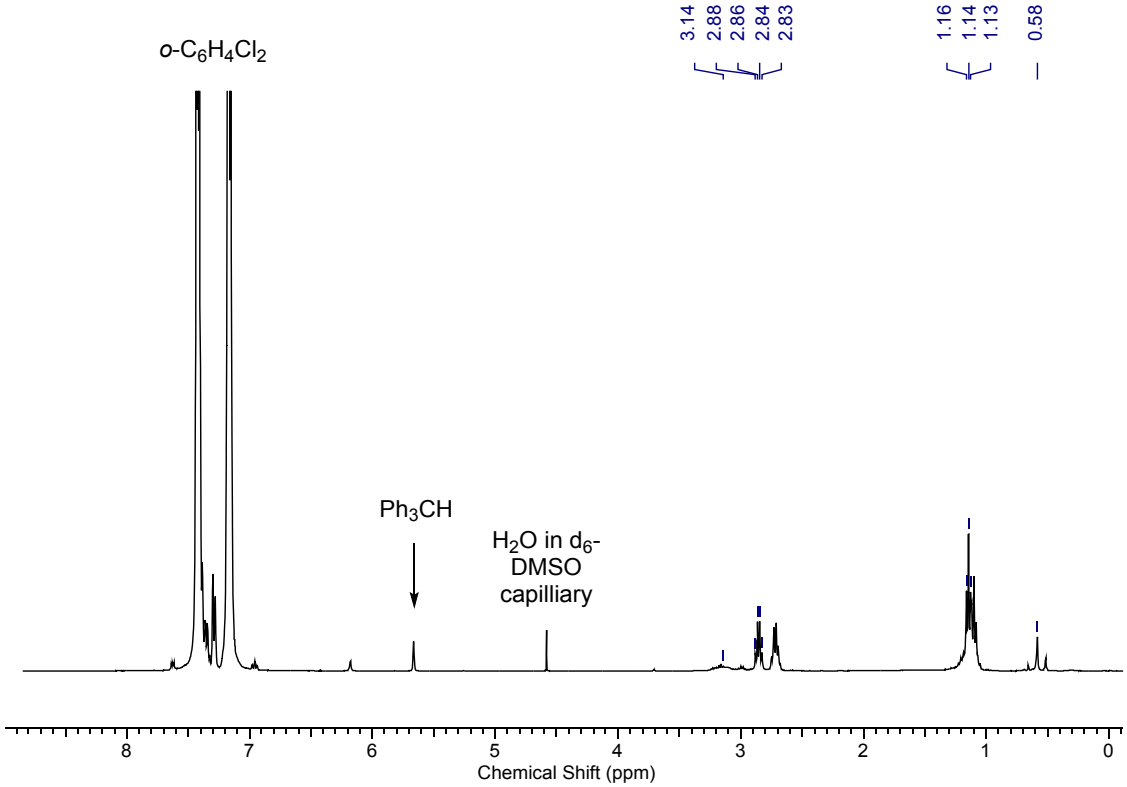

Minor unidentified products are also observed, e.g., Et_3N derived species at 3.14 ppm.

^{1}H {^{11}B} NMR Spectrum: In situ NMR of boroxine formation and NEt_3 boronium

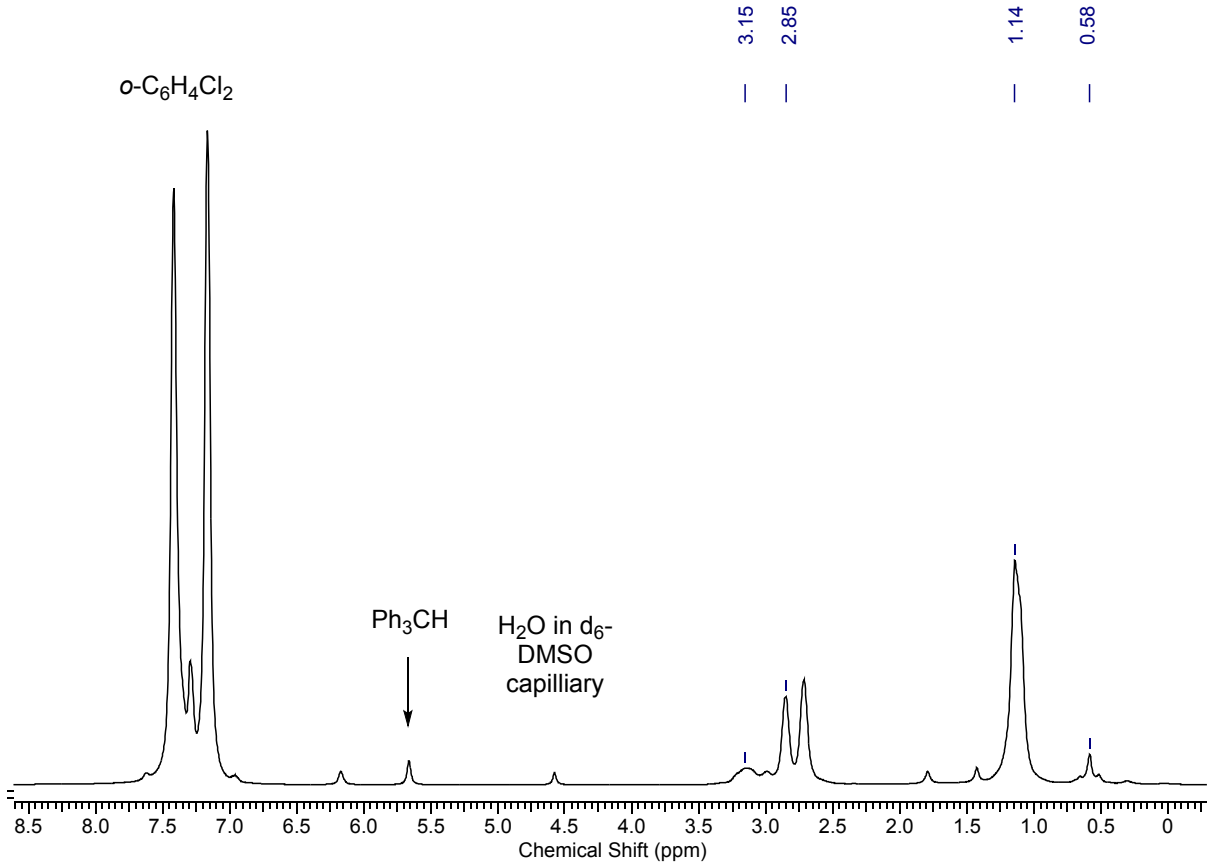

^{11}B NMR Spectrum: In situ NMR of boroxine formation and NEt_3 boronium

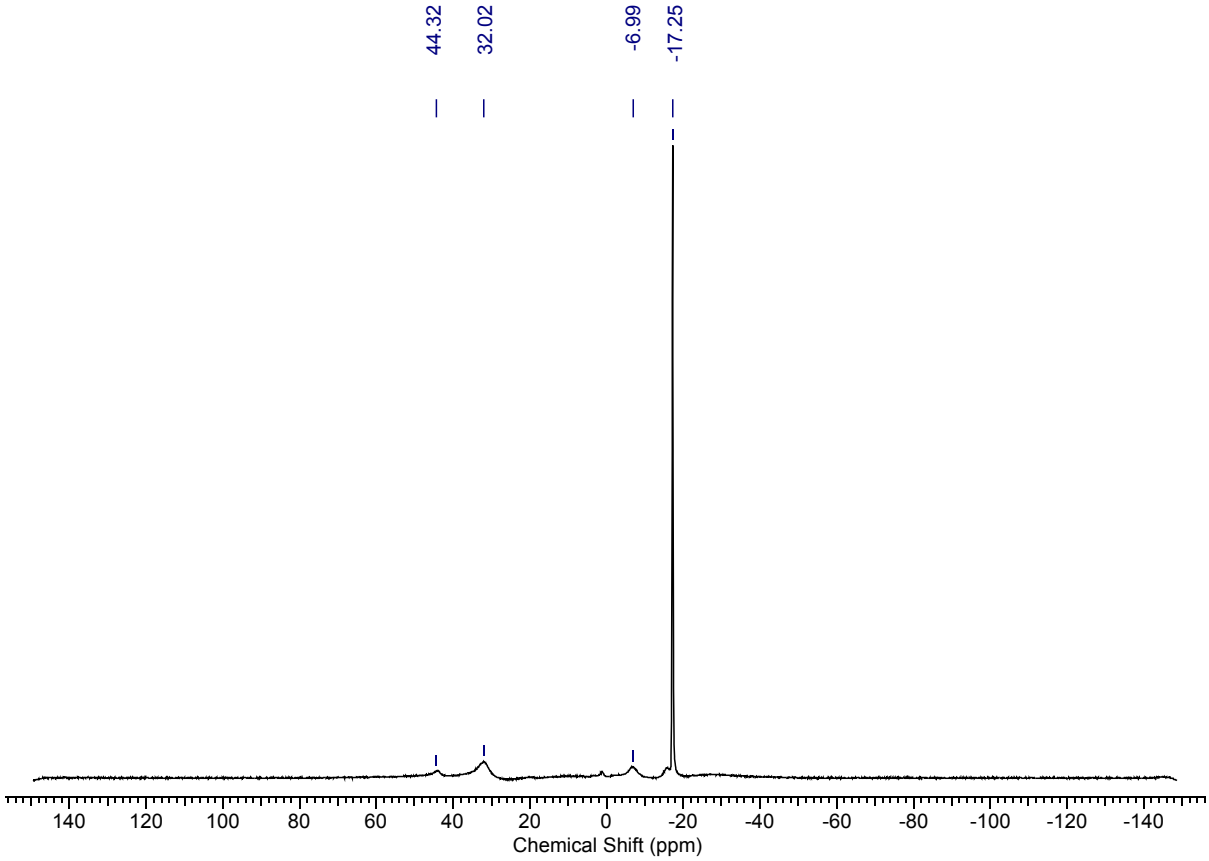

^{11}B {^{1}H} NMR Spectrum: In situ NMR of boroxine formation and NEt_3 boronium

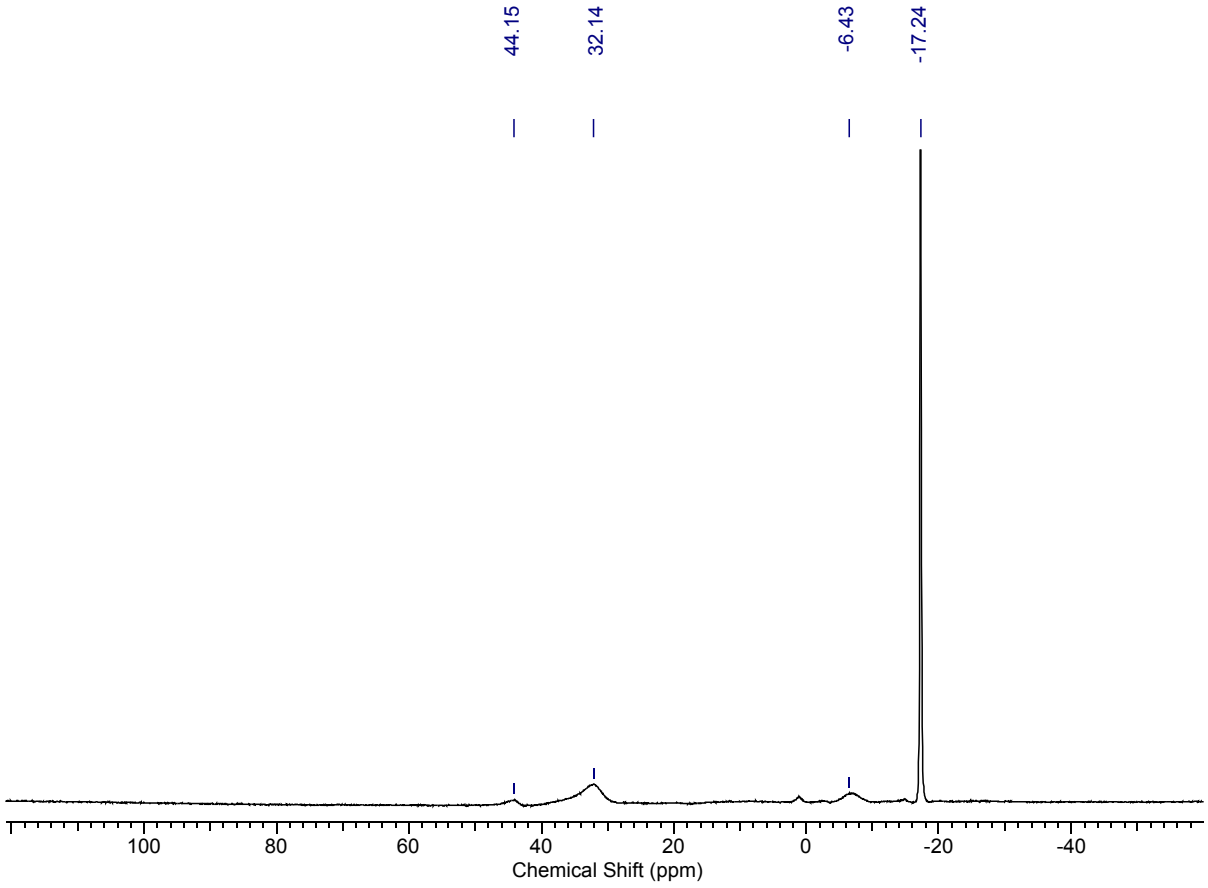

^{13}C {^{1}H} NMR spectrum: In situ NMR of boroxine formation and NEt_3 boronium

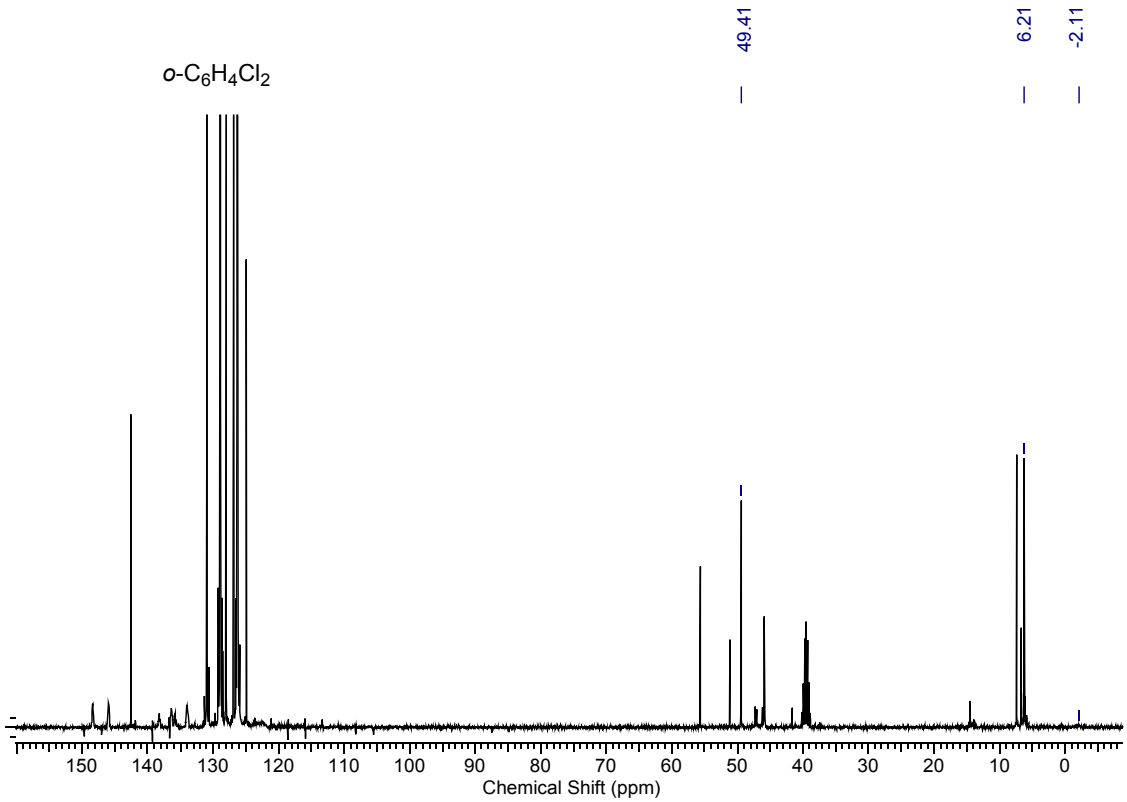

^{19}F {^{1}H} NMR Spectrum: In situ NMR of boroxine formation and NEt_3 boronium

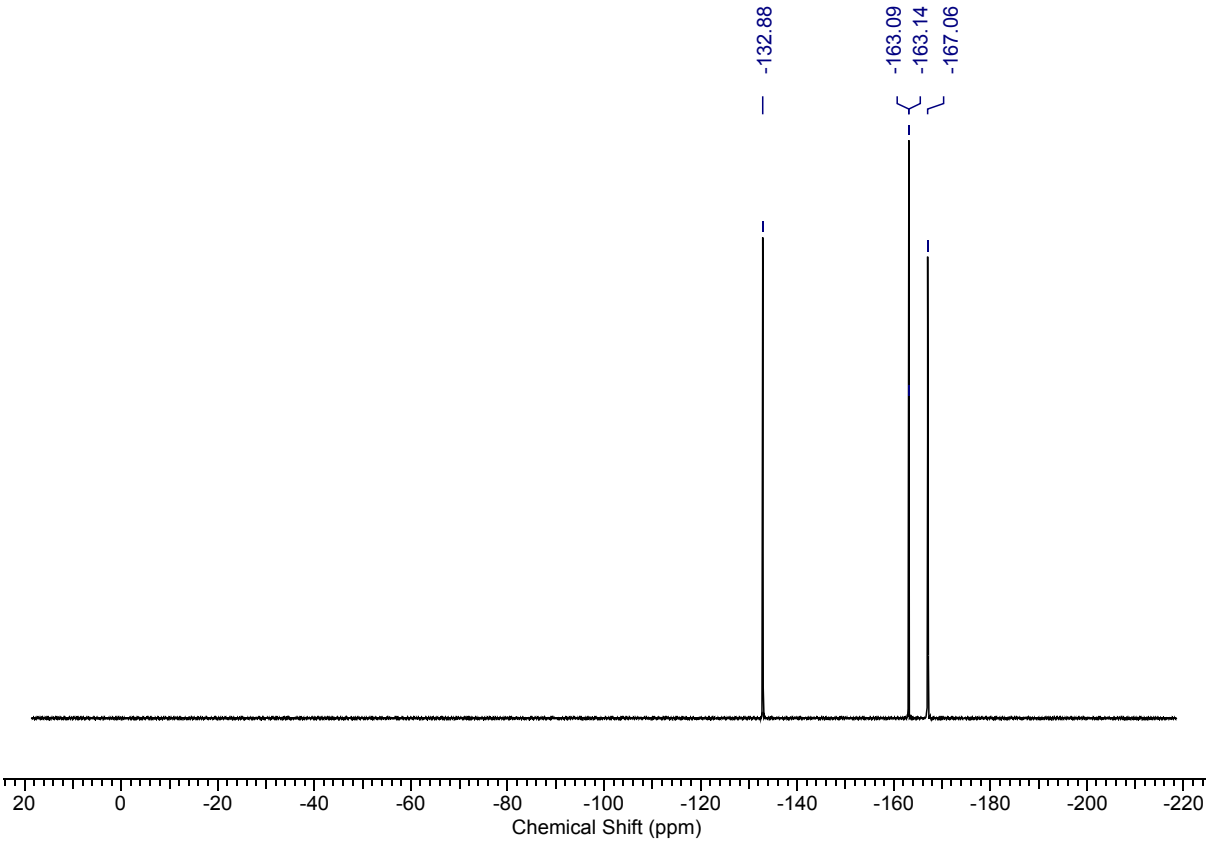

12.5

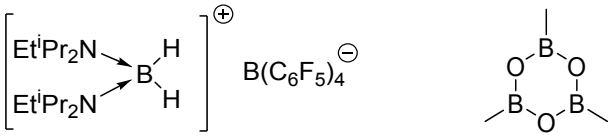

^{1}H NMR Spectrum: In situ NMR of boroxine formation and Hunig's Base boronium

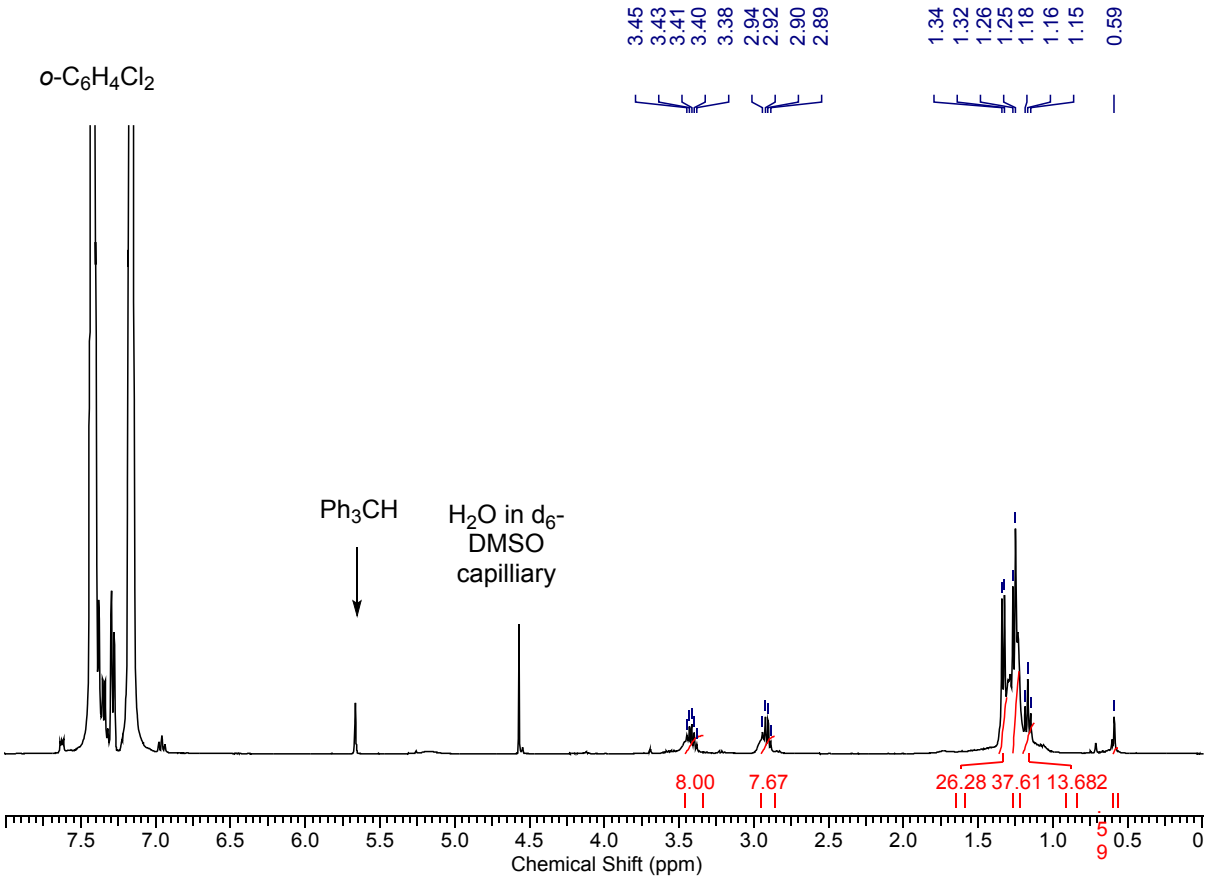

^{1}H {^{11}B} NMR Spectrum: In situ NMR of boroxine formation and Hunig's Base boronium

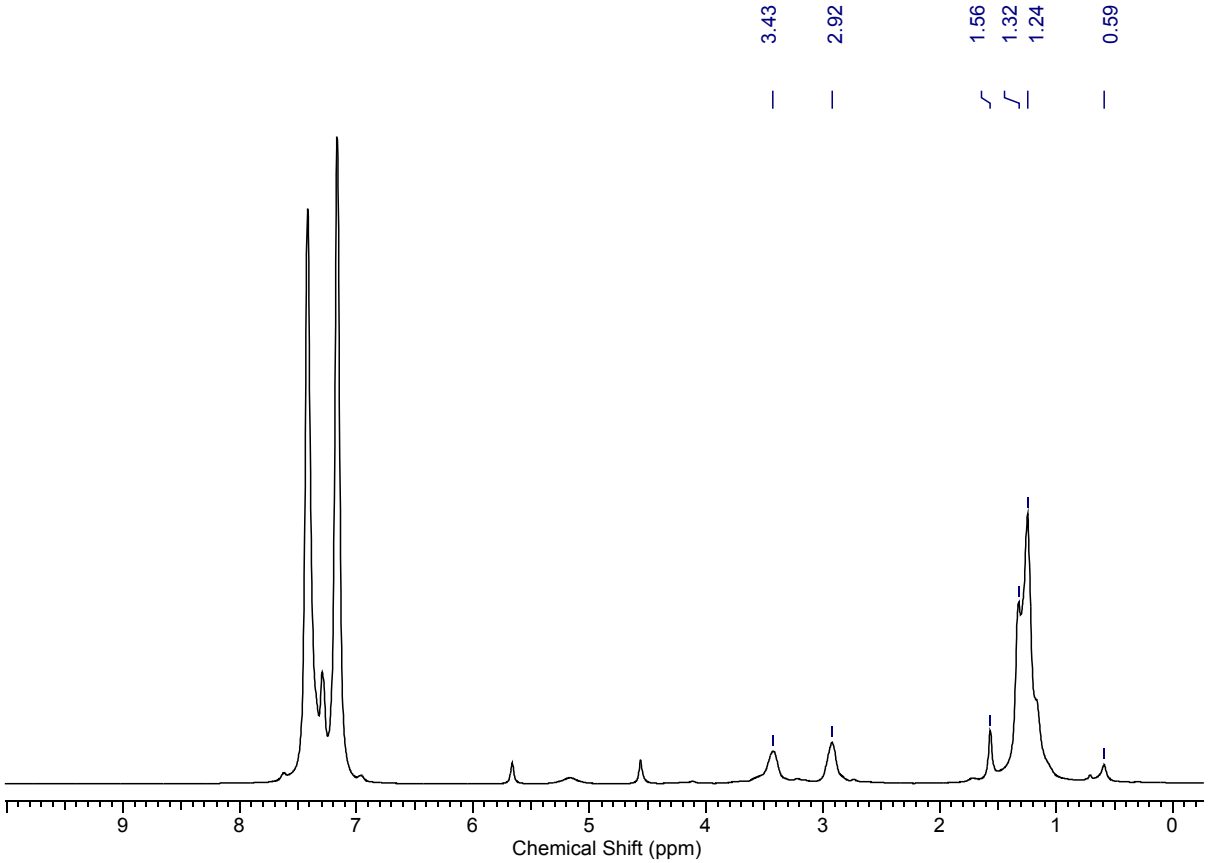

^{11}B NMR Spectrum: In situ NMR of boroxine formation and Hunig's Base boronium

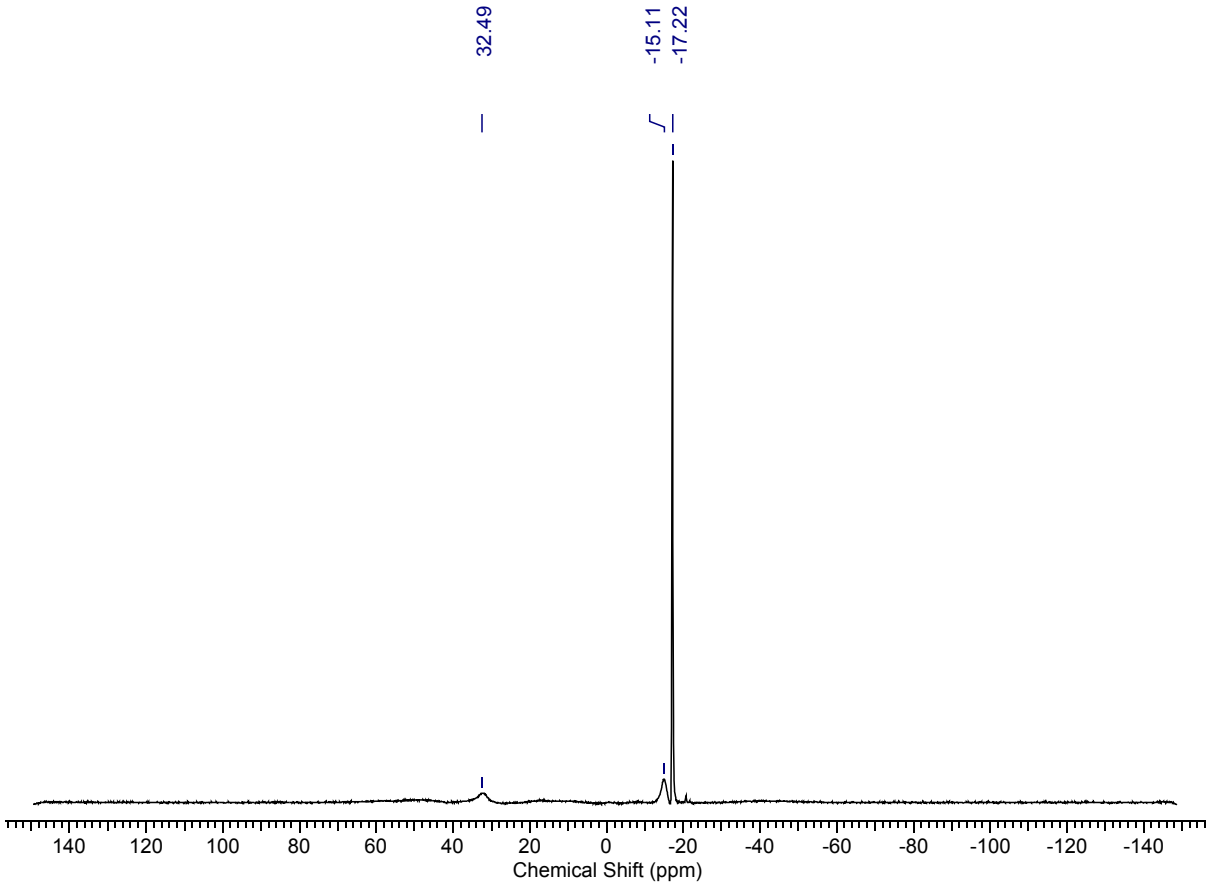

^{11}B {^{1}H} NMR Spectrum: In situ NMR of boroxine formation and Hunig's Base boronium

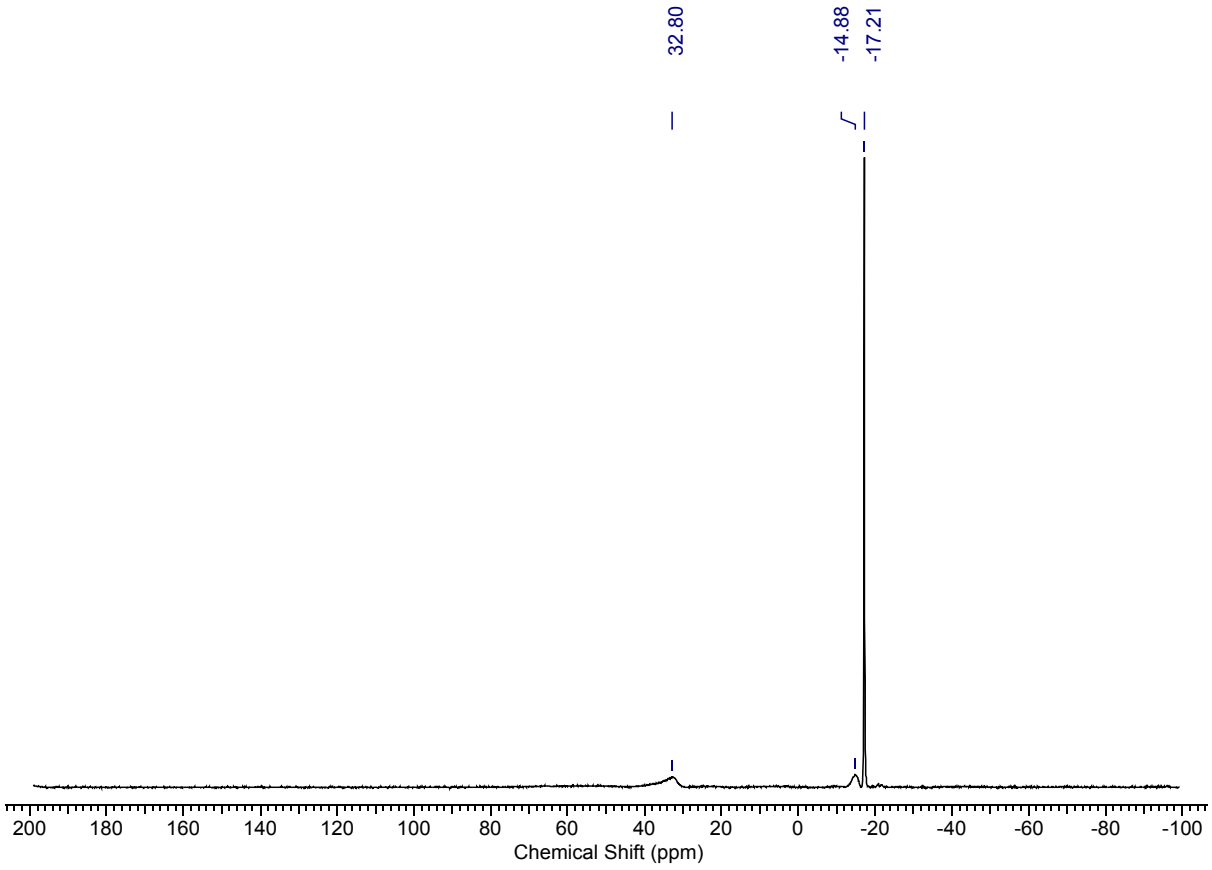

^{13}C {^{1}H} NMR Spectrum: In situ NMR of boroxine formation and Hunig's Base boronium

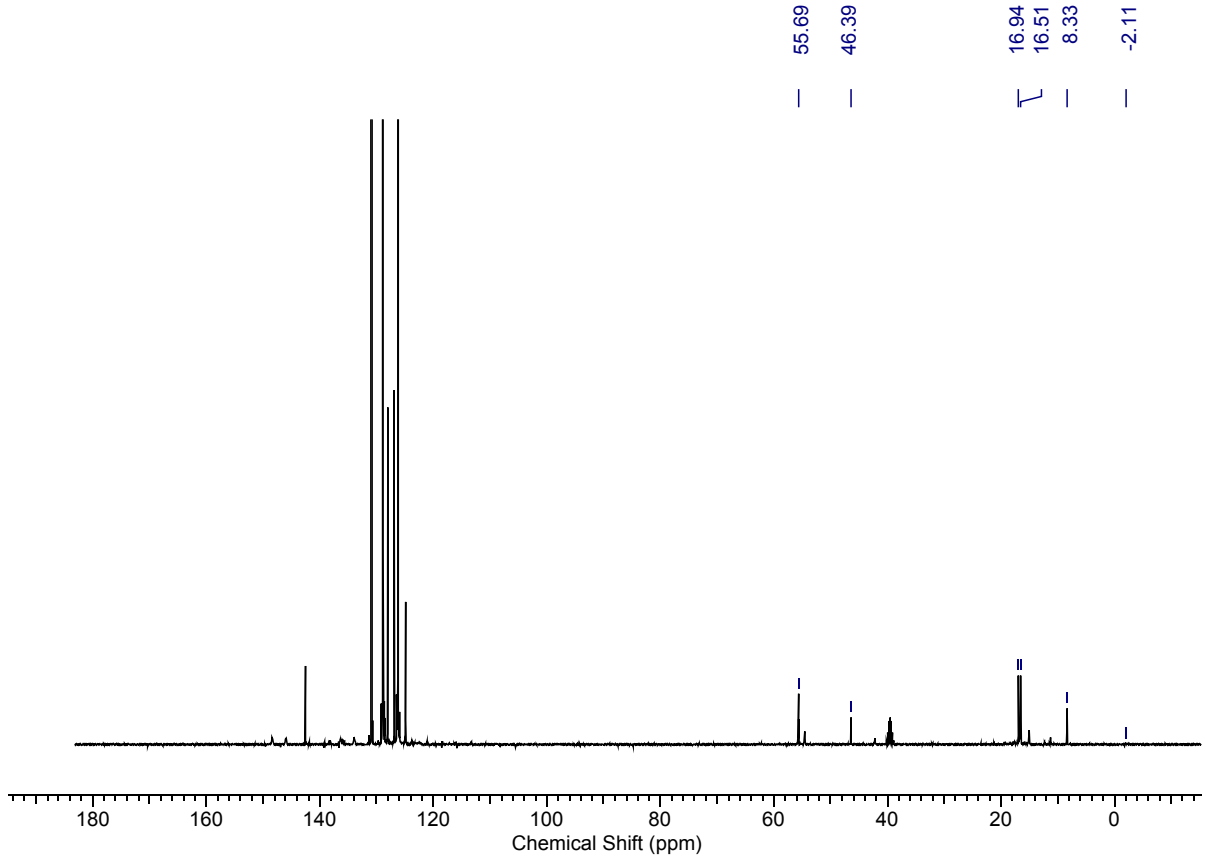

^{19}F {^{1}H} NMR Spectrum: In situ NMR of boroxine formation and Hunig's Base boronium

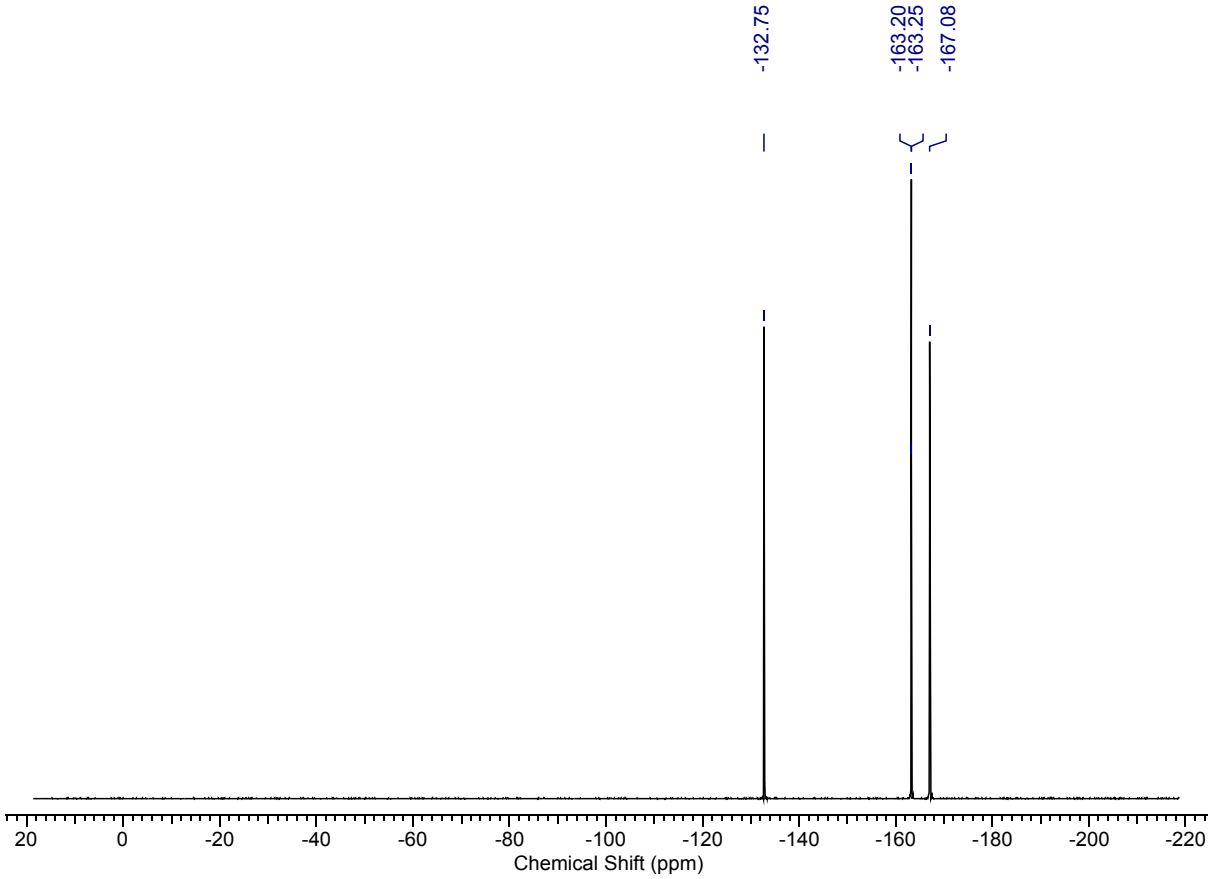

For comparison below are the ^{1}H (blue) and $^{1}H\{^{11}B\}$ (red) NMR spectra in o-DCB/d_6-DMSO capillary of the starting amine borane $Et^{i}Pr_2NBH_3$ to confirm its absence from the above spectra.

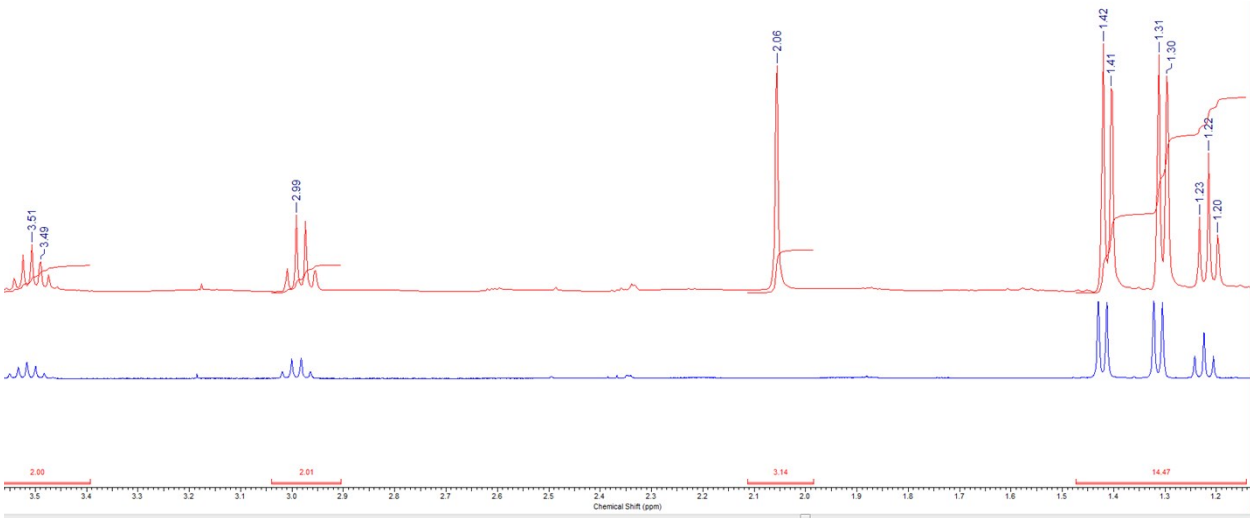

12.5

^{13}C {^{1}H} NMR spectrum: Overlay of 1 under an atmosphere of ^{13}CO, blue spectrum t = 0, green spectrum heated to 60 °C overnight, red spectrum heated 100 °C overnight.

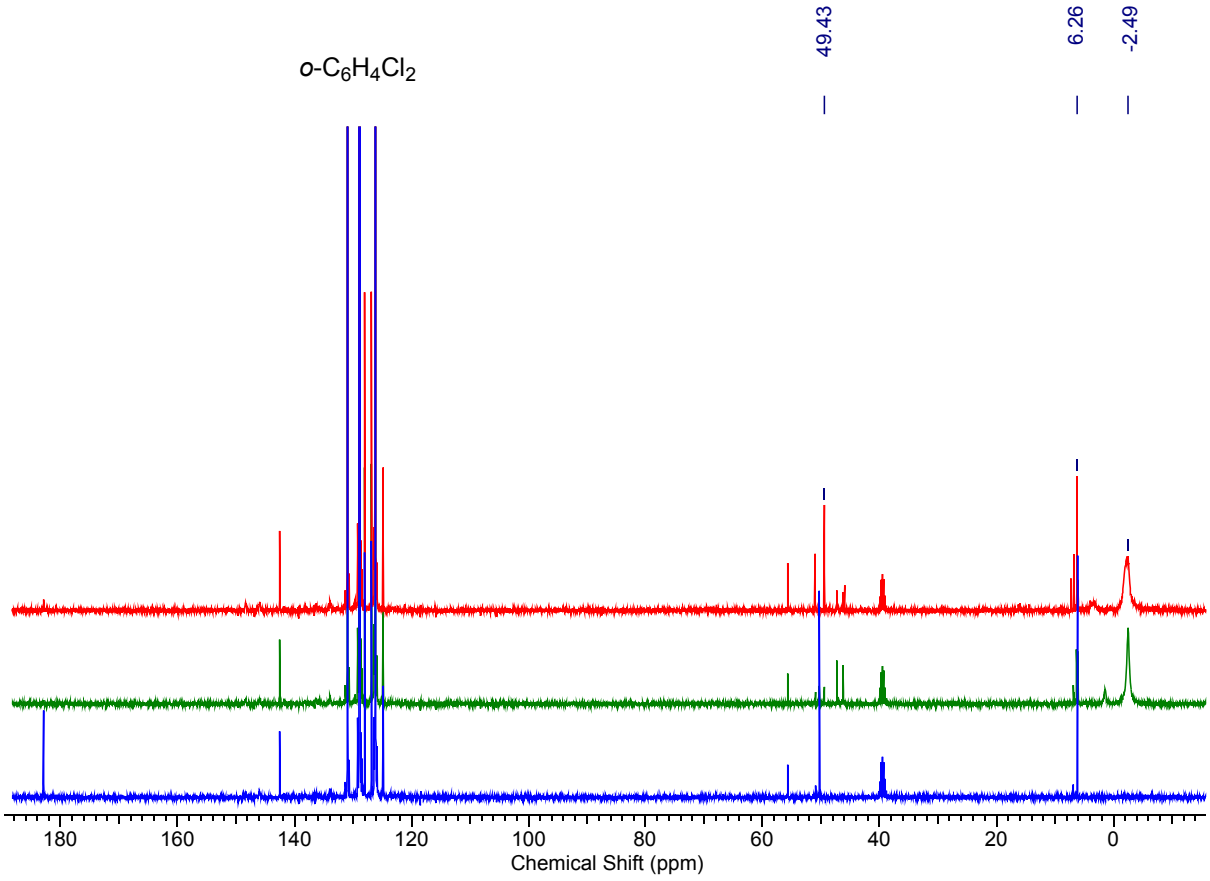

12.6

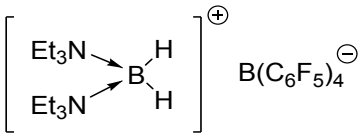

^{1}H NMR Spectrum: In situ NMR of independent formation of NEt_3 boronium

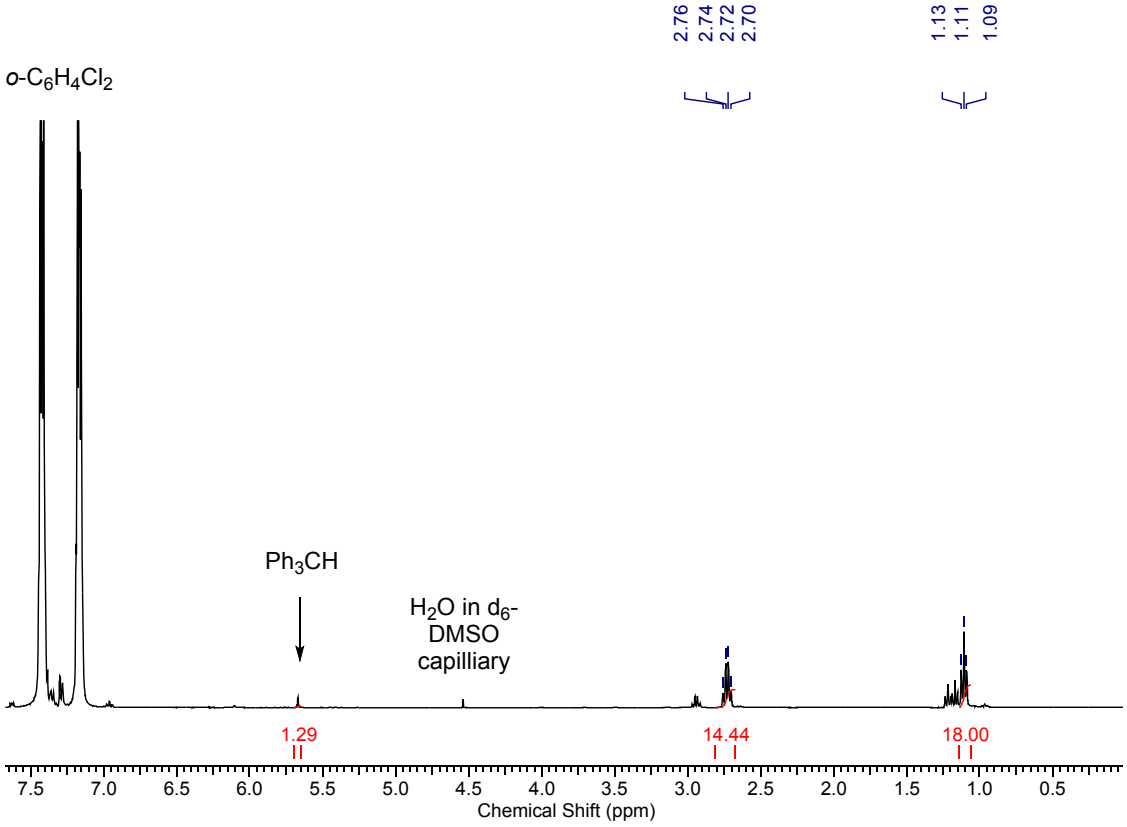

^{1}H {^{11}B} NMR Spectrum: In situ NMR of independent formation of NEt_3 boronium

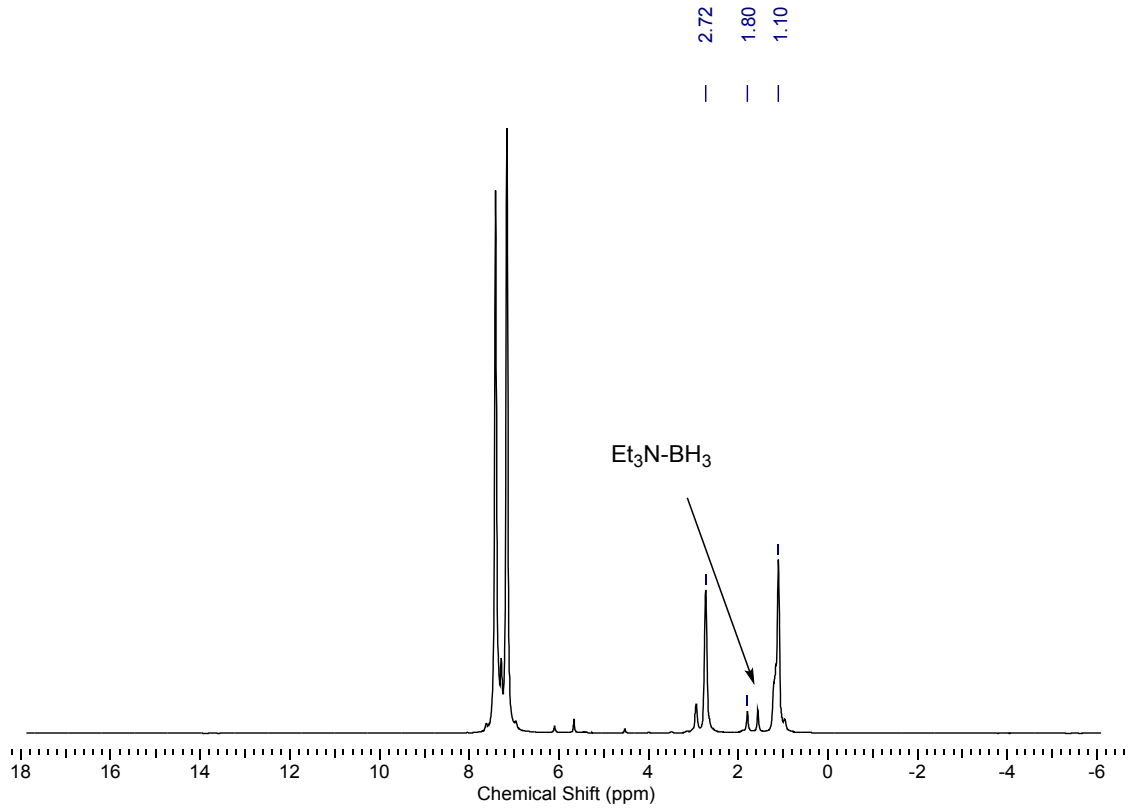

^{11}B NMR Spectrum: In situ NMR of independent formation of NEt_3 boronium

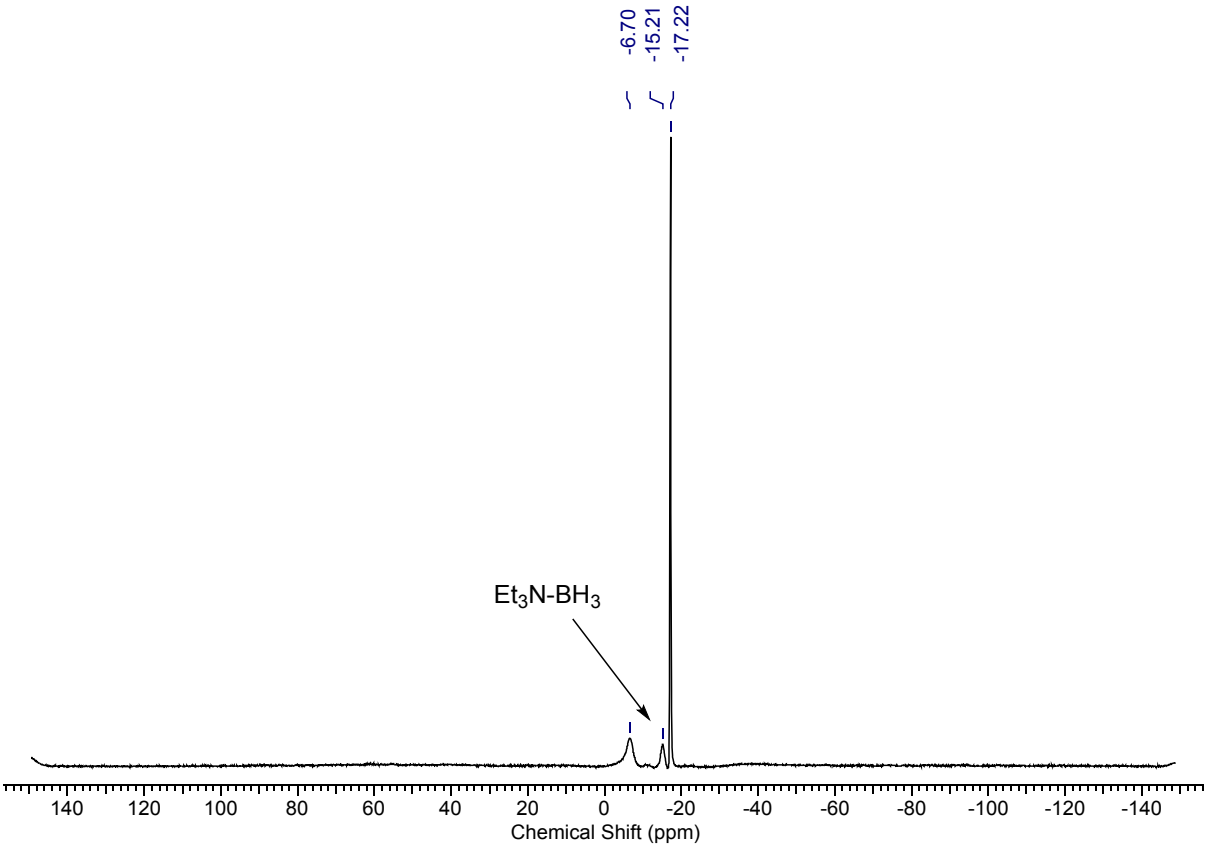

^{11}B {^{1}H} NMR Spectrum: In situ NMR of independent formation of NEt_3 boronium

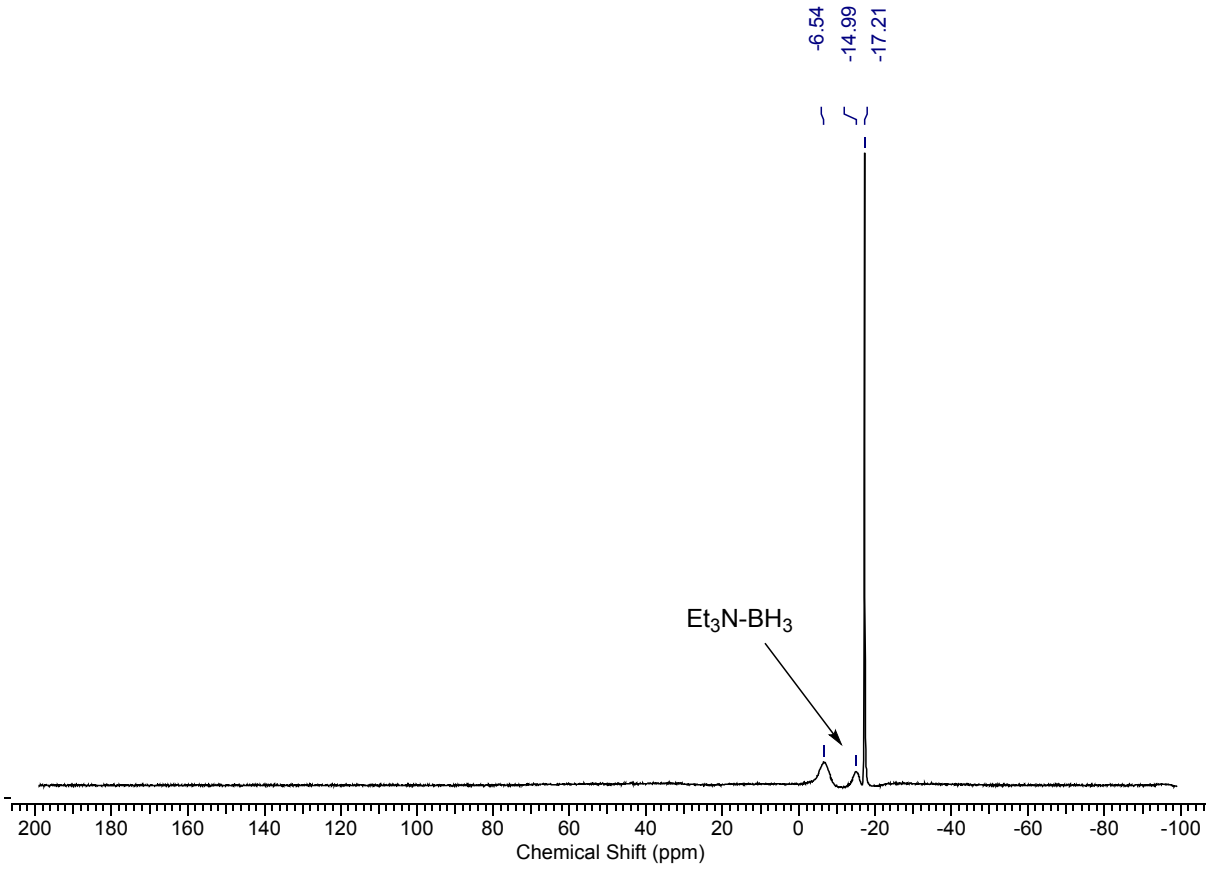

^{13}C {^{1}H} NMR spectrum: In situ NMR of independent formation of NEt_3 boronium

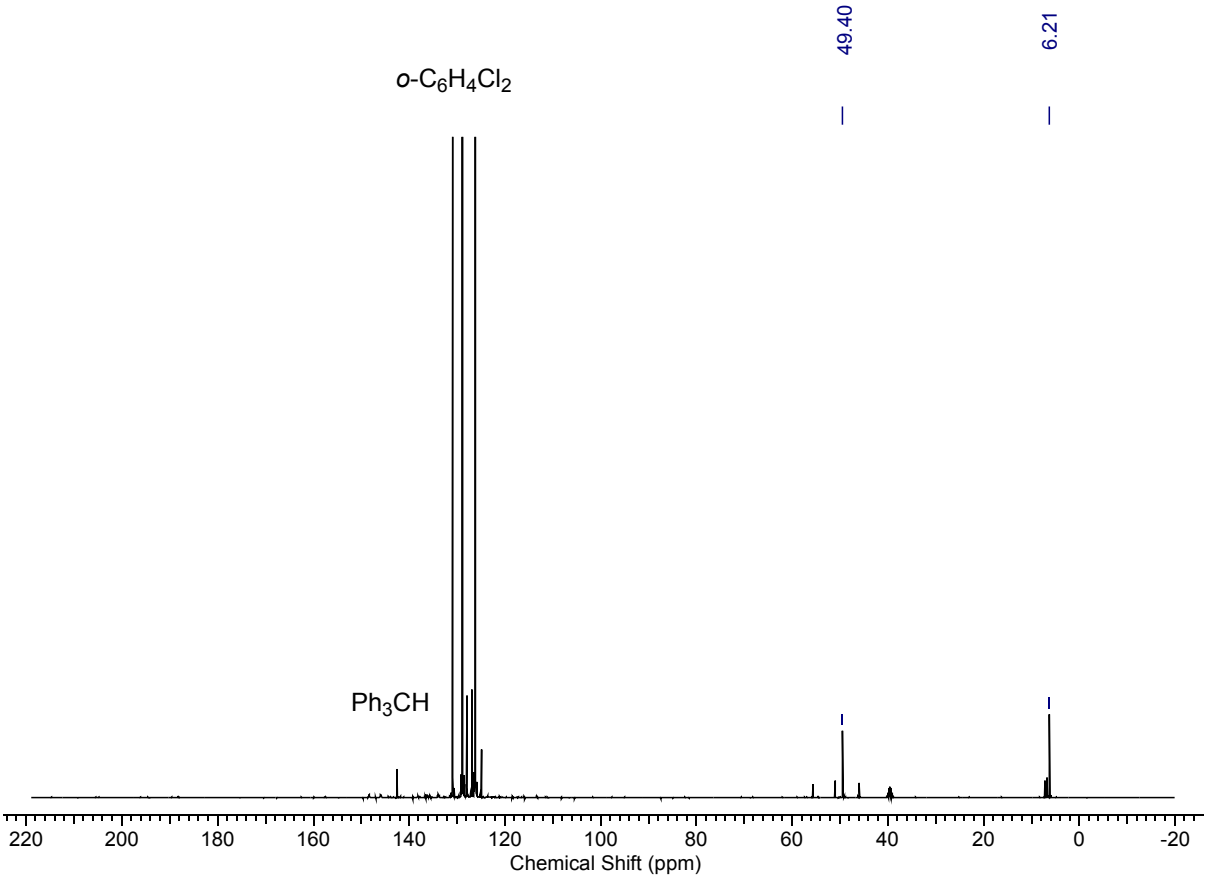

^{19}F {^{1}H} NMR Spectrum: In situ NMR of independent formation of NEt_3 boronium

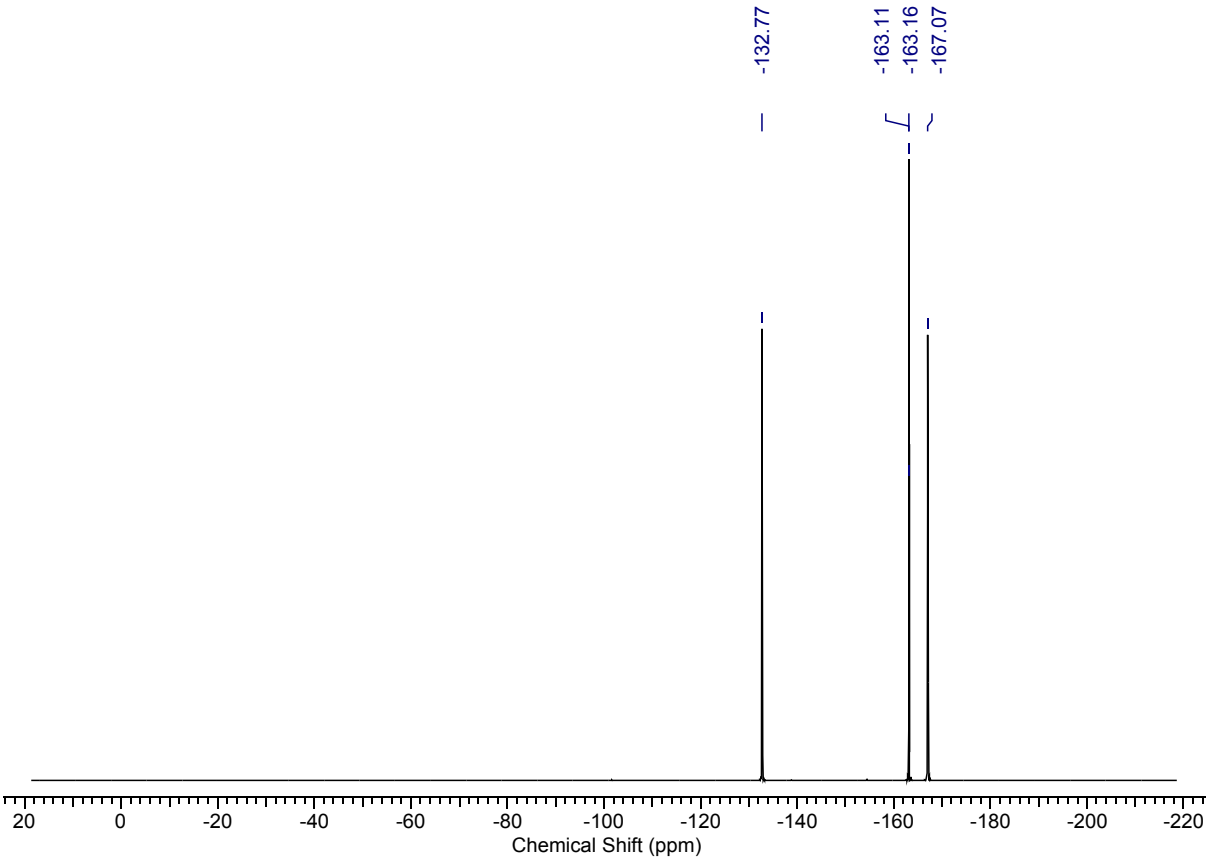

12.7

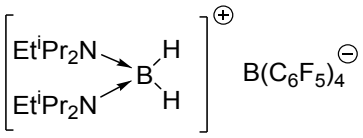

^{1}H NMR Spectrum: In situ NMR of independent formation of Hunig's Base boronium

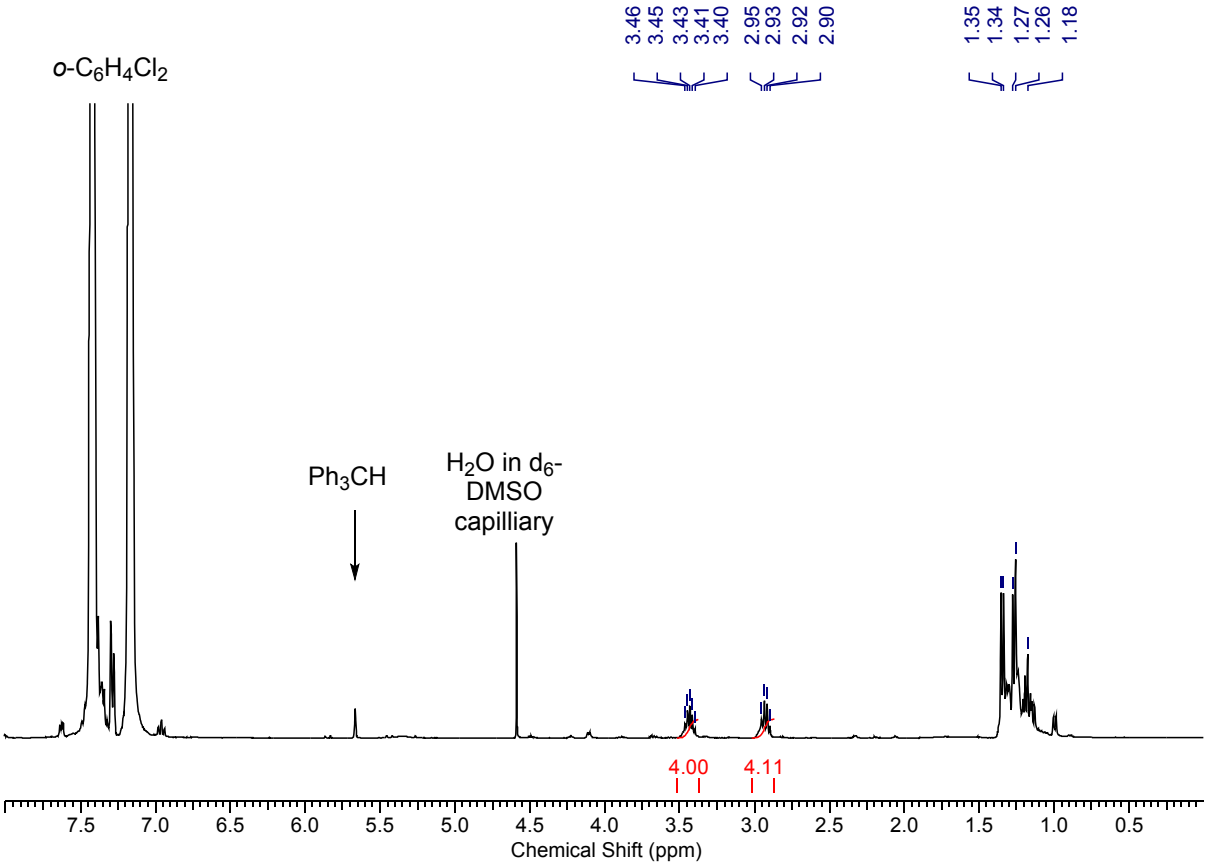

^{1}H {^{11}B} NMR Spectrum: In situ NMR of independent formation of Hunig's Base boronium

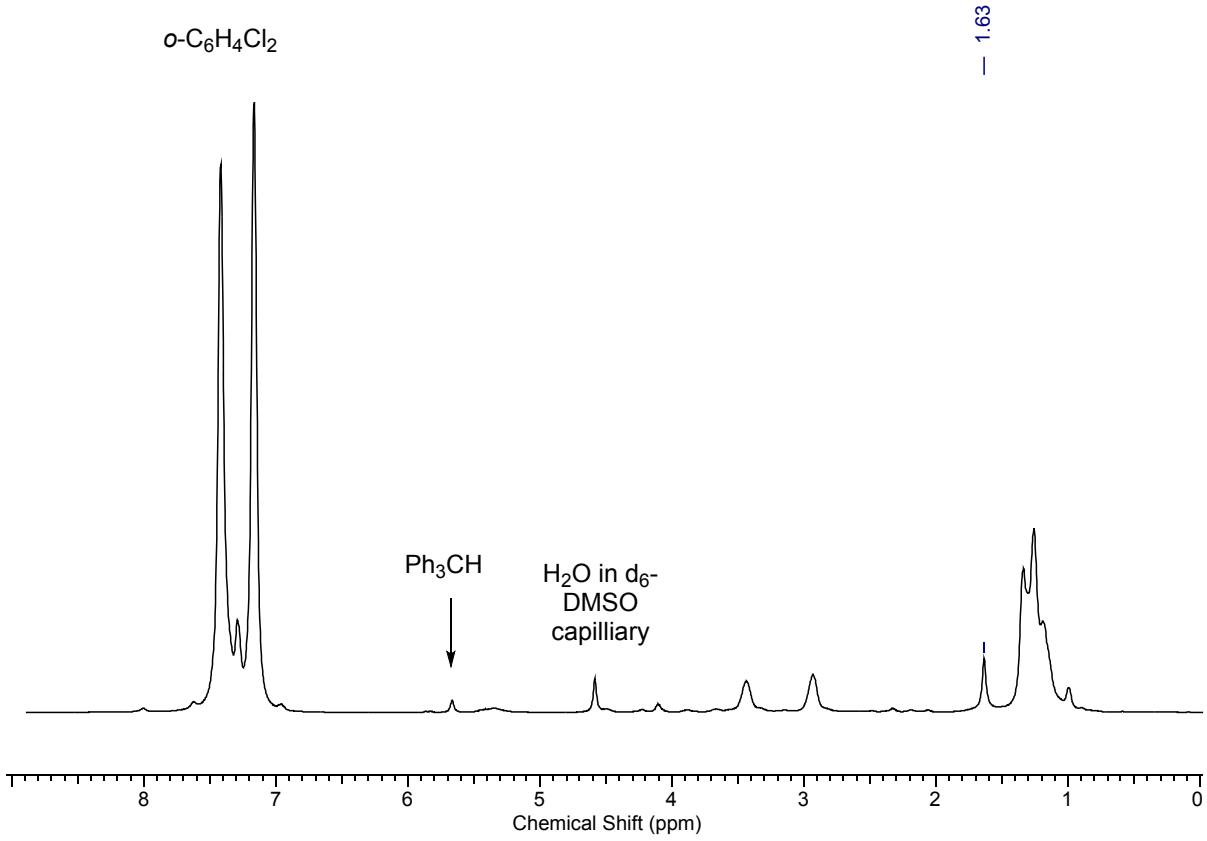

^{11}B NMR Spectrum: In situ NMR of independent formation of Hunig's Base boronium

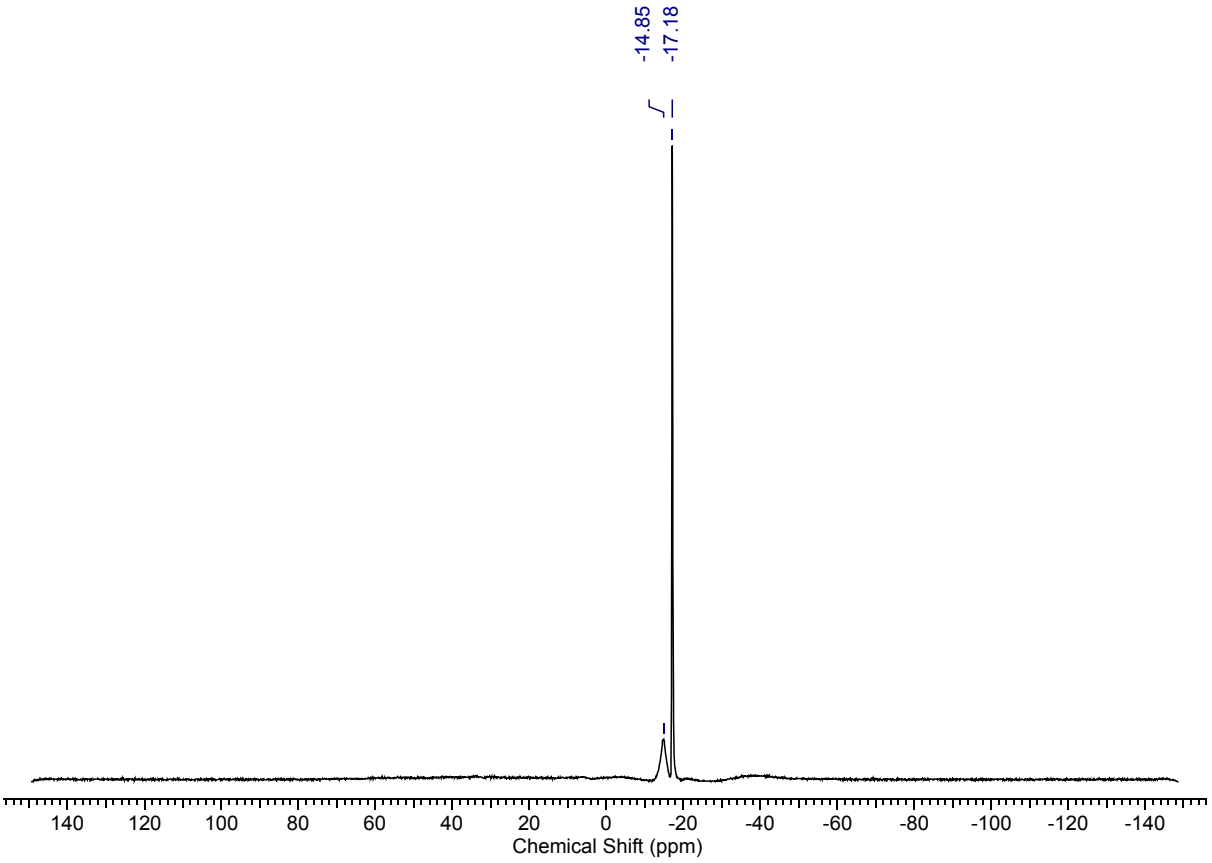

^{11}B {^{1}H} NMR Spectrum: In situ NMR of independent formation of Hunig's Base boronium

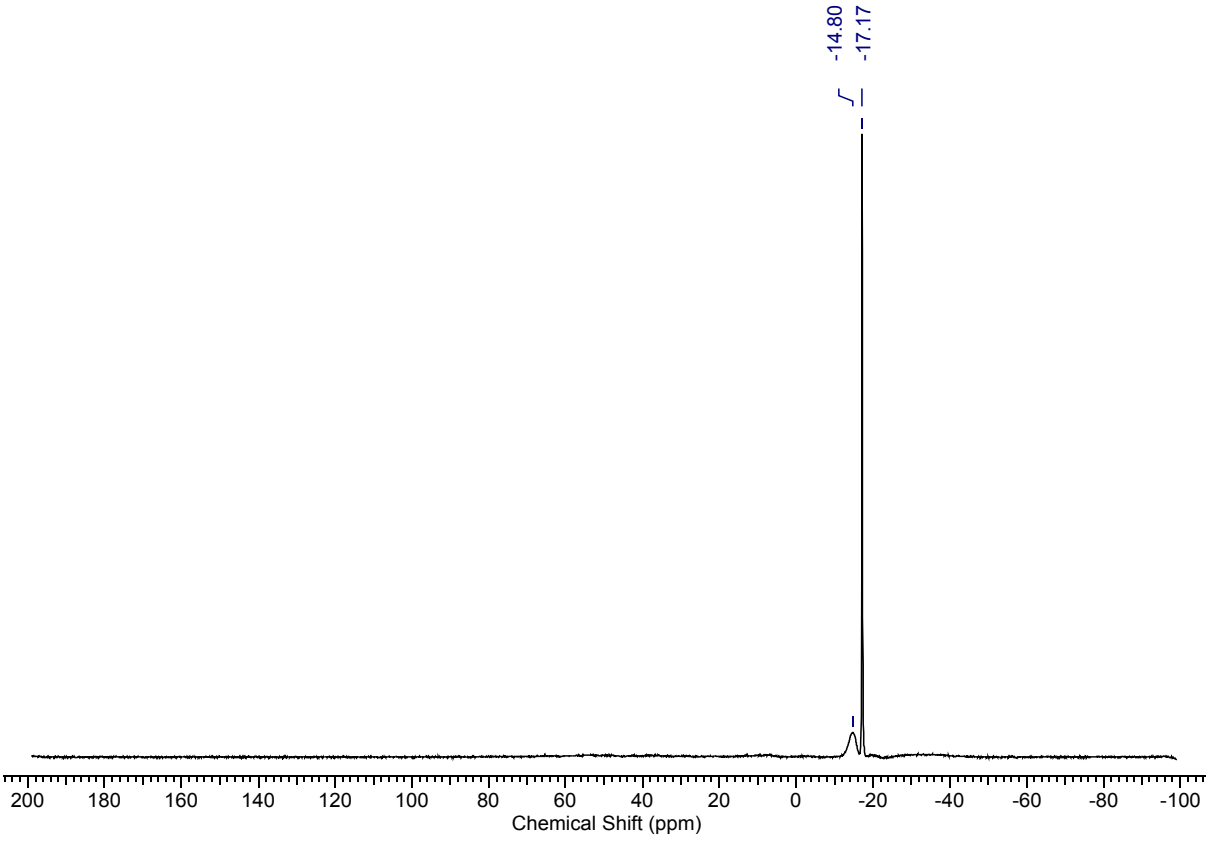

^{13}C {^{1}H} NMR spectrum: In situ NMR of independent formation of Hunig's Base boronium

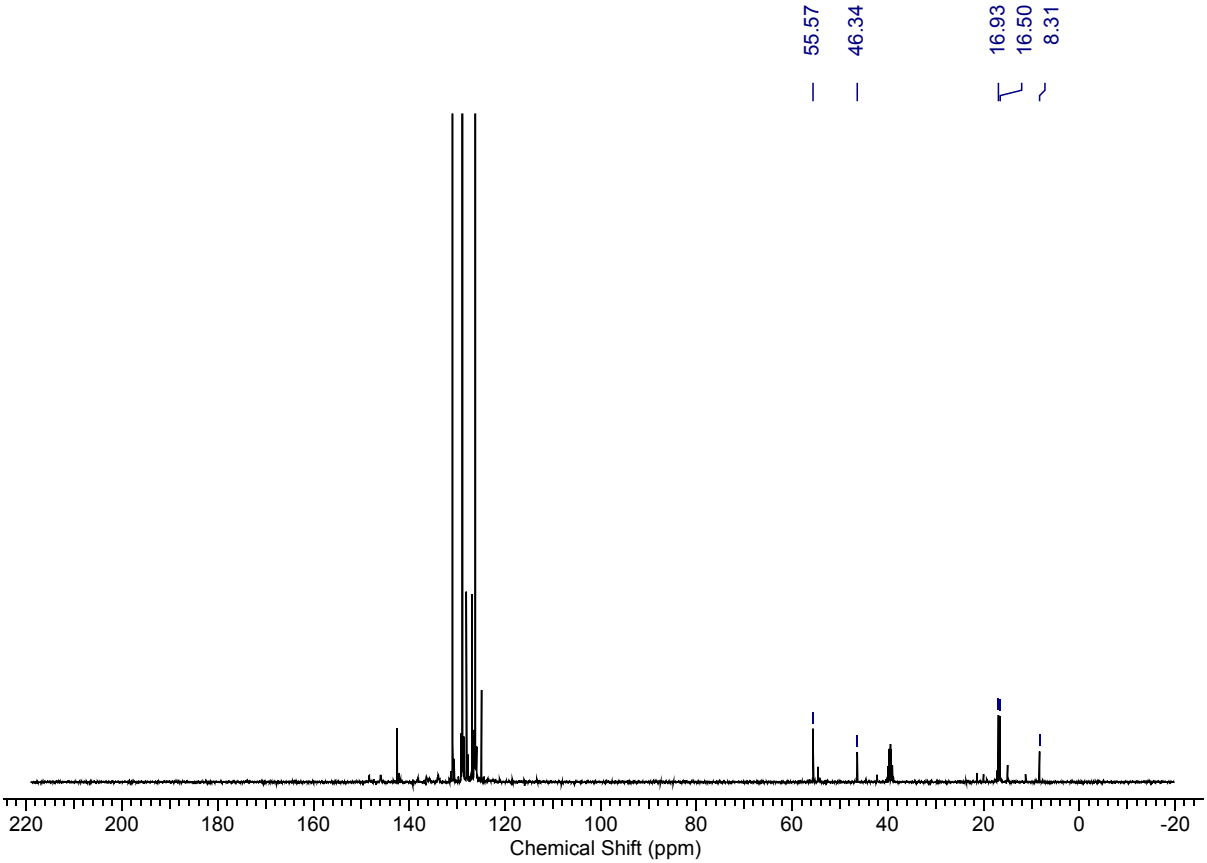

^{19}F {^{1}H} NMR Spectrum: In situ NMR of independent formation of Hunig's Base boronium

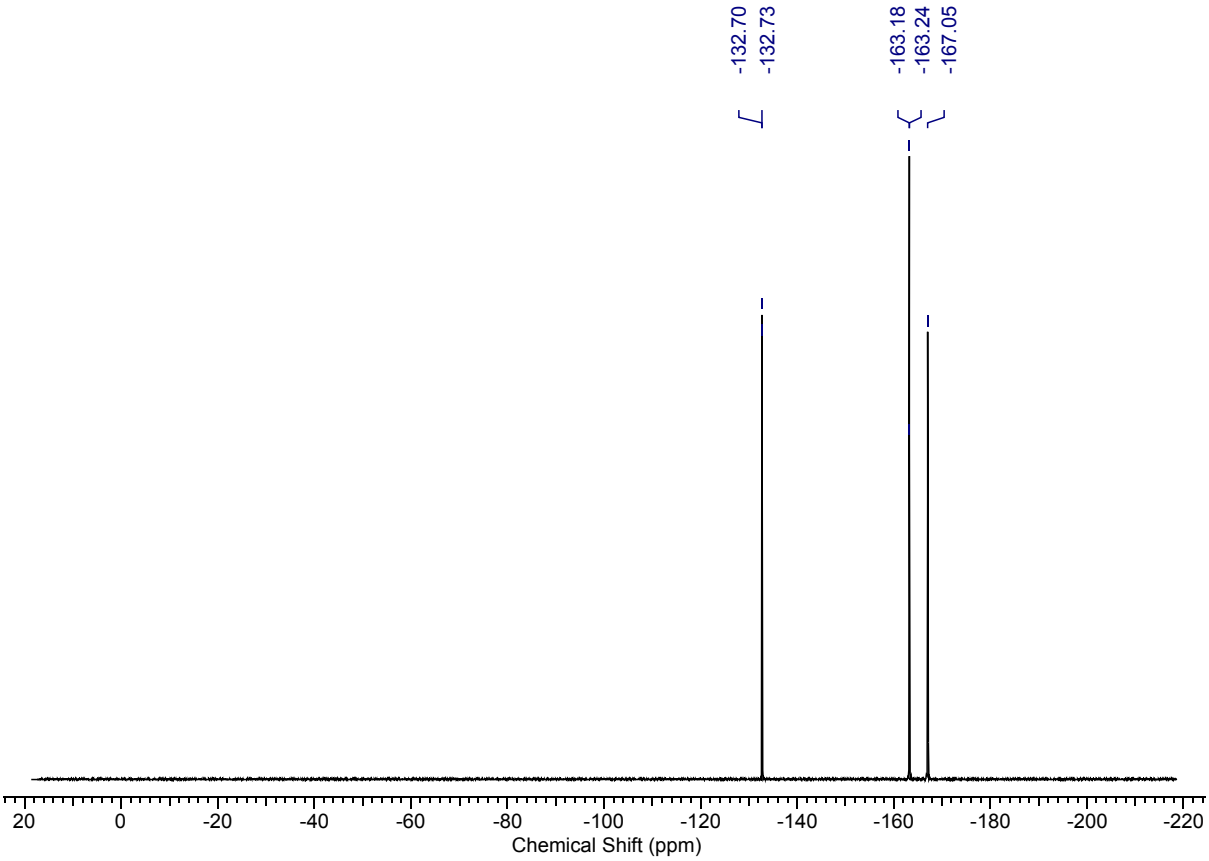

12.8

^{1}H NMR Spectrum: Boroxine in *o*-$C_6H_4Cl_2$

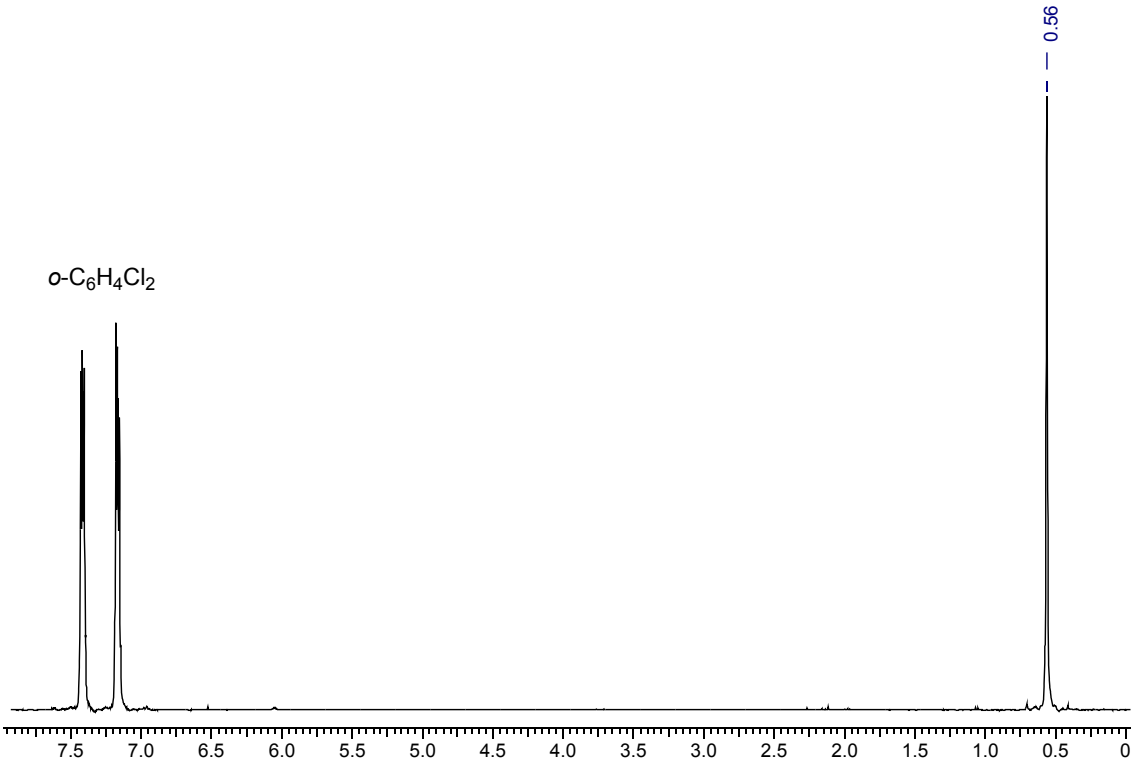

^{11}B NMR Spectrum: Boroxine in *o*-$C_6H_4Cl_2$

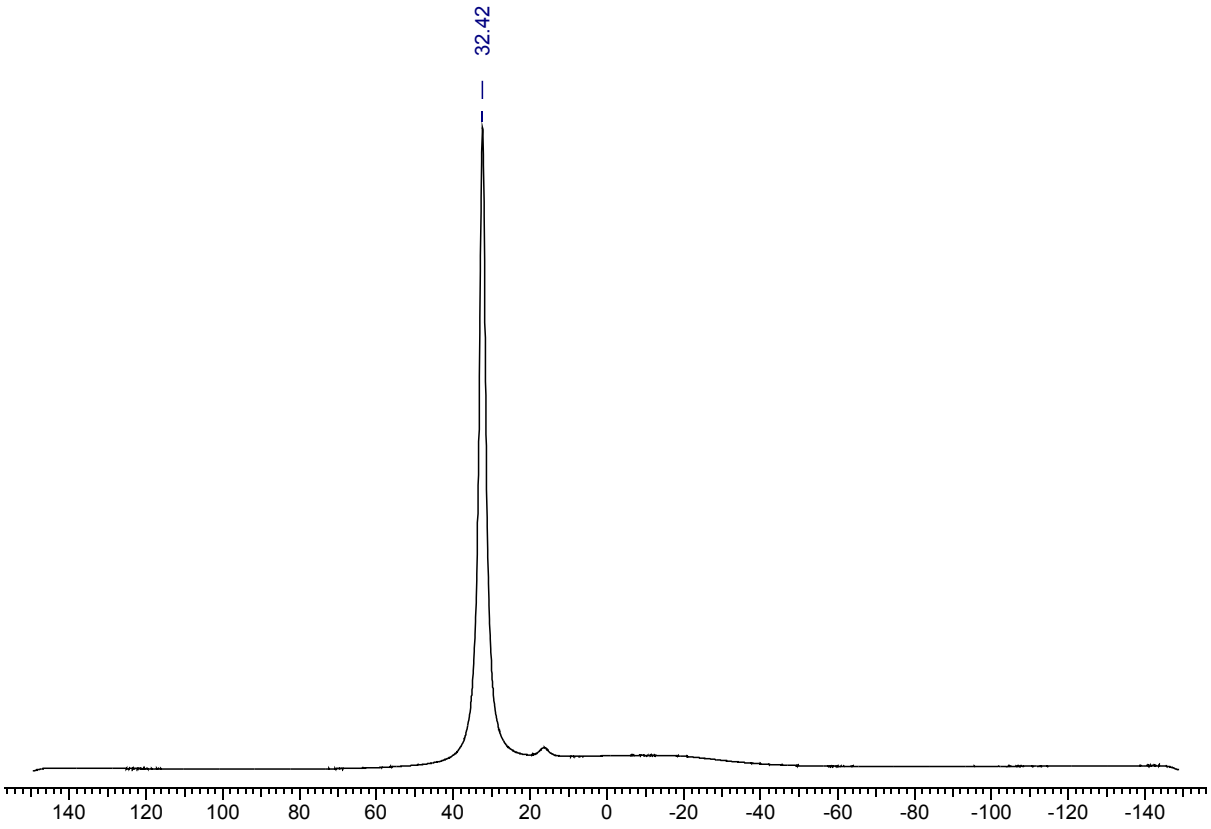

^{13}C {^{1}H} NMR Spectrum: Boroxine in *o*-$C_6H_4Cl_2$

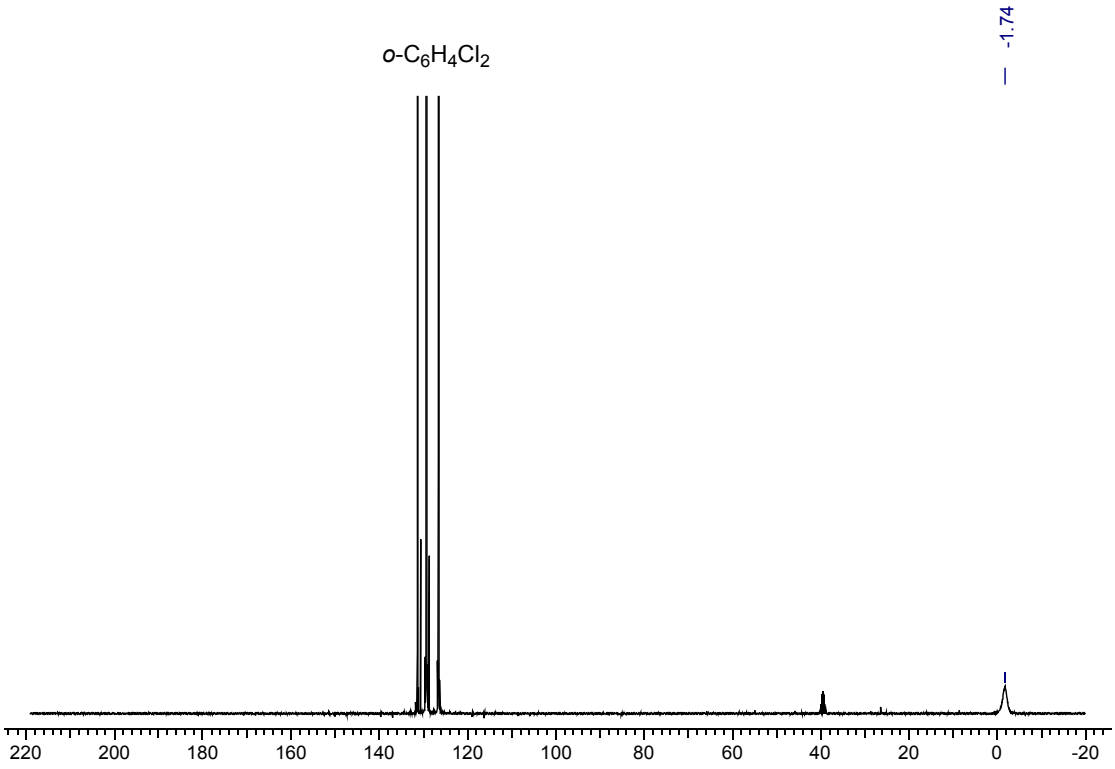

12.9 VT NMR Spectroscopy

^{1}H NMR Spectrum: -70 °C 1 charged with CO in CD_2Cl_2

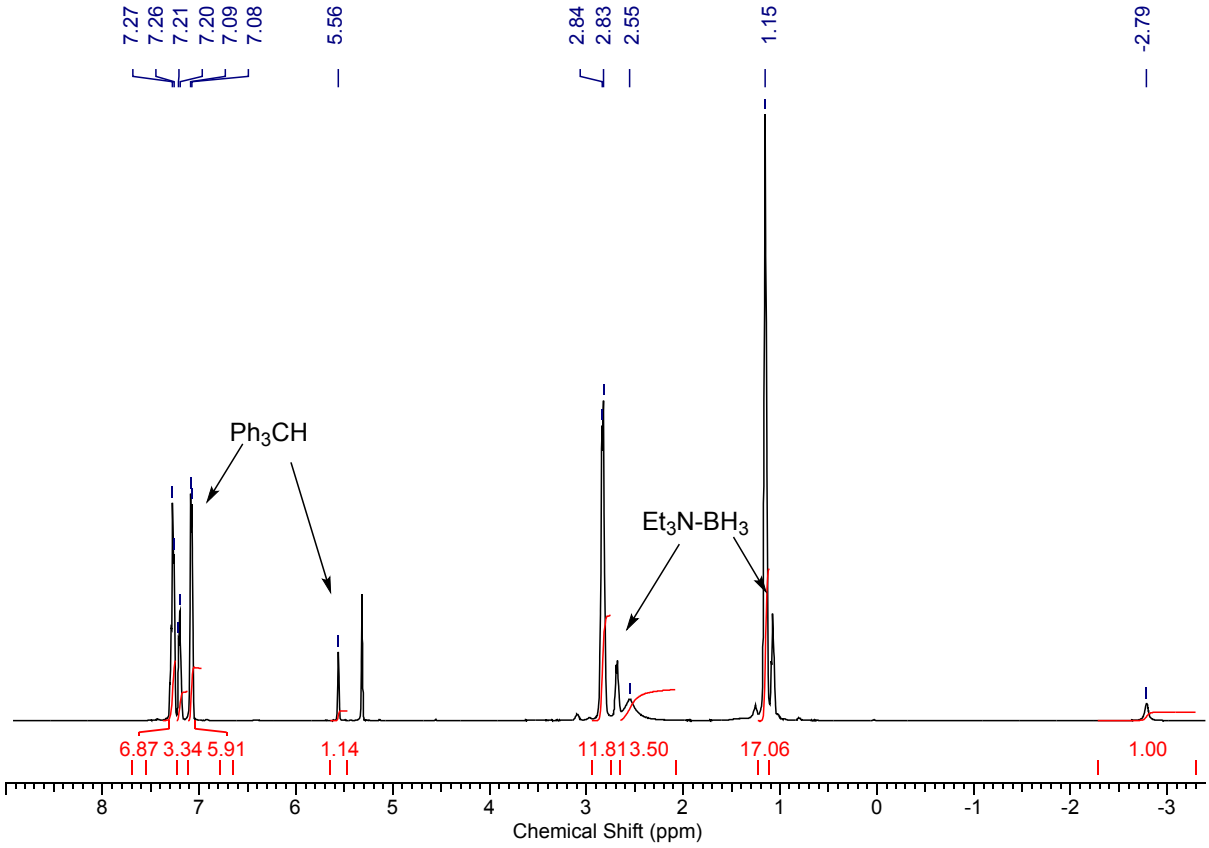

^{11}B NMR Spectrum: -70 ^{o}C 1 charged with CO

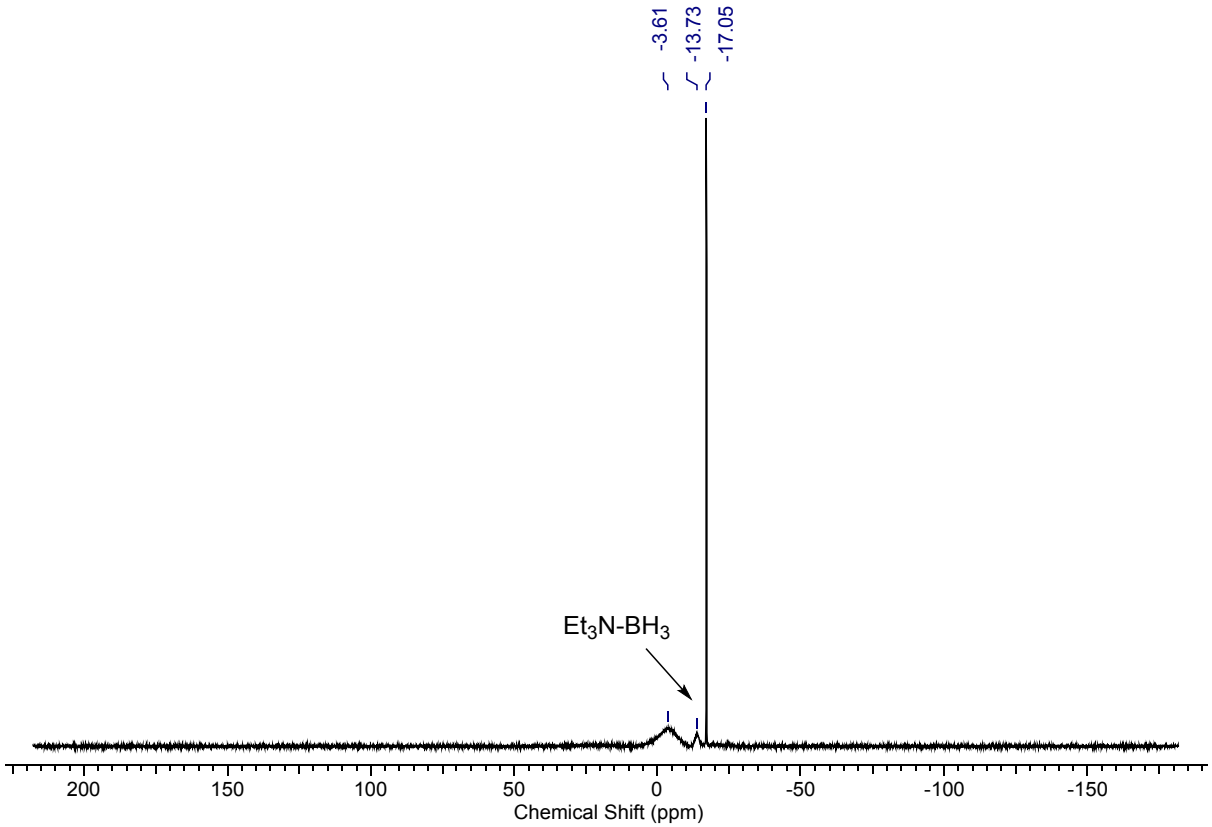

12.10

^{1}H NMR Spectrum: In situ NMR of reaction catalytic in Trityl Salt- Addition of Excess Hunig's base borane 24 h at 60 °C

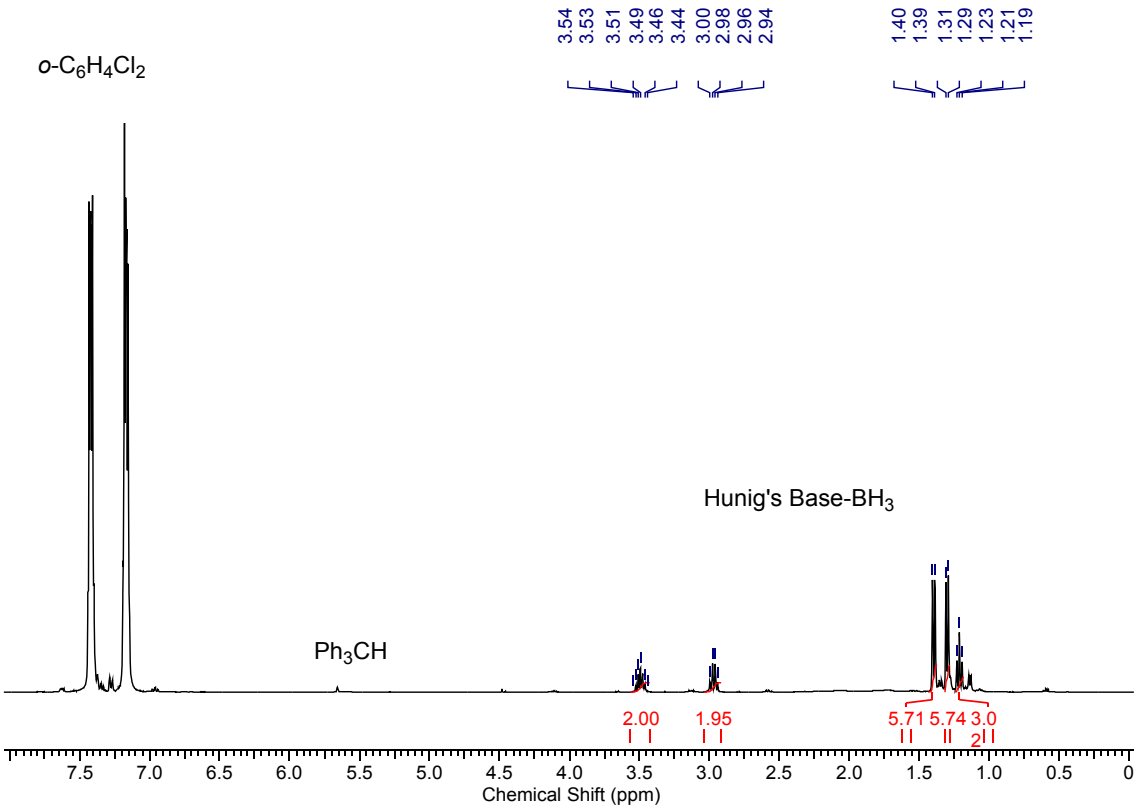

^{1}H {^{11}B} NMR Spectrum: In situ NMR of reaction catalytic in Trityl Salt- Addition of Excess Hunig's base borane 24 h at 60 °C

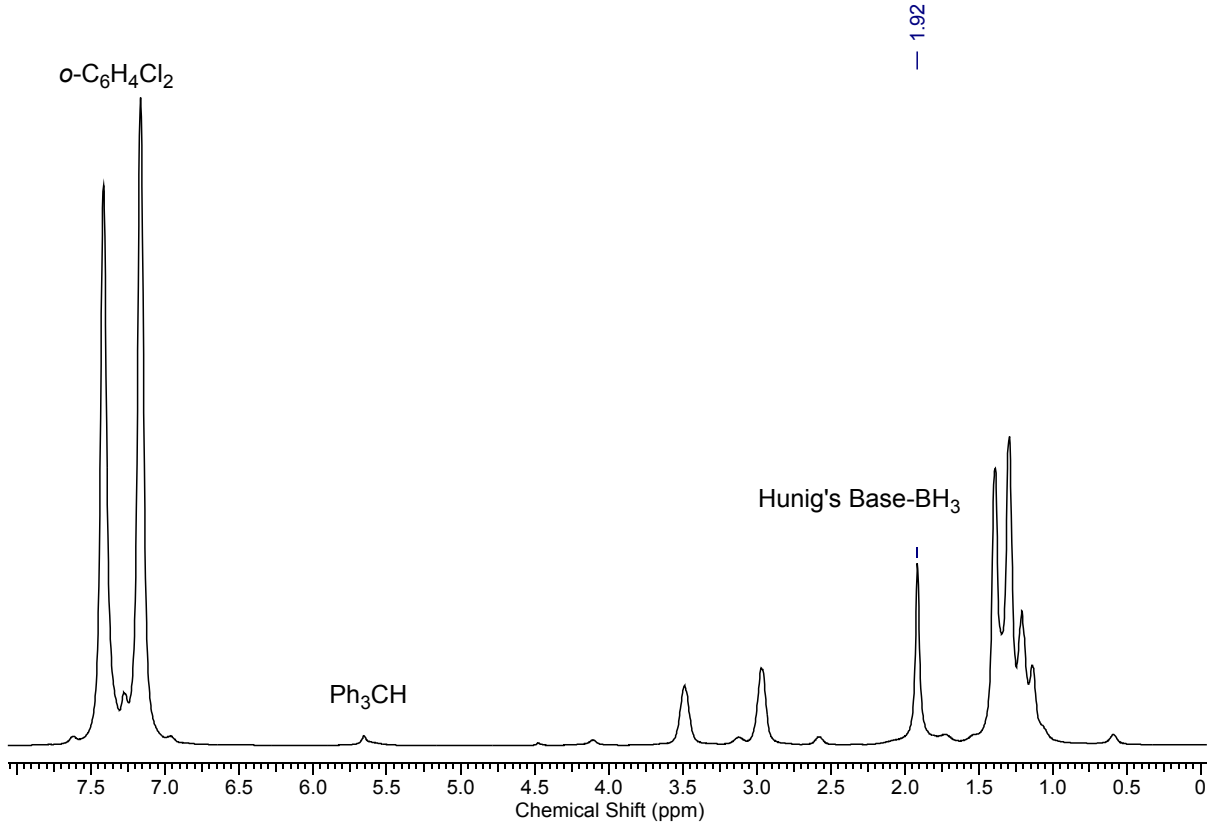

^{11}B NMR Spectrum: In situ NMR of reaction catalytic in Trityl Salt- Addition of Excess Hunig's base borane 24 h at 60 °C

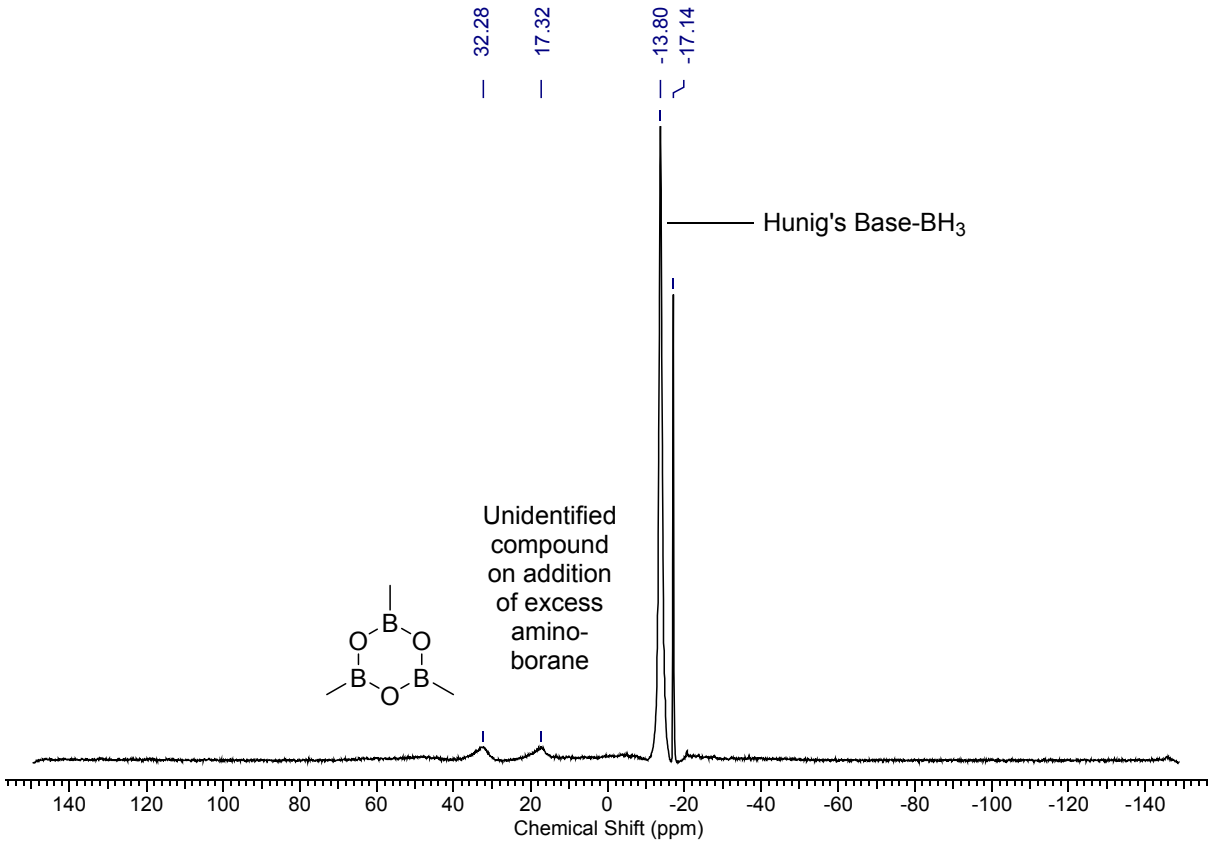

^{11}B {^{1}H} NMR Spectrum: In situ NMR of reaction catalytic in Trityl Salt- Addition of Excess Hunig's base borane 24 h at 60 °C

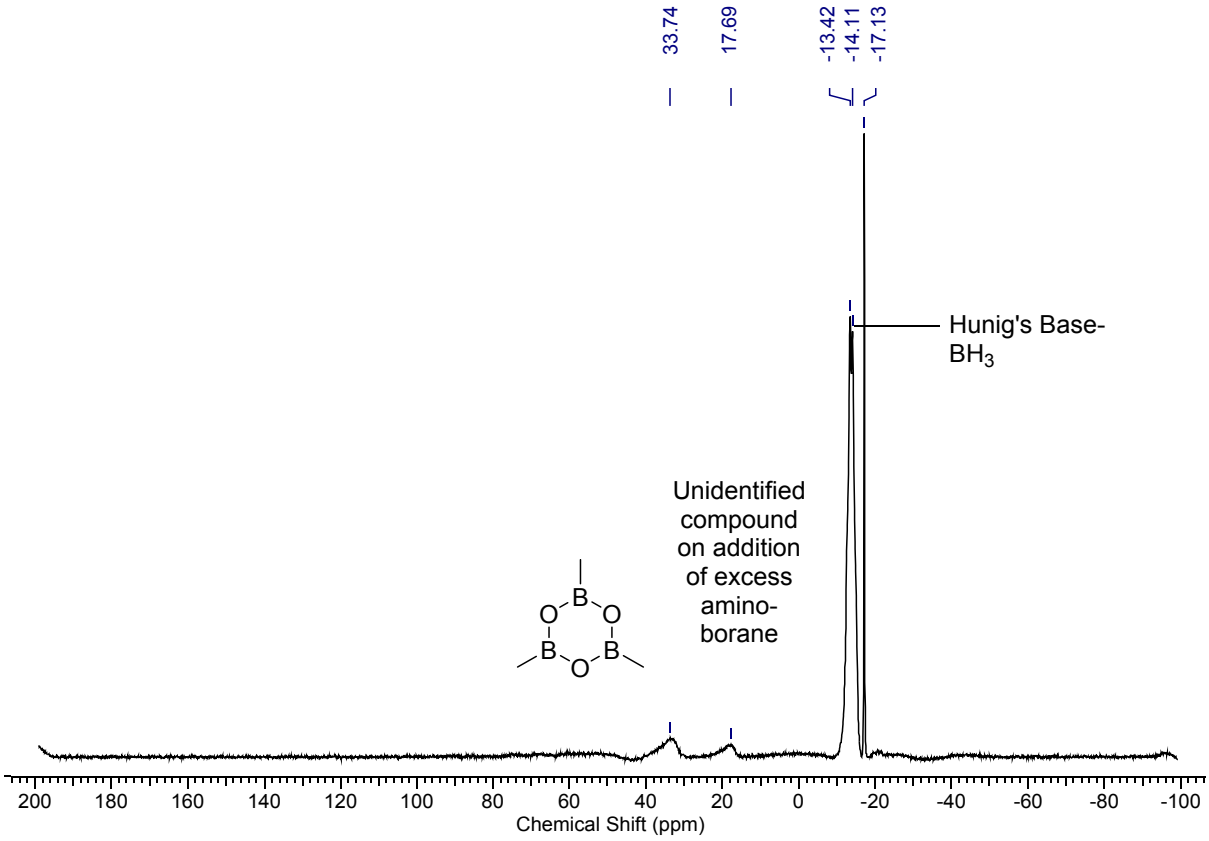

^{19}F {^{1}H} NMR Spectrum: In situ NMR of reaction catalytic in Trityl Salt- Addition of Excess Hunig's base borane 24 h at 60 °C

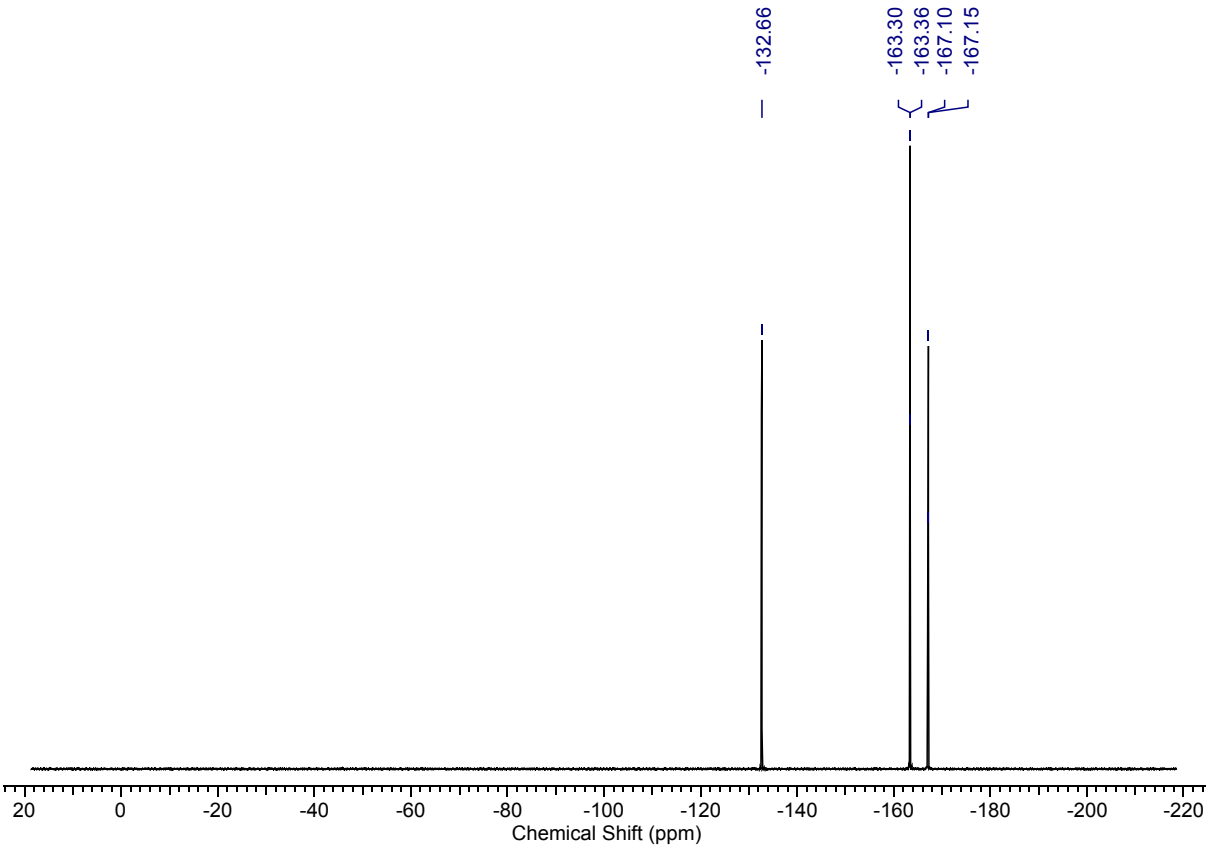

12.11

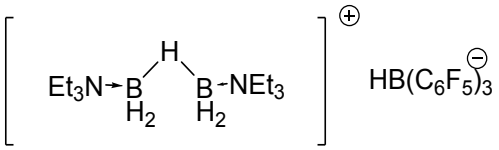

^{1}H NMR Spectrum: In situ NMR of triethylamine Borane Activation with $B(C_6F_5)_3$

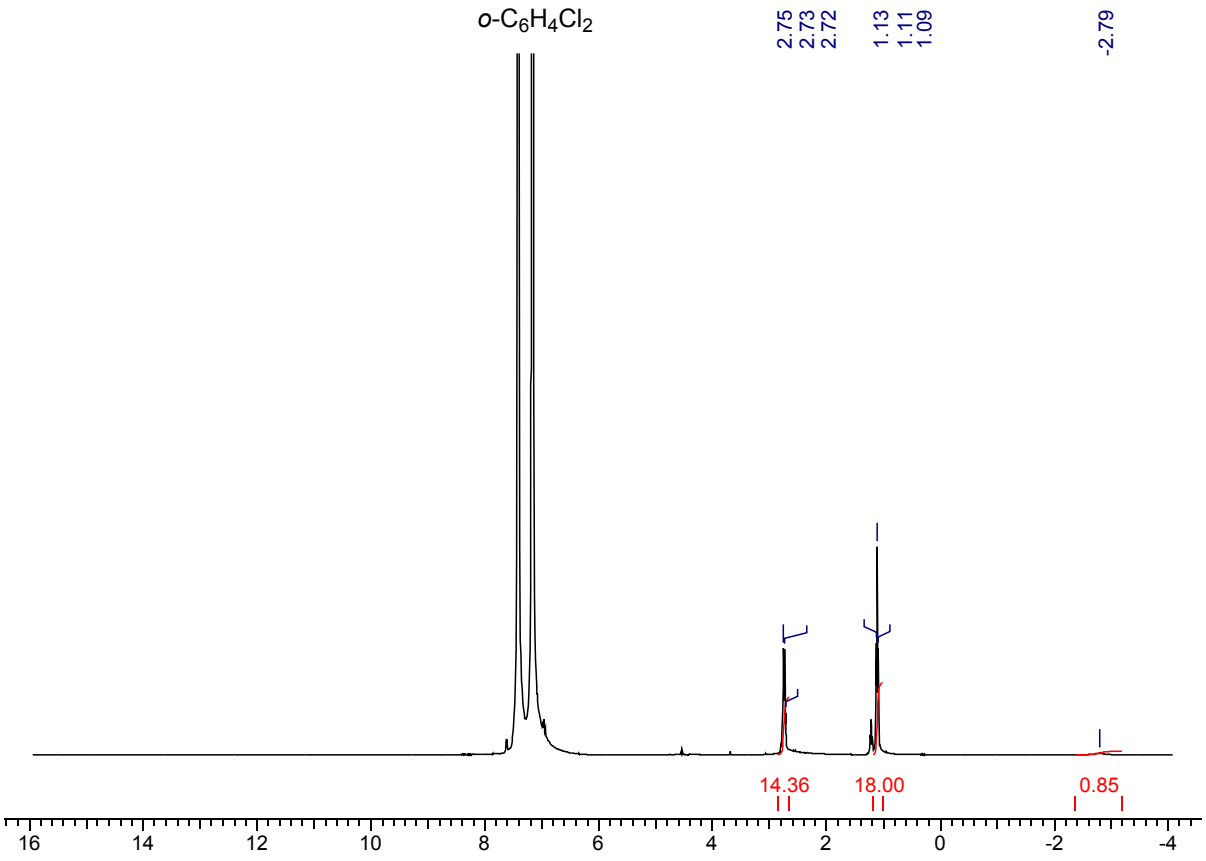

^{1}H {^{11}B} NMR Spectrum: In situ NMR of triethylamine Borane Activation with $B(C_6F_5)_3$

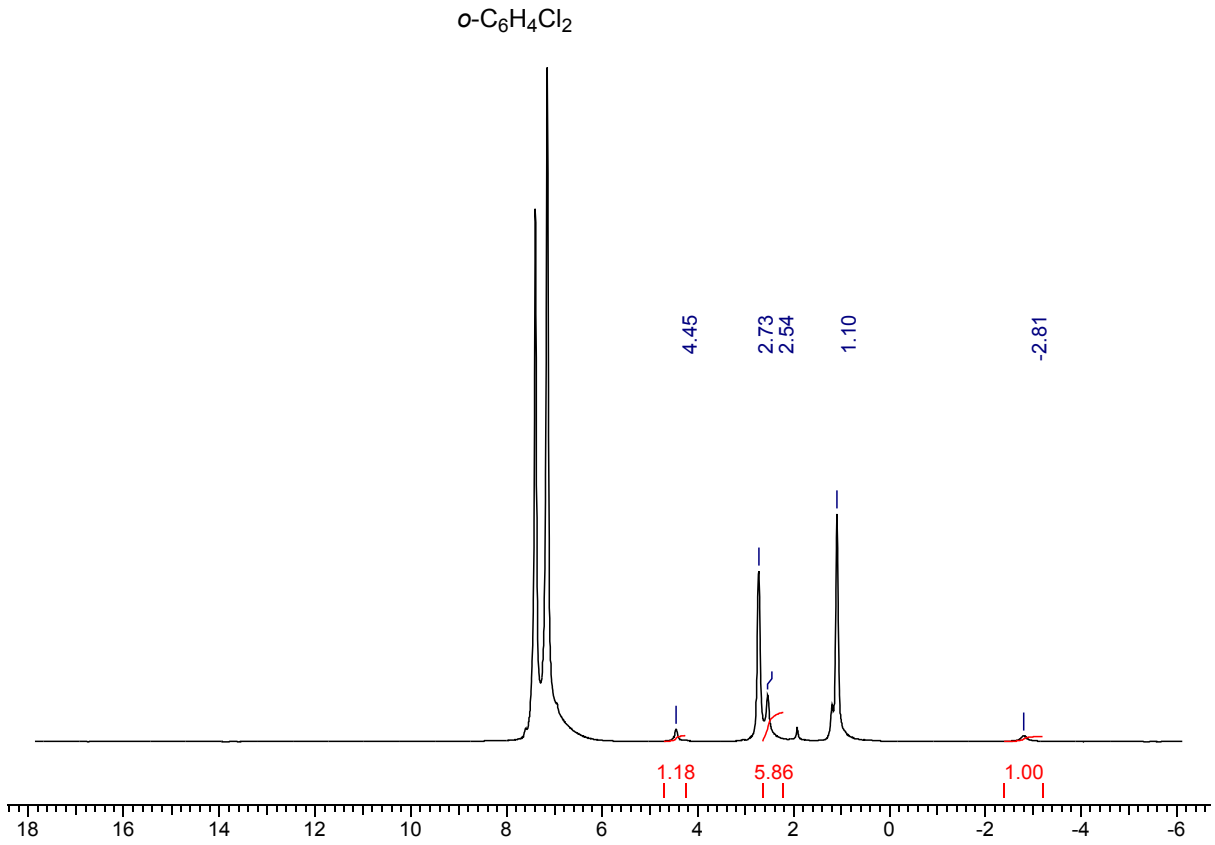

^{11}B NMR Spectrum: In situ NMR of triethylamine Borane Activation with $B(C_6F_5)_3$

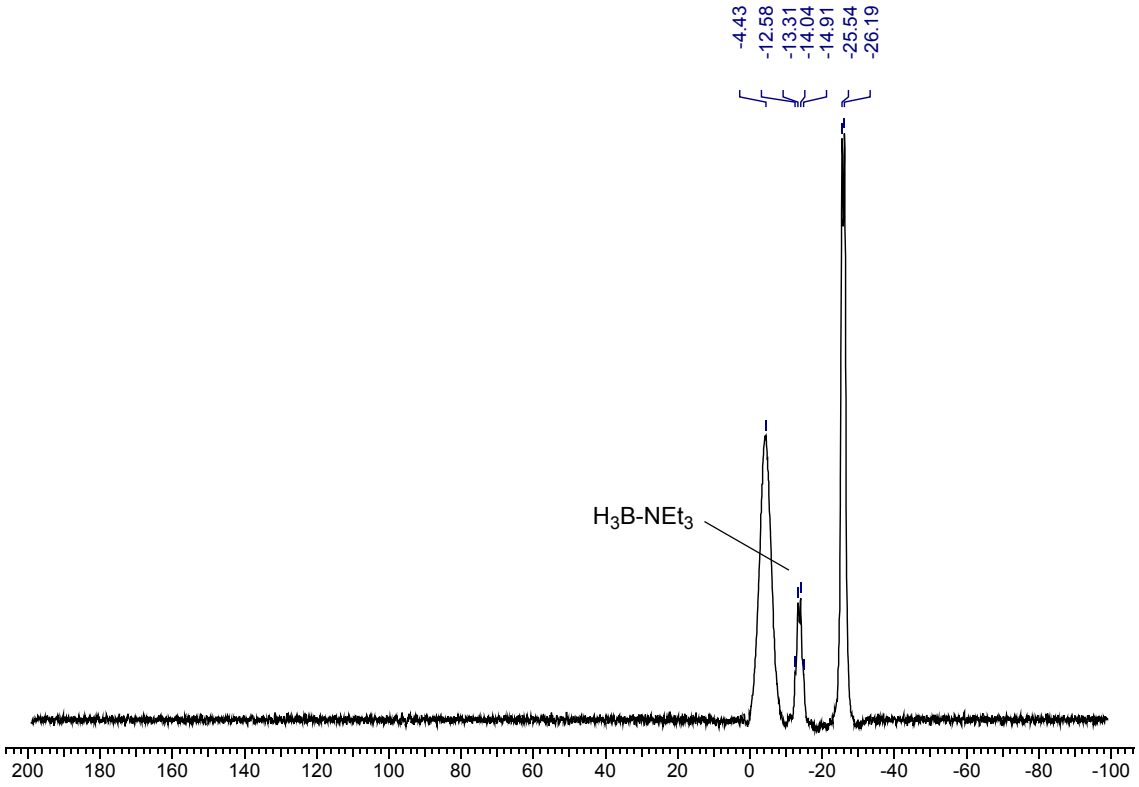

^{11}B {^{1}H} NMR Spectrum: In situ NMR of triethylamine Borane Activation with $B(C_6F_5)_3$

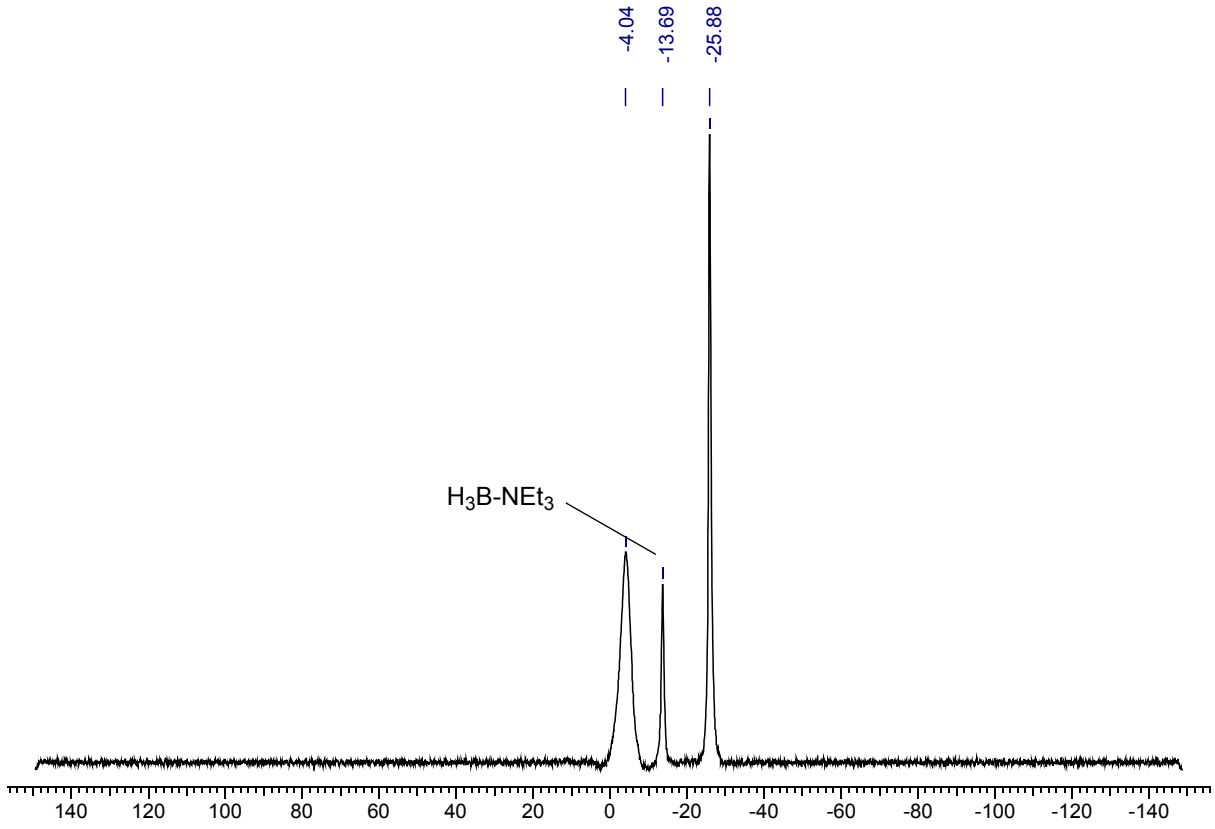

^{19}F {^{1}H} NMR Spectrum: In situ NMR of triethylamine Borane Activation with $B(C_6F_5)_3$

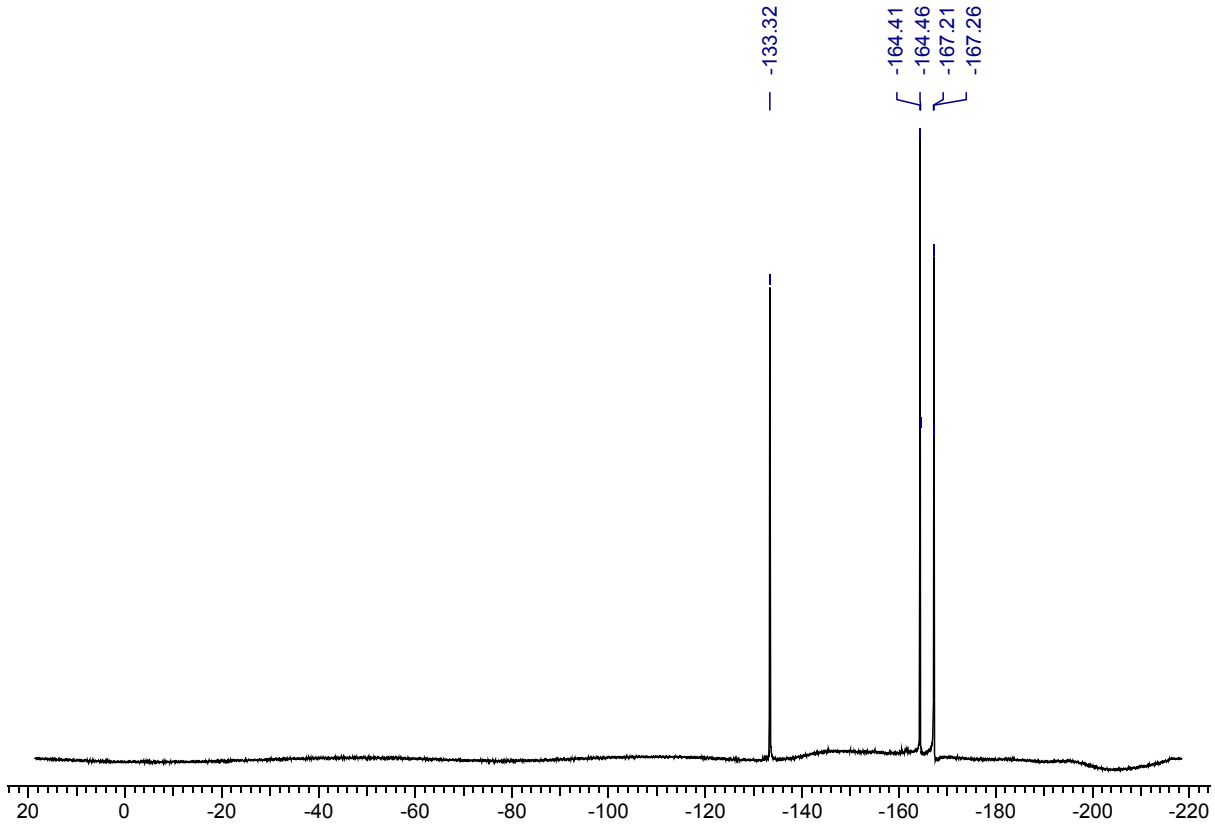

13.12

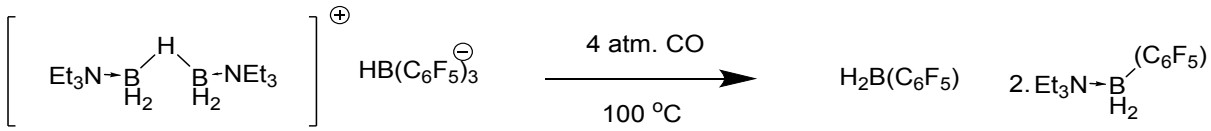

^{1}H NMR Spectrum: In situ NMR of triethylamine Borane Activation with $B(C_6F_5)_3$ under CO heat 100 °C 24 h

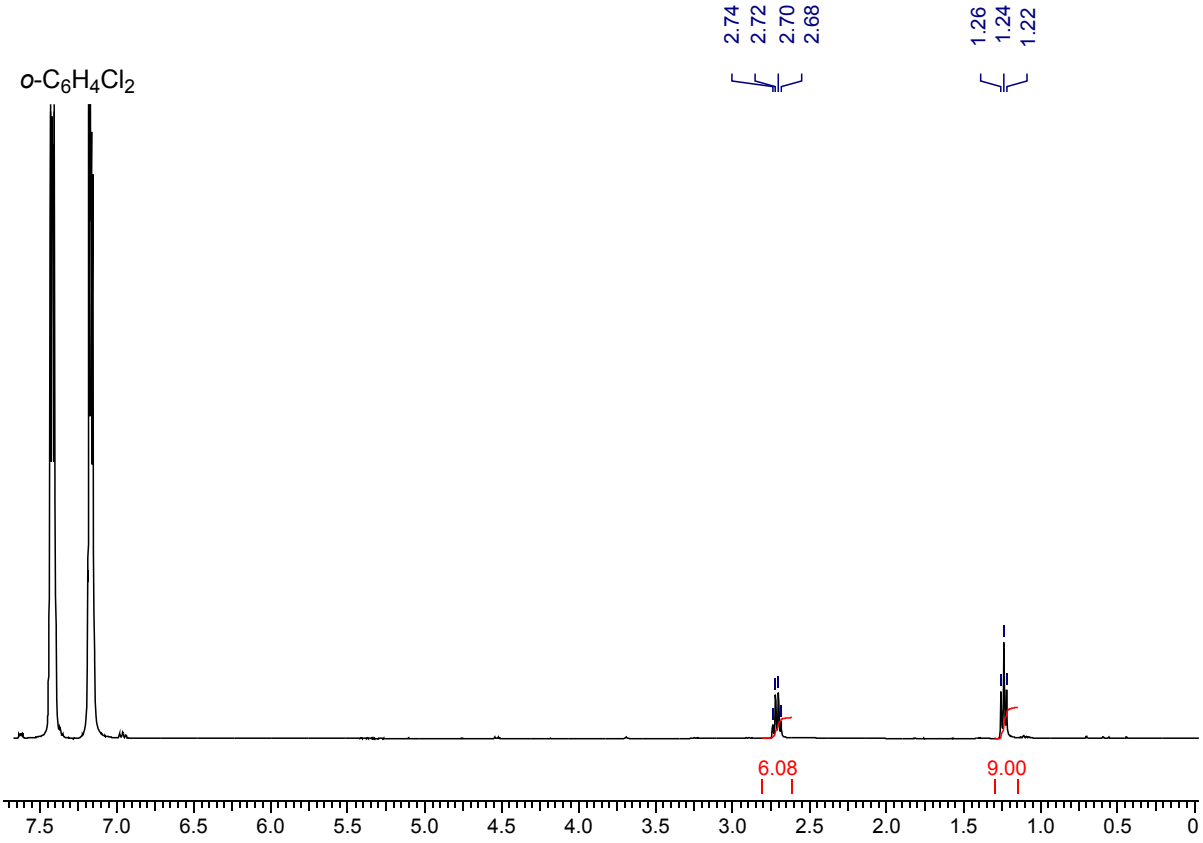

^{1}H {^{11}B} NMR Spectrum: In situ NMR of triethylamine Borane Activation with $B(C_6F_5)_3$ under CO heat 100 °C 24 h

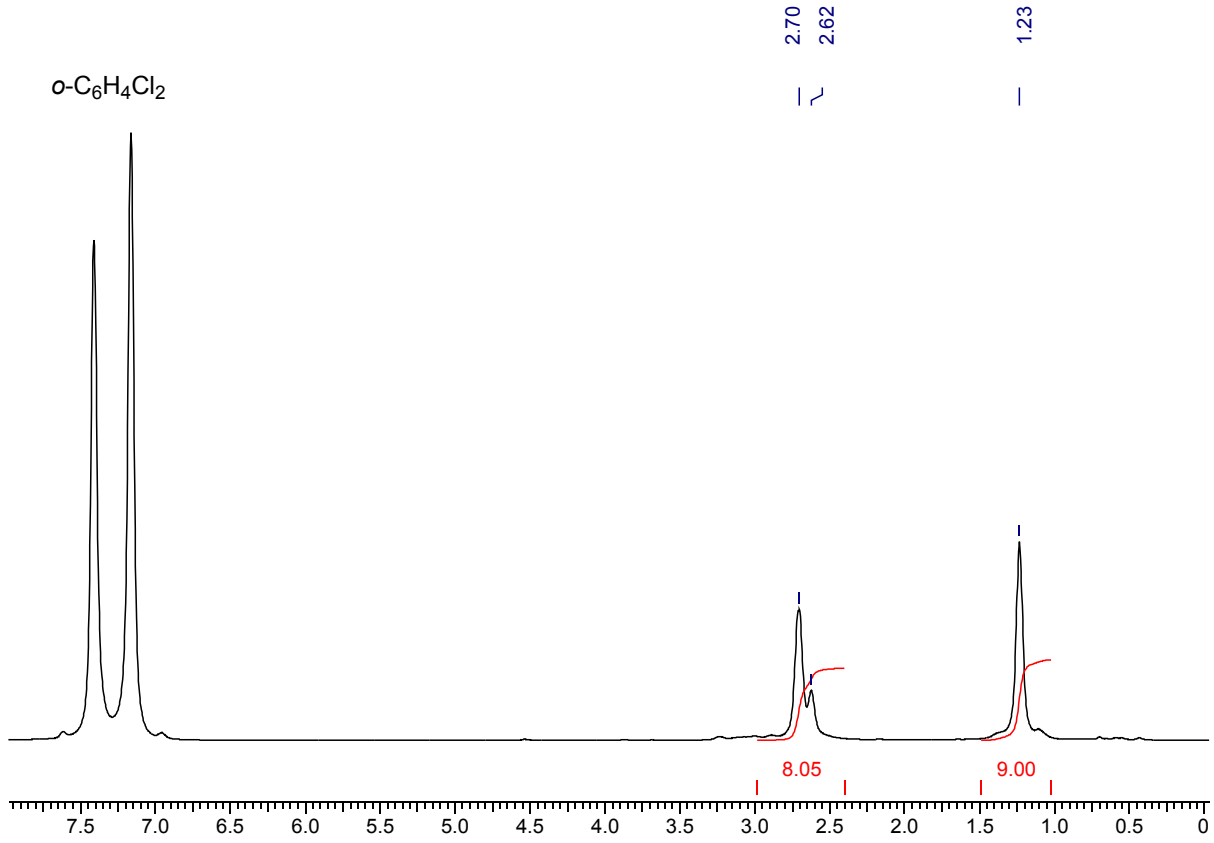

^{11}B NMR Spectrum: In situ NMR of triethylamine Borane Activation with $B(C_6F_5)_3$ under CO heat 100 °C 24 h

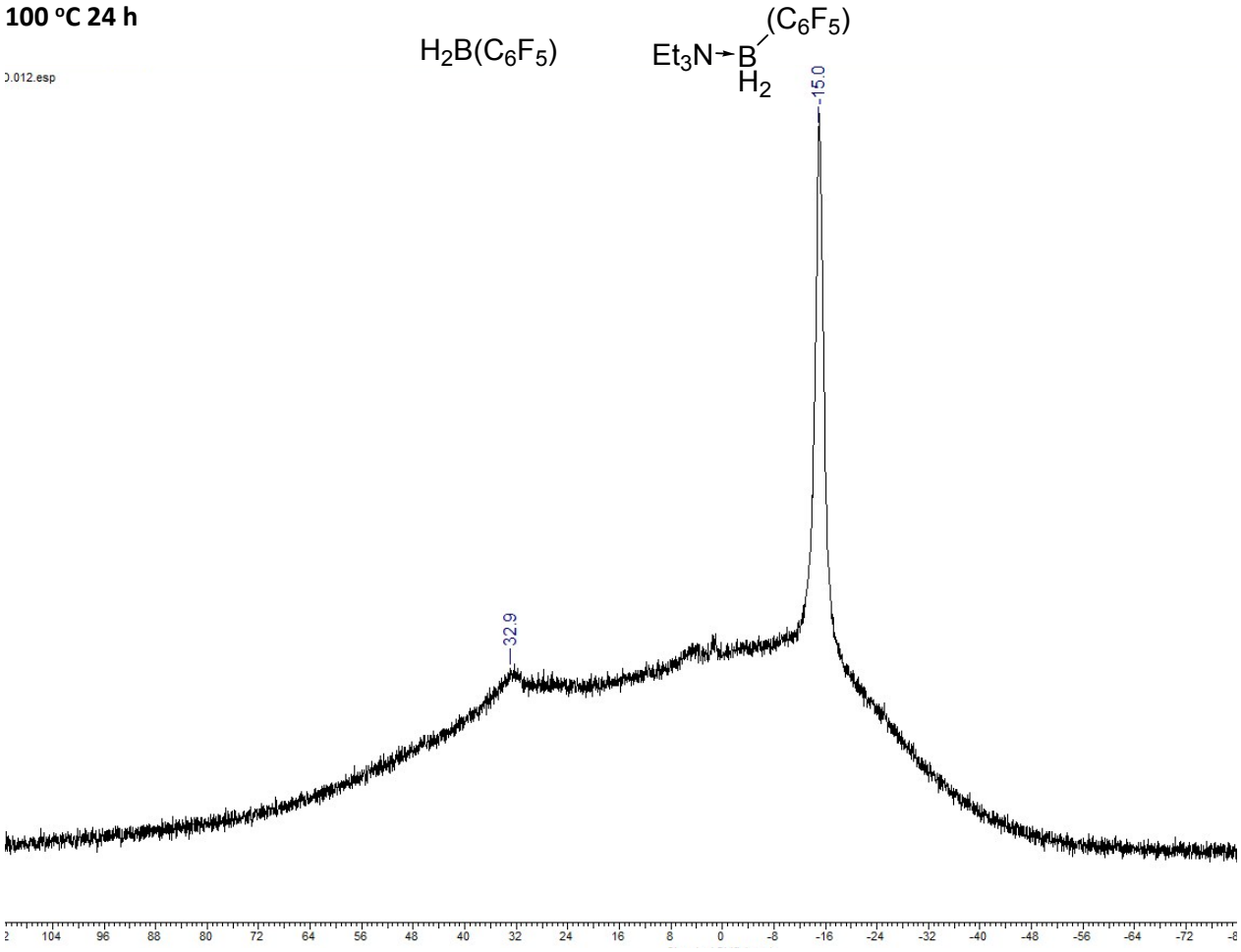

^{11}B {^{1}H} NMR Spectrum: In situ NMR of triethylamine Borane Activation with $B(C_6F_5)_3$ under CO heat 100 ^{o}C 24 h

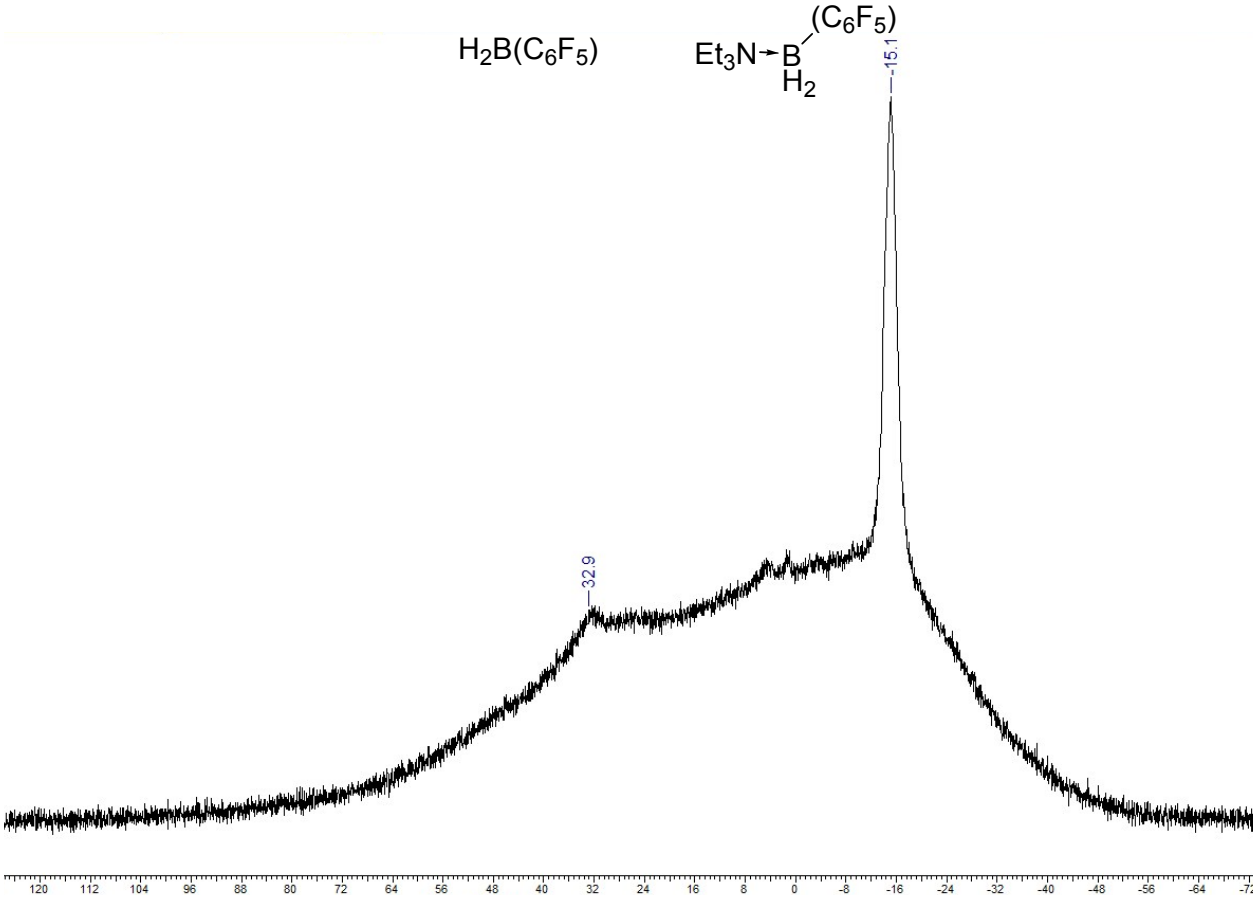

^{19}F {^{1}H} NMR Spectrum: In situ NMR of triethylamine Borane Activation with $B(C_6F_5)_3$ under CO heat 100 °C 24 h

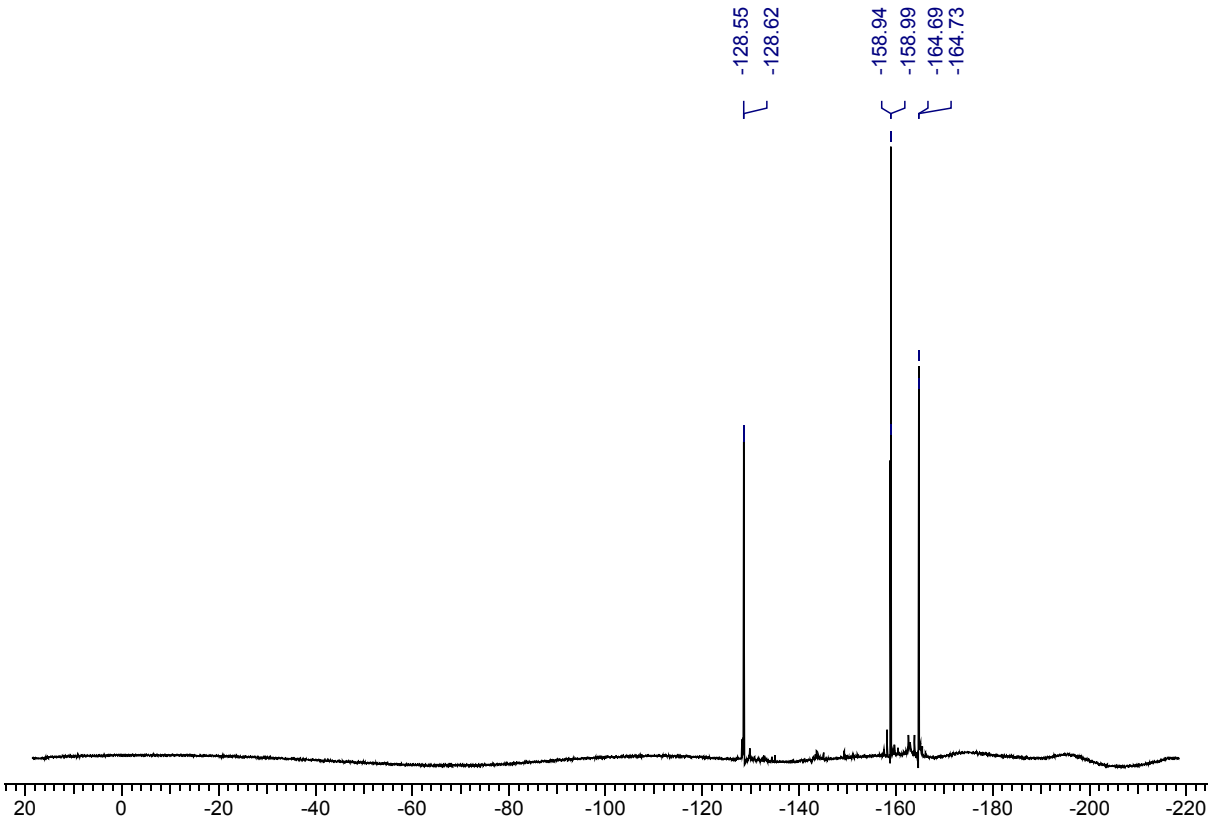

13. X-Ray Crystallography

Data for compounds **3** and **5** and were recorded on an Agilent Supernova diffractometer, with Mo Ka radiation (mirror monochromator, l=0.7107). The CrysAlisPro[3] software package was used for data collection, cell refinement and data reduction. For all data sets the CrysAlisPro software package was used for empirical absorption corrections, which were applied using spherical harmonics, implemented in SCALE3 ABSPACK scaling algorithm.

Structures **3** and **5** were solved using direct methods[4] and refined against F^2 using the Crystals[5] software package. Non-hydrogen atoms were refined anisotropically. Hydrogen atoms were all located in a difference map and repositioned geometrically. Experimental details are given below in Table 1.

Crystallographic data for **3** and **5** have been deposited with the Cambridge Crystallographic Data Center under the references: 1058783; and 1058784. These data can be obtained free of charge from The Cambridge Crystallographic Data Centre (CCDC) *via* www.ccdc.cam.ac.uk/data _request/cif.

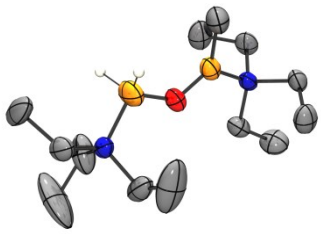

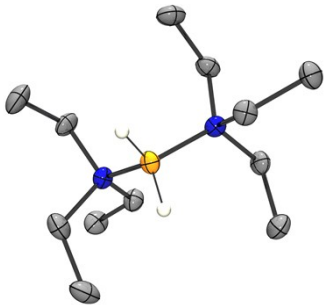

Table 1 Crystal data and structure refinement for 3 and 5.

Identification code	Compound 3 (1058783)	Compound 5 (1058784)
Empirical formula	$C_{37}H_{33}B_3F_{20}N_2O$	$C_{36}H_{32}B_2F_{20}N_2$
Formula weight	934.08	894.25
Temperature/K	150	150.0
Crystal system	monoclinic	triclinic
Space group	$P2_1/c$	P-1
a/Å	15.3222(4)	8.7661(5)
b/Å	15.0233(6)	13.7257(7)
c/Å	17.8625(6)	15.8543(8)
α/°	90	82.373(4)
β/°	98.977(3)	83.288(4)
γ/°	90	81.661(4)
Volume/Å^3	4061.4(2)	1861.44(17)
Z	4	2
ρ_{calc}g/cm^3	1.528	1.595
μ/mm^{-1}	0.154	0.163
F(000)	1888.0	904.0

Crystal size/mm^3	0.1 × 0.1 × 0.2	0.4 × 0.2 × 0.05
Radiation	MoKα (λ = 0.71073)	Mo Kα (λ = 0.71073)
2Θ range for data collection/°	6.524 to 58.032	6.674 to 57.796
Index ranges	-20 ≤ h ≤ 18, -12 ≤ k ≤ 19, -23 ≤ l ≤ 23	-11 ≤ h ≤ 11, -17 ≤ k ≤ 18, -21 ≤ l
Reflections collected	18395	14253
Independent reflections	9153 [R_{int} = 0.0330, R_{sigma} = 0.0661]	8377 [Rint = 0.0323, Rsigma =
Data/restraints/parameters	9153/0/575	8377/0/555
Goodness-of-fit on F^2	1.031	1.046
Final R indexes [I>=2σ (I)]	R_1 = 0.0626, wR_2 = 0.1316	R1 = 0.0581, wR2 = 0.0951
Final R indexes [all data]	R_1 = 0.1015, wR_2 = 0.1524	R1 = 0.0938, wR2 = 0.1126
Largest diff. peak/hole / e $Å^{-3}$	0.56/-0.32	0.27/-0.25

14. Computational Details

Calculations were performed using the Gaussian09 suite of programmes.[6] Geometries were optimised with the DFT method using M06-2X functional[7] and 6-311G(d,p) as a basis set. All stationary geometry optimizations were full, with no restrictions. All stationary points were characterised as a minima or transitions state by vibrational analysis. Transition states had one imaginary frequency, whose normal mode corresponded to the expected motion. Solvent effects of the dichloromethane were introduced using the self consistent field approach, by means of the integral equation formalism polarisable continuum model (IEFPCM).[8]

Full Cartesian coordinates of the optimised structures are provided below.

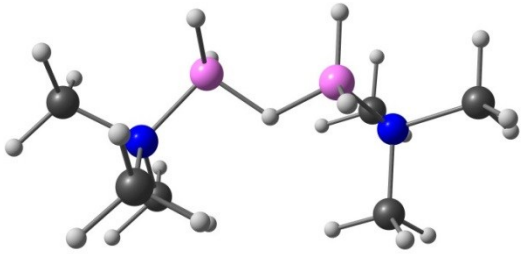

$[(H_2B(NMe_3))_2(\mu\text{-}H)]^+$

E(RM062X) = -401.449546086

N	3.513318000	10.832979000	8.909767000
N	0.571135000	9.305415000	6.067496000
C	4.528320000	11.864614000	9.275850000
H	4.804723000	11.734473000	10.322506000
H	5.402353000	11.740105000	8.639529000
C	-0.144860000	10.610649000	6.090783000
H	0.059600000	11.114442000	7.034741000
H	-1.216545000	10.435938000	5.989816000
C	4.094169000	9.480516000	9.134954000
H	4.986159000	9.377629000	8.519993000
H	4.348655000	9.367527000	10.189116000
C	2.316776000	11.013301000	9.774434000
H	1.595967000	10.227146000	9.556015000
H	1.875566000	11.986959000	9.568715000
C	0.254757000	8.601809000	4.789685000
H	-0.818544000	8.417348000	4.743472000
H	0.563584000	9.229579000	3.956368000
C	0.107472000	8.463760000	7.202630000
H	0.313956000	8.979418000	8.138874000
H	0.639605000	7.514800000	7.178535000
B	3.176624000	11.062806000	7.371214000
B	2.149325000	9.513472000	6.081042000
H	2.461618000	10.207003000	5.167303000
H	2.713699000	8.472829000	6.227902000
H	3.364509000	8.724732000	8.846695000
H	4.096121000	12.851987000	9.123101000
H	2.612624000	10.949661000	10.82193000
H	-0.966245000	8.294981000	7.114062000
H	0.798217000	7.658939000	4.764367000
H	0.214817000	11.222378000	5.265563000
H	2.251754000	10.128917000	7.243171000
H	2.604252000	12.097216000	7.212418000
H	4.143691000	10.838101000	6.717300000

CO

E(RM062X) = -113.308362705

C	-3.646472000	4.030527000	7.632363000
O	-2.524977000	4.030527000	7.632363000

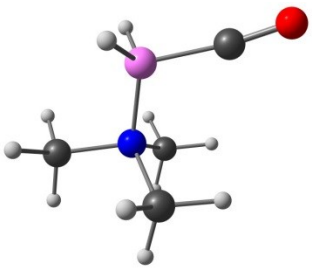

$[(Me_3N)BH_2\text{-}CO]^+$ **2_{Me}**

E(RM062X) = -313.653076176

N	3.716563000	10.896590000	8.983481000
C	4.503481000	12.170304000	9.004586000
H	4.756328000	12.405188000	10.038003000
H	5.408749000	12.034065000	8.416255000
C	4.551721000	9.806008000	9.569520000
H	5.433601000	9.666219000	8.947732000
H	4.845768000	10.086088000	10.580352000
C	2.485003000	11.082316000	9.807633000
H	1.914194000	10.154118000	9.819797000
H	1.887867000	11.880452000	9.371568000
B	3.370225000	10.616396000	7.475094000
H	3.969888000	8.884905000	9.605579000
H	3.895746000	12.964716000	8.576186000
H	2.773582000	11.341162000	10.825868000
H	2.633843000	11.438964000	7.016410000
H	4.342866000	10.387044000	6.818820000
C	2.519476000	9.261108000	7.341569000
O	1.926704000	8.345479000	7.124034000

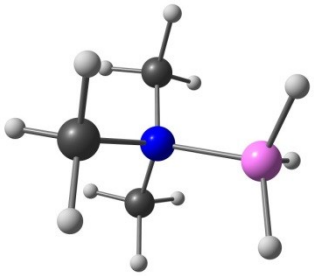

Me_3NBH_3

E(RM062X) = -201.093840399

N	3.799269000	10.840444000	8.999463000
C	4.427094000	12.182367000	8.969840000
H	4.627713000	12.523709000	9.987966000
H	5.357466000	12.120413000	8.407908000
C	4.711876000	9.894653000	9.683817000
H	5.643783000	9.841759000	9.123689000
H	4.906671000	10.236133000	10.702977000
C	2.526945000	10.917433000	9.754992000
H	2.073001000	9.928151000	9.776000000
H	1.859503000	11.610691000	9.246018000
B	3.513359000	10.331747000	7.481776000
H	4.245221000	8.911308000	9.702947000
H	3.749563000	12.873875000	8.471906000
H	2.718319000	11.262281000	10.773655000
H	2.765494000	11.146357000	6.984814000
H	4.591642000	10.295487000	6.928187000
H	3.005517000	9.235354000	7.580110000

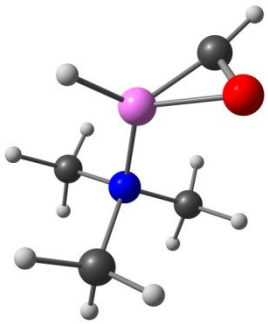

4

E(RM062X) = -313.620915771

N	3.800399000	10.799877000	8.996213000
C	4.405491000	12.169197000	8.996634000
H	4.511641000	12.501857000	10.028544000
H	5.380881000	12.122597000	8.516314000
C	4.698477000	9.862641000	9.742601000
H	5.677324000	9.860697000	9.267517000
H	4.779729000	10.205119000	10.773577000

C	2.470417000	10.846459000	9.672232000
H	2.035587000	9.848766000	9.682158000
H	1.820261000	11.537138000	9.134888000
B	3.730792000	10.328813000	7.514387000
H	4.266704000	8.863486000	9.710962000
H	3.751174000	12.846141000	8.449416000
H	2.611006000	11.195592000	10.694047000
C	2.375544000	10.276982000	6.802232000
O	2.694607000	9.168087000	7.271397000
H	1.457659000	10.453555000	6.243159000
H	4.768781000	10.257788000	6.958944000

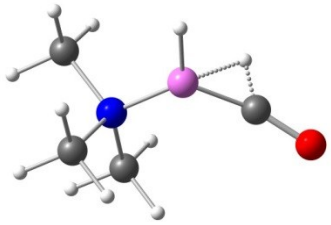

$TS_{2\rightarrow4}$

E(RM062X) = -313.596309197

N	3.783234000	10.783151000	9.017775000
C	4.422940000	12.137716000	8.906589000
H	4.610520000	12.510484000	9.912653000
H	5.357055000	12.041688000	8.357702000
C	4.723922000	9.849584000	9.742161000
H	5.658865000	9.786698000	9.188530000
H	4.900907000	10.265246000	10.732968000
C	2.506198000	10.890402000	9.794671000
H	2.058822000	9.902052000	9.881218000
H	1.832636000	11.573041000	9.278706000
B	3.623065000	10.141468000	7.642995000
H	4.258346000	8.868432000	9.824335000
H	3.741661000	12.802634000	8.379309000
H	2.737225000	11.280449000	10.784202000
H	2.211667000	10.837703000	6.838125000
H	4.501732000	10.226477000	6.863454000
C	2.271877000	9.677567000	7.192700000
O	1.370898000	8.949768000	6.981696000

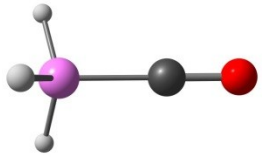

H_3B-CO

E(RM062X) = -139.945292811

B	3.389056000	10.644901000	7.483558000
C	2.567973000	9.337637000	7.354652000
O	1.974955000	8.391466000	7.263694000
H	4.376964000	10.433989000	6.830997000
H	2.664201000	11.489707000	7.028355000
H	3.586991000	10.745711000	8.665765000

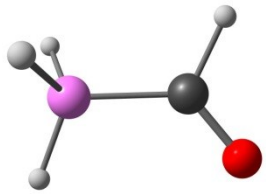

$[H_3B\text{-}CHO]^-$

E(RM062X) = -140.649856147

B	3.389056000	10.644901000	7.483558000
C	2.567973000	9.337637000	7.354652000
O	1.974955000	8.391466000	7.263694000
H	4.376964000	10.433989000	6.830997000
H	2.664201000	11.489707000	7.028355000
H	3.586991000	10.745711000	8.665765000

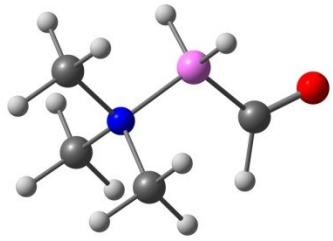

$(Me_3N)BH_2$-CHO

E(RM062X) = -314.409418054

N	3.734573000	10.922591000	9.002127000
C	4.517289000	12.182599000	9.041505000

H	4.777093000	12.421809000	10.074852000
H	5.420879000	12.051422000	8.449027000
C	4.559689000	9.831277000	9.578734000
H	5.453791000	9.712727000	8.969082000
H	4.837253000	10.080287000	10.604807000
C	2.506970000	11.100186000	9.818291000
H	1.930685000	10.176707000	9.812116000
H	1.913123000	11.901802000	9.382589000
B	3.354935000	10.599129000	7.456898000
H	3.988650000	8.904472000	9.571690000
H	3.915469000	12.981500000	8.612337000
H	2.779250000	11.351698000	10.845200000
C	2.502441000	9.239773000	7.319385000
O	2.115420000	8.815010000	6.246727000
H	2.227911000	8.623468000	8.219025000
H	4.403782000	10.487903000	6.864465000
H	2.700099000	11.536645000	7.063179000

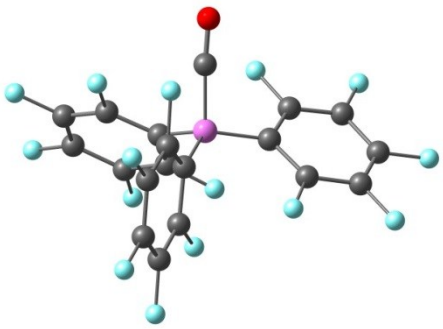

$(C_6F_5)_3B$-CO

E(RM062X) = -2321.48687874

B	-0.355124000	-1.448985000	0.799040000
C	1.193693000	-1.505581000	0.310883000
C	1.753791000	-2.501078000	-0.478341000
C	2.048503000	-0.467091000	0.662937000
C	3.068680000	-2.448388000	-0.918486000
C	3.363103000	-0.381406000	0.250806000
C	3.875649000	-1.386610000	-0.553180000
C	-1.134727000	-0.057534000	0.483877000
C	-2.279370000	0.254900000	1.204206000
C	-0.804243000	0.818100000	-0.540280000
C	-3.059915000	1.367665000	0.953785000
C	-1.561168000	1.944266000	-0.823870000
C	-2.690425000	2.220931000	-0.072831000
C	-1.301953000	-2.690449000	0.396714000
C	-1.629218000	-2.835650000	-0.944439000
C	-1.887062000	-3.590423000	1.267449000
C	-2.471191000	-3.827460000	-1.407714000

C	-2.742925000	-4.596363000	0.846881000
C	-3.033017000	-4.713635000	-0.499935000
F	1.578153000	0.520555000	1.441056000
F	4.132035000	0.639235000	0.614605000
F	5.134364000	-1.332666000	-0.964323000
F	3.560171000	-3.417647000	-1.684080000
F	-2.656771000	-0.565010000	2.201429000
F	-3.417873000	3.297944000	-0.336256000
F	-4.145486000	1.621982000	1.676441000
F	-1.212344000	2.760917000	-1.813118000
F	-3.845833000	-5.672360000	-0.924973000
F	-3.284095000	-5.439175000	1.720927000
F	0.263242000	0.603724000	-1.312302000
F	-1.635471000	-3.506158000	2.584332000
F	-1.090488000	-1.997352000	-1.837806000
F	-2.747679000	-3.944049000	-2.702643000
C	-0.165705000	-1.419796000	2.429087000
O	0.072327000	-1.319512000	3.511308000
F	1.047047000	-3.564818000	-0.866142000

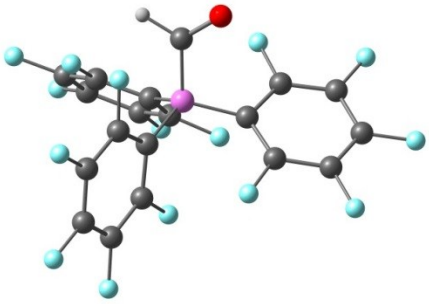

$[(C_6F_5)_3B\text{-}CHO]^-$

E(RM062X) = -2322.23574882

B	-0.312344000	-1.413806000	0.900686000
C	1.189108000	-1.477610000	0.257543000
C	1.742650000	-2.504093000	-0.489717000
C	2.076457000	-0.450448000	0.563831000
C	3.061760000	-2.508594000	-0.929123000
C	3.393548000	-0.411755000	0.151548000
C	3.894162000	-1.457033000	-0.607019000
C	-1.155653000	-0.053405000	0.498473000
C	-2.387109000	0.178686000	1.104105000
C	-0.794165000	0.902193000	-0.442520000
C	-3.187304000	1.278585000	0.843711000
C	-1.562930000	2.019697000	-0.733475000
C	-2.766233000	2.214969000	-0.082348000
C	-1.274119000	-2.657298000	0.442139000
C	-1.605077000	-2.801697000	-0.899107000
C	-1.868432000	-3.572178000	1.293131000

C	-2.443718000	-3.788743000	-1.380759000
C	-2.722350000	-4.576395000	0.857570000
C	-3.010271000	-4.685584000	-0.488871000
F	1.648073000	0.603158000	1.279041000
F	4.188299000	0.613720000	0.471512000
F	5.162405000	-1.444769000	-1.017956000
F	3.531063000	-3.527627000	-1.655339000
F	-2.882243000	-0.709998000	1.986205000
F	-3.514675000	3.284087000	-0.350756000
F	-4.355968000	1.439541000	1.468476000
F	-1.157122000	2.905912000	-1.646076000
F	-3.824243000	-5.645146000	-0.928274000
F	-3.270848000	-5.431788000	1.723930000
F	0.336176000	0.786934000	-1.154893000
F	-1.642404000	-3.521601000	2.616844000
F	-1.071462000	-1.964385000	-1.802895000
F	-2.713936000	-3.893479000	-2.684312000
C	-0.092134000	-1.388005000	2.530028000
O	0.958533000	-1.639537000	3.085102000
H	-0.950501000	-1.099544000	3.177100000
F	1.026958000	-3.586453000	-0.841466000

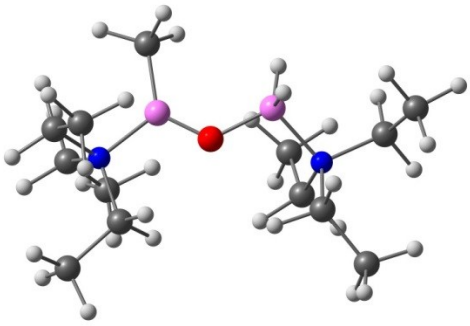

3

E(RM062X) = -750.725468583

O	2.389991000	9.787499000	7.224494000
N	3.729200000	10.807577000	8.988825000
N	0.341964000	9.369304000	5.909040000
C	3.993645000	12.294816000	9.007560000
H	4.250294000	12.567687000	10.031451000
H	4.880641000	12.456397000	8.396298000
C	0.679212000	11.839861000	5.339442000
H	0.440530000	11.731136000	4.281518000
H	1.762333000	11.808395000	5.453704000
H	0.328276000	12.823906000	5.655781000
C	2.581689000	10.828505000	11.267120000
H	2.689707000	11.902255000	11.424972000
H	3.388576000	10.310819000	11.787438000

H	1.644595000	10.522890000	11.733860000
C	2.831027000	13.122893000	8.488181000
H	2.494211000	12.782609000	7.504937000
H	3.166375000	14.154595000	8.381898000
H	1.980453000	13.117712000	9.169995000
C	-0.017302000	10.800428000	6.203599000
H	0.222881000	10.967166000	7.254230000
H	-1.098041000	10.895328000	6.087120000
C	-1.768532000	8.532683000	7.102147000
H	-2.264203000	8.236587000	6.176172000
H	-2.145005000	9.509944000	7.404804000
H	-2.060099000	7.817041000	7.872300000
C	-0.088514000	7.536619000	4.188981000
H	-0.416975000	7.422084000	3.155097000
H	-0.734471000	6.914871000	4.810187000
H	0.933975000	7.169074000	4.263220000
C	4.958200000	10.119389000	9.537339000
H	5.786180000	10.412582000	8.893444000
H	5.149736000	10.536491000	10.526203000
C	4.707663000	10.583679000	6.455956000
H	5.032392000	9.613133000	6.066262000
H	5.588134000	11.111493000	6.818213000
H	4.312268000	11.129821000	5.593670000
C	4.829098000	8.606598000	9.588003000
H	4.518122000	8.189638000	8.626205000
H	4.126482000	8.277110000	10.353579000
H	5.806214000	8.187889000	9.829104000
C	2.502680000	10.457710000	9.796995000
H	2.342823000	9.389523000	9.668797000
H	1.662616000	10.953224000	9.315122000
C	-0.183719000	9.011220000	4.547558000
H	-1.221588000	9.348846000	4.493183000
H	0.394244000	9.596790000	3.834526000
C	-0.252297000	8.497405000	6.981503000
H	0.218046000	8.816903000	7.912969000
H	0.091278000	7.484055000	6.780779000
B	3.545492000	10.349202000	7.478267000
B	1.955373000	9.158198000	5.940825000
H	2.417554000	9.698454000	4.968651000
H	2.169471000	7.973665000	5.978077000

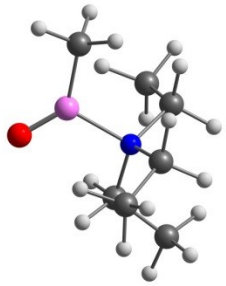

$(Et_3N)(CH_3)BO$

E(RM062X) = -432.400339986

O	2.356976000	9.740649000	7.234608000
N	3.798579000	10.844405000	8.985950000
C	4.344358000	12.234436000	8.925279000
H	4.634286000	12.536138000	9.934647000
H	5.257040000	12.182308000	8.331296000
C	2.615296000	11.235500000	11.206314000
H	2.929740000	12.276416000	11.305761000
H	3.294258000	10.610656000	11.789774000
H	1.625098000	11.148744000	11.656417000
C	3.376930000	13.240210000	8.320984000
H	2.968423000	12.883487000	7.372380000
H	3.910865000	14.171715000	8.129990000
H	2.546711000	13.463426000	8.991901000
C	4.847565000	9.974009000	9.607136000
H	5.721136000	10.032185000	8.957773000
H	5.132696000	10.413115000	10.566633000
C	4.700200000	10.553192000	6.425842000
H	4.580702000	9.927949000	5.539338000
H	5.697476000	10.368336000	6.833036000
H	4.690900000	11.594495000	6.084409000
C	4.421224000	8.525227000	9.783343000
H	4.021404000	8.111860000	8.855545000
H	3.668117000	8.412354000	10.564223000
H	5.293718000	7.938891000	10.073990000
C	2.516837000	10.789569000	9.755567000
H	2.154408000	9.768145000	9.674223000
H	1.800386000	11.395881000	9.204993000
B	3.482371000	10.275801000	7.414646000

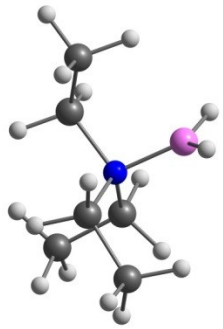

$[(Et_3N)BH_2]^+$

E(RM062X) = -318.222318049

N	0.209341000	9.289047000	5.860302000
C	0.406120000	11.803380000	5.723062000
H	0.190032000	11.866665000	4.657691000
H	1.492783000	11.782411000	5.865696000
H	0.049633000	12.720408000	6.191818000
C	-0.285997000	10.625843000	6.395341000
H	-0.084010000	10.621510000	7.466225000
H	-1.362938000	10.653923000	6.237391000
C	-1.642562000	7.917402000	6.942272000
H	-2.074312000	7.553768000	6.009791000
H	-2.187730000	8.803210000	7.269121000
H	-1.785759000	7.144348000	7.697696000
C	0.013457000	7.690348000	3.908853000
H	-0.315070000	7.659721000	2.870003000
H	-0.472057000	6.868463000	4.435022000
H	1.093611000	7.528876000	3.917658000
C	-0.360959000	9.044837000	4.480709000
H	-1.442308000	9.159409000	4.558215000
H	0.020441000	9.842721000	3.845796000
C	-0.150746000	8.173062000	6.830180000
H	0.269739000	8.466907000	7.791444000
H	0.374539000	7.277657000	6.494224000
B	1.727002000	9.429411000	5.850583000
H	2.288806000	9.421784000	4.814707000
H	2.234143000	9.539490000	6.909800000

15. References

1. De Vries, T. S.; Vedejs, E., *Organometallics*, **2006**, 26, 3079.
2. Menard, G.; Stephan, D. W.; *Dalton Trans,* **2013**, 42, 5447.
3. CrysAlisPro, Agilent Technologies, Version 1.171.35.19 (release 27-10-2011 CrysAlis171 .NET (compiled Oct 27 2011,15:02:11)
4. SIR92, Altomare, A.; Cascarano, G.; Giacovazzo, C.; Guagliardi, A.; Burla, M. C.; Polidori, G.; Camalli, M. *J. Appl. Cryst.* **1994**, 27, 435.
5. Olex2.refine (Bourhis, L. J.; Dolomanov, O. V.; Gildea, R. J.; Howard, J. A. K.; Puschmann, H. in preparation, 2011)
6. Gaussian 09, Revision C1, Frisch, M. J.; Trucks, G. W.; Schlegel, H. B.; Scuseria, G. E.; Robb, M. A.; Cheeseman, J. R.; Scalmani, G.; Barone, V.; Mennucci, B.; Petersson, G. A.; Nakatsuji, H.; Caricato, M.; Li, X.; Hratchian, H. P.; Izmaylov, A. F.; Bloino, J.; Zheng, G.; Sonnenberg, J. L.; Hada, M.; Ehara, M.; Toyota, K.; Fukuda, R.; Hasegawa, J.; Ishida, M.; Nakajima, T.; Honda, Y.; Kitao, O.; Nakai, H.; Vreven, T.; Montgomery, Jr., J. A.; Peralta, J. E.; Ogliaro, F.; Bearpark, M.; Heyd, J. J.; Brothers, E.; Kudin, K. N.; Staroverov, V. N.; Kobayashi, R.; Normand, J.; Raghavachari, K.; Rendell, A.; Burant, J. C.; Iyengar, S. S.; Tomasi, J.; Cossi, M.; Rega, N.; Millam, J. M.; Klene, M.; Knox, J. E.; Cross, J. B.; Bakken, V.; Adamo, C.; Jaramillo, J.; Gomperts, R.; Stratmann, R. E.; Yazyev, O.; Austin, A. J.; Cammi, R.; Pomelli, C.; Ochterski, J. W.; Martin, R. L.; Morokuma, K.; Zakrzewski, V. G.; Voth, G. A.; Salvador, P.; Dannenberg, J. J.; Dapprich, S.; Daniels, A. D.; Farkas, Ö.; Foresman, J. B.; Ortiz, J. V.; Cioslowski, J.; Fox, D. J. Gaussian, Inc., Wallingford CT, **2009**.
7. Zhao Y.; Truhlar D. G., *Theor. Chem. Acc.* **2008**, 120, 215.
8. Mennucci B.; Cancès E.; Tomasi J., *J. Phys. Chem. B* **1997**, 101, 10506.